



Università degli Studi di Ferrara

DOTTORATO DI RICERCA IN  
FISICA

CICLO XXIV

COORDINATORE Prof. Filippo Frontera

# A scanning device for wide band infrared reflectography

Settore Scientifico Disciplinare FIS/07

**Dottorando**

Dott. Peccenini Eva

---

**Tutore**

Prof. Gambaccini Mauro

---

**Cotutore**

Prof. Petrucci Ferruccio

---

Anni 2009/2011



# Contents

**INTRODUCTION..... 7**

**CHAPTER 1**

**STUDY AND CONSERVATION OF CULTURAL HERITAGE..... 9**

**1.1 THE SCIENTIFIC EXAMINATION OF ARTWORKS ..... 11**

**1.2 THE BASIC STRUCTURE OF A PAINTING ..... 11**

**1.3 INTERACTION BETWEEN ELECTROMAGNETIC RADIATION AND PICTORIAL LAYERS..... 14**

**1.4 A PROTOCOL FOR IMAGE DIAGNOSTICS OF PAINTINGS..... 19**

**CHAPTER 2**

**WIDE BAND INFRARED REFLECTOGRAPHY ..... 31**

**2.1 RESULTS AND IMPROVEMENTS OF IR IMAGING OF PAINTINGS ..... 33**

**2.2 TRADITIONAL DEVICES FOR IR IMAGING ..... 37**

**2.3 ADVANTAGES OF SCANNING SYSTEM..... 39**

**2.4. THEORY OF IR REFLECTOGRAPHY..... 41**

**2.5. KUBELKA-MUNK DIFFUSION THEORY ..... 42**

**2.6 WIDE BAND RANGE ..... 48**

**2.6.1 TEST PAINTING ..... 48**

**2.6.2 RESULTS ..... 51**

**2.6.3 DISCUSSION ..... 56**

**CHAPTER 3**

**SCANNING DEVICE ..... 59**

**3.1 PROJECT FOR A SCANNING DEVICE FOR WIDE BAND IR REFLECTOGRAPHY ..... 61**

**3.2 SCANNING SYSTEM ..... 62**

**3.3 MECHANICAL SYSTEM ..... 63**

**3.4 ACQUISITION DEVICE ..... 64**

**3.5 SAFETY SYSTEM ..... 67**

**3.6 OPTICAL SYSTEM ..... 68**

**3.7 DETECTORS ..... 70**

**3.8 SOFTWARE ..... 75**

**CHAPTER 4**

**SYSTEM OPTIMIZATION ..... 79**

**4.1 OPTICAL TARGET ..... 81**

**4.2 SPATIAL RESOLUTION OF THE SCANNING SYSTEM ..... 83**

**4.3 OVERHEATING REDUCTION ..... 88**

4.3.1 “*RETURN OF PRODIGAL SON*” ..... 88

4.3.2 “*MADDALENA PENITENTE*” ..... 92

**CHAPTER 5**

**APPLICATIONS ..... 99**

**5.1 VIRGIN WITH CHILD AND SAINTS ..... 101**

**5.2 PORTRAIT OF CARDINAL MAZARINO ..... 108**

**5.3 LANDSCAPE BY GUGLIELMO CIARDI ..... 112**

**5.4 FLOWERS ..... 116**

**5.5 LANDSCAPE 20<sup>TH</sup> CENTURY ..... 120**

**5.6 FIVE PAINTINGS BY THE SAME ARTIST: EDOARDO PAZZINI ..... 125**

**CHAPTER 6**

**CONCLUSIONS ..... 135**

**ACKNOWLEDGEMENTS..... 139**



# Introduction

Diagnostics in the cultural heritage field is an important resource to investigate art history, issues, execution techniques, materials and state of conservation of an artwork. In this field the main concern is preservation and, for this reason, new *non-invasive* and *non-destructive* technologies have been developed.

At the Department of Physics in Ferrara, imaging for cultural heritage, using electromagnetic radiation, from visible light to X-rays is applied and studied.

A diagnostics protocol has been defined to standardize the study approach on paintings considering that each painting is a particular case, and the protocol must be adapted to the needs that the artwork itself requires.

This work consists in the development of a scanning devices for wide band infrared Reflectography, to extend the applications of the reflectographic technique, and how it is inserted in the diagnostic protocol.

The success of IR Reflectography to reveal the underdrawing in paintings since XIV up to XVI century depends on the peculiar technique of painters in that period. Thin and uniform pictorial layers, covering high contrast drawings on white priming allow a good detection of underdrawing details.

Paintings of late sixteenth century have dark preparations and thick paint layers, so Reflectography doesn't get the same good results.

Extension of the spectral band to longer wavelengths is a tool to improve reflectographic capability.





---

---

**CHAPTER 1**

**STUDY AND CONSERVATION OF  
CULTURAL HERITAGE**

---

---



## 1.1 The scientific examination of artworks

**A** work of art lives a long time, and the passage of time inevitably produces changes. This is the result of natural process or it is due to human intervention, that changes its original features.

A methodical investigation of physical properties of art materials may be a tool to clear the distortion of time and to return to the primary meanings.

In the Archaeometry Laboratory at Physics Department of Ferrara University an image diagnostics protocol to study paintings is followed. This includes visual observation and image diagnostics techniques: raking light, close-up photographs, UV-fluorescence, IR Reflectography, X-ray radiography. This is usually accepted and adopted by many diagnostics services through the world.

During the latest years instrumentations and devices have been added, designed and built in the lab to enhance non-invasive approach to the study of pictorial artworks.

This work will be focused, in particular, on the development of a scanning device for wide band IR reflectography.

A short description will follow, on the structure of painting and on the interaction between electromagnetic radiation and pictorial materials.

## 1.2 The basic structure of a painting

In the traditional form in Western Europe since Middle Age, a painting has a complex structure in layers. Each layer has a specific function to guarantee the stability in time of the object.

The base of a painting is the support, made of wood or canvas. The wooden supports are made by many tables assembled by joints or glue. Often, in the ancient paintings the support in wood is covered of light canvas, to limit movements of wood due to the thermo-hygrometric changes.

Since XV century, canvas gradually replaces the wooden support, because of its evident advantage: easy to transport, better suited for large paintings, minor susceptibility to climate changes.

The tradition has imposed a "regola d'arte" to suggest to the artists the right features of paintings. Over time the rule of art was abandoned. The introduction of new execution techniques and of new materials, more suitable to express the creativity of the artist, will be destined to become the main feature of the Twentieth Century Art.

The support is covered by *preparation* layer. It is made by chalk and animal glue applied by increasingly finer layers. On the last layer, called priming, is applied the *preparatory drawing*. Sometimes the priming is colourful for aesthetic function.

The underdrawing is made using a black pigment applied by brush or stick.

On the priming is applied the paint layer, composed by pigments and binders.

Inorganic pigments are fine coloured powders in suspension into the binder. In ancient times this substances were obtained by milling coloured earths (for instance, ochre) or minerals (lapis lazuli, malachite). The level of milling established the final effect.

Also organic dyes were used, precipitated on inert materials and soluble into the binder. They are extracted from plants (saffron) or animals (murex). These have a weak opacity and were used on the paint for lighting effects.

After the Industrial Revolution, namely at the beginning of XIX century, synthetic pigments invaded the art market. They are often organic compounds, while many were made to substitute expensive natural products by industrial formulates.

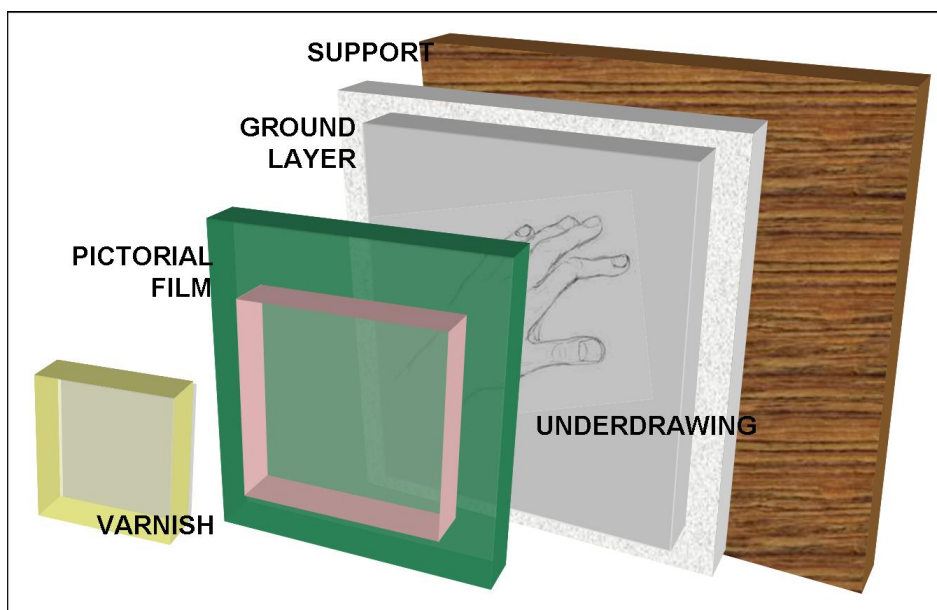


Fig. 1.1. Structure of a painting.

The binder or *medium* imparts adhesion and cohesion to pigments, and strongly influences many optical properties, such as transparency and gloss, and physical properties such as durability, flexibility. Moreover, it should be able to dry in a short time.

Clearly, the choice of medium is heavily limited by these requirements and by the technologic limits of the time.

The choice of the binder establishes the pictorial techniques: *tempera* is based on animal glue as a binder, *oil* is usually linseed oil and *mixed technique* means coexistence of different products.

The tempera technique was used in paintings of Middle Ages and Renaissance. The medium used, generally, was egg yolk diluted in water.

Since XV century the tempera was replaced by drying oils. In the time of transition the pictorial technique is called mixed, because the oil was mixed with yolk egg, milk or casein. After this transition time, oils were used alone. Drying oils were extracted by plants as: linseed, poppy-seed, nut.

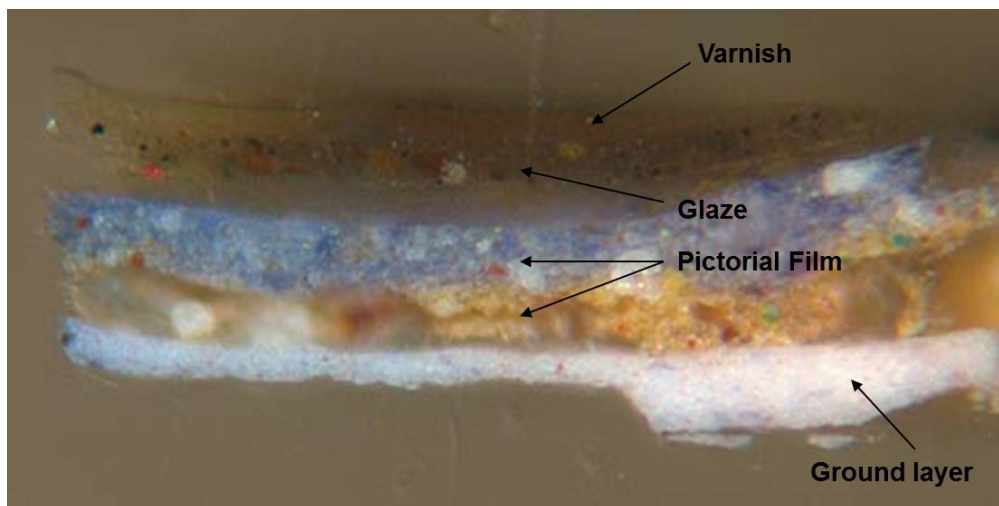


Fig. 1.2. Cross section of a painting. Unknown Italian artists, 'Portrait Group', repainted in early 20th century, oil and tempera on wood. From the National Gallery of London website [12].

In the Contemporary Art ready-to-use commercial colours are employed, composed by a pigment and synthetic binders like acrylic, vinyl, alkyd, resins. These compounds have a high opacity. Therefore, the paint layers are thinner than in oil painting.

The final layer is the *varnish*, applied on the painting layer to protect the surface and increase the gloss effect. The substances employed are natural resin like arabic gum, copal, dammar.

However, in Contemporary Art there are no more rules. The artwork is the free expression of the artist and, often, this description is not applicable.

### 1.3 Interaction between electromagnetic radiation and pictorial layers

The observation of a painting in visible light from 380 up to 760 nm implies different phenomena: specular reflection, refraction, absorption, scattering.

*Specular reflection* happens on the surface and depends on its smoothness and glossiness. In paintings, incident light is partly reflected on the smooth and glossy varnish, and part penetrates in the pictorial layer. It is refracted by binder, scattered and absorbed by pigment.

*Selective absorption*, of part of the spectrum of incident light, is responsible for the feeling of colours, on the contrary, the non-absorbed part is scattered by interaction with particles of pigment.

*Scattering* of light by a pictorial layer depends by particles dimension and concentration in binder.

Due to opacity of pictorial layer, part of the light can reach the background, partly be absorbed and scattered again.

The painting may assume particular tonality through the selective absorption of preparatory layer; especially when under the layer there is a coloured pigment. This is the cases of coloured preparation: like the use of green pigment under the faces in the paintings of XIV century, or the use of red pigment under the blue of mantle of Virgin Mary to intensify its chromatic tone.

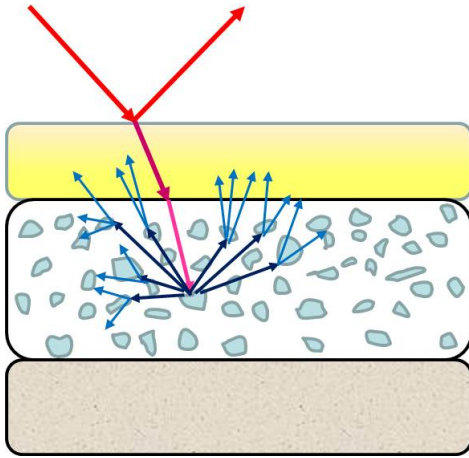


Fig. 1.3. Interaction between visible radiation and pictorial layer.

Scattering decreases with increasing wavelength.

Infrared, is less scattered than visible. The long wavelength allows to IR radiation to be less scattered and offers better transmission through inhomogeneous medium.

The lower backscatter of infrared radiation relative to visible makes possible to investigate the underdrawing in paintings.

IR penetrates the paint layer, where it is scattered by the pigment, like for visible light. But, differently by the visible, part of this can pass through the pictorial layer, where it is reflected back by the white priming and absorbed by black line of drawing.

The near-infrared (NIR) is comprised from  $0,75\ \mu\text{m}$  up to  $3\ \mu\text{m}$ . It may be also absorbed by materials, producing electronic transitions in some substances.

While molecular vibrations and rotations, characteristic of many atomic binding, by middle-infrared (MIR  $3\text{-}25\ \mu\text{m}$ ) and far-infrared (FIR  $25\text{-}150\ \mu\text{m}$ ) radiation are induced. Several spectroscopic techniques use MIR and FIR to investigate the chemical composition: FTIR and Raman spectroscopy.

Moreover, radiation emitted by room temperature bodies, due to thermal agitation, falls in the MIR region. The strong temperature dependence of the thermal radiation makes possible the thermal imaging of bodies

Due to its shorter wavelength, UV radiation is more scattered by surface layer, so it is not penetrating more than the varnish layer.

The greater energy of the UV radiation takes to evidence fluorescence phenomenon.

When a molecular electron absorbs energy from ultraviolet radiation shifts on the outermost orbital, but this “excited” state is unstable and the molecule returns to its steady state, emitting radiation at lower energy, that is, greater wavelength.

Therefore, this fluorescence can be observed in visible light.

In the electromagnetic spectrum, the X-ray band at even higher energies: 1 to 500 keV

In X-ray interaction with matter three processes can occur, depending on X-ray energy and the atomic number of the target: photoelectric effect, Compton scattering and pair production.

Photoelectric is the absorption of a photon by the atom. It may happen only when the energy of the photon is enough to eject an electron from its orbit.

In Compton scattering, the incident photon transfers part of its energy to the electron collided. The scattered photon has lower energy than the incident photon and thus a higher wavelength.

Pair production happens when the photon annihilates creating an electron-positron pair.

This effect has threshold energy of 1,022 MeV, for energy to mass conversion.

At the low energies (1-100 KeV), used in applications to paintings, photoelectric effect dominates.

X-rays transmission through a target of thickness  $x$  is expressed by

$$I = I_0 e^{-\mu x}$$

where  $I$  is the number of photons emerging from the target,  $I_0$  the number of photons impinging on the target and  $\mu$  is the total linear attenuation coefficient.

The linear attenuation coefficient  $\mu$ , which includes the attenuation of beam by any effect, is depending by the atomic number of elements and the energy of X-ray.



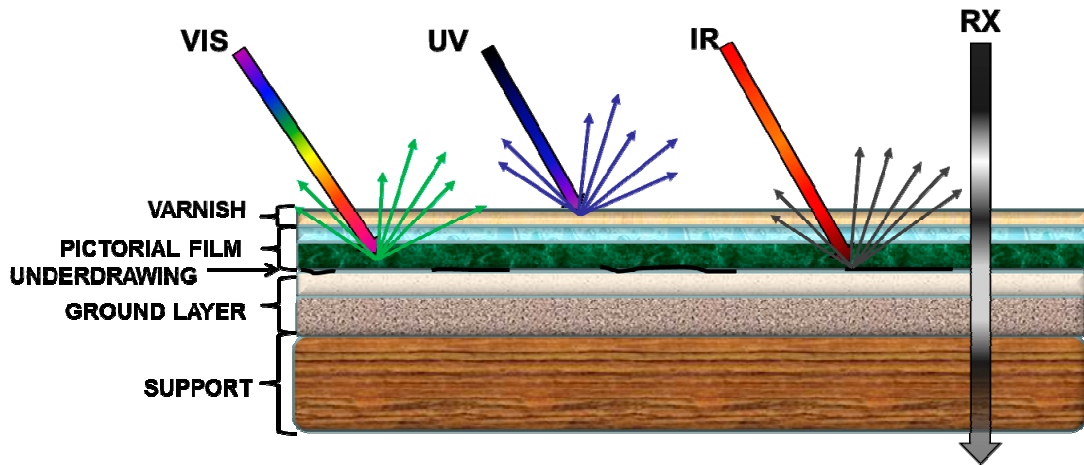


Fig. 1.4. Interaction between different electromagnetic radiations and painting layers.

X-rays, as UV radiation, induce fluorescence in the materials.

The X incident radiation of sufficient energy dislodges an inner electron by photoelectric effect, the atom becomes an ion and an outer electron replaces the vacancy of electron. When this happens, energy is released as emitted radiation with lower energy than the primary incident X-rays and is termed fluorescent radiation. Since the energy of the emitted photon is characteristic of a transition between two electron orbitals in a particular element, the resulting fluorescent X-rays are characteristic of the atom and can be used to recognize a spectrum of elements present in the sample.

Physical diagnostics techniques in Cultural Heritage use different bands of the electromagnetic spectrum to obtain information on artwork structure and on the nature of the materials.

In table 1.1 image and spectroscopic techniques are shown.

E.M. RADIATION	RANGE $\lambda$	IMAGE DIAGNOSTICS TECHNIQUE	SPECTROSCOPIC TECHNIQUE
IR	0,7 - 2,5 $\mu\text{m}$	IR Reflectography	UV-VIS-NIR Reflectance spectroscopy
	3-15 $\mu\text{m}$	IR Thermography	Furier transform infrared spectroscopy (FTIR) Raman spectroscopy
VIS	380-760 nm	Raking light, Specular reflected light Trans-irradiation Image spectroscopy	Diffuse reflectance spectroscopy
UV	250-400nm	UV fluorescence	UV-VIS-NIR Reflectance spectroscopy
RX	1-100 KeV	X-ray radiography	X-ray fluorescence (XRF)

Tab.1.1 summary of non-invasive imaging and spectroscopic techniques

Common to all the techniques mentioned is the non-invasiveness, important aspects in the study of Cultural Heritage.

The sample involves damage, microscopic, but still a defect on objects characterized by uniqueness, therefore, it must be minimized.

Sampling in artworks is becoming a practices less supported by museums and institutions, thus favoring non-invasive techniques.

## 1.4 A protocol for image diagnostics of paintings

The image diagnostics of an artwork includes several techniques. The first advantage of this important resource is its absolute non-invasiveness. Second, its feature gets information from large areas, or totality, of the painting.

The definition of a diagnostics protocol is important to standardize the study of paintings but, at the same time, each painting is a peculiar case, and the protocol must be adapted to the required information and possibly revised according to the results of each step.

The first step is visual observation. It is possible to see the consistence of the pictorial layer, the state conservation of surfaces and of the support.

In temporary exhibitions the *condition report* of artworks is requested at the opening of packaging for insurance purposes. Due to the amount of artworks to be examined in a limited time, this operation is often based only on visual observation [6].

In this case the condition report of a painting contains:

- A brief description of artwork – types of support, pictorial techniques as declared by the artist or the provider.
- A brief characterization of pictorial technique, the form of brushstrokes: thin or thick, uniform or patchy, flat or projecting.
- The state conservation of surfaces. It is important to remark the presence of *craquelures*, that may change during the exhibition. Obviously it is mandatory to signal the presence of accidental damages: scratches, abrasions, stains, spots, halos etc...

This descriptive part is usually accompanied with a sketch or photo of the artwork with a map of damages, each of them, must be documented by photos.

In figure 1.5 are shown some photos of a condition report, made during the installation of Italia Pavilion about 54th International Art Exhibition of Venice Biennale.

The condition report assumes a different meaning when it is done before a restoration; the process is longer and careful, though often it is based too on visual observation.

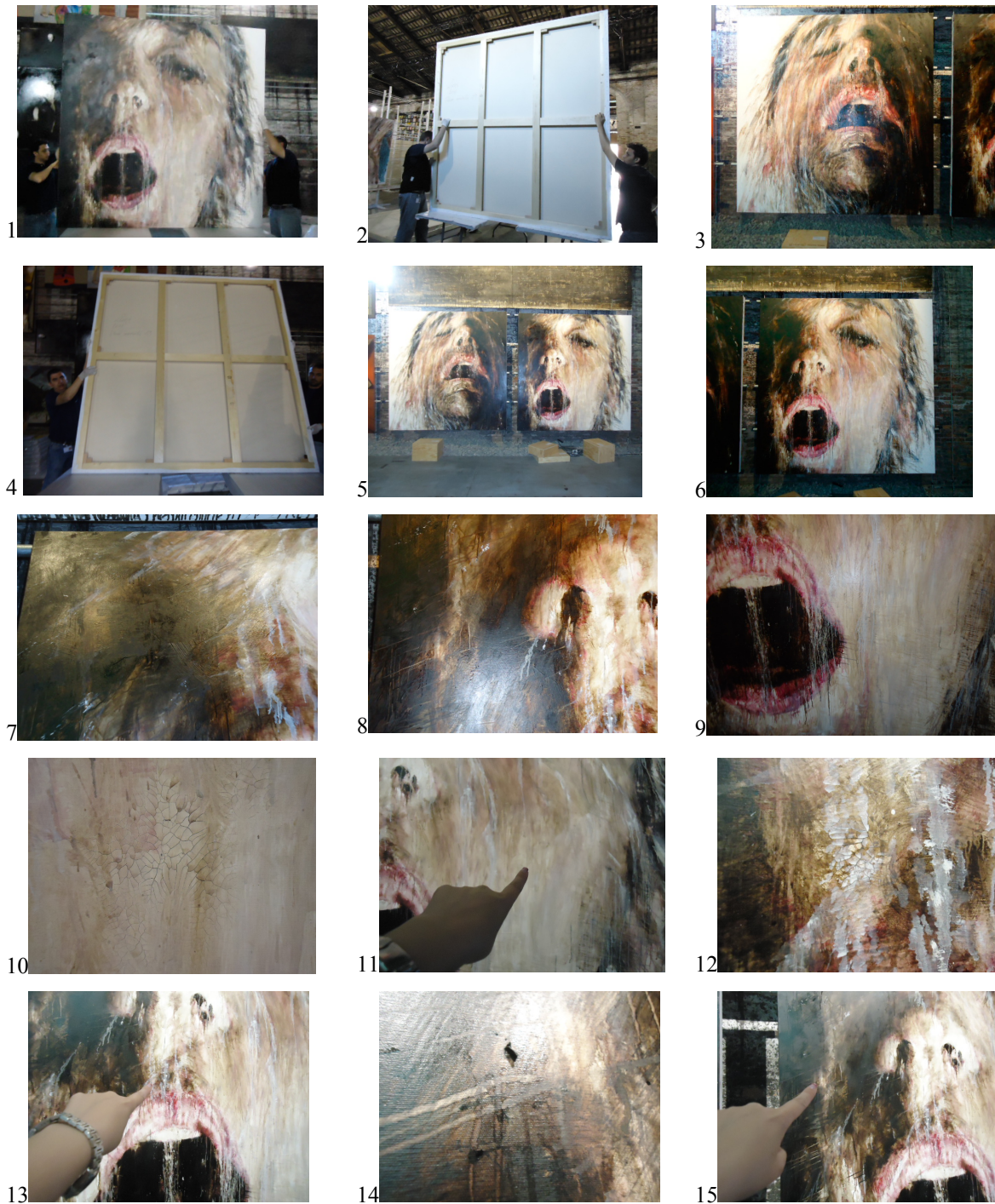


Fig. 1.5. F. Leone, *Flussi Immobili*, mixed technique on canvas, 2011. Some photos from the Condition Report. Courtesy of 54th International Art Exhibition of Venice Biennale. 1)-2)-3)-4) Recto and verso photos of the paintings during the opening of the packaging 5) Paintings hang to the wall. 6)-7)-8)-9) close-up photos. 10)-11)-12)-13) Detail of craquelures and indication of position on the surface. 14)-15) detail of projecting elements and indication of position on the surface.

A good photographic documentation of *recto* and *verso*, under uniform illumination must be done including color and grayscale target to evaluate exposure and reproduction fidelity.

Details must be documented by close-up photo.



Fig. 1.6. G. De Chirico, *Ettore e Andromaca*, 1958, oil on canvas, Casa Museo Remo Brindisi, Comacchio. Photographic documentation: a) recto, b) verso, c) detail in raking light, d) detail in transillumination.

For the case of application, inspection by Raking light is first technique of image diagnostics to investigate the pictorial surface.

Raking light is particularly effective in revealing the morphology of *impasto*, showing the marks made by brush or palette knife. It highlights distinctive aspects of a structure like a presence of a seams or joins in the support, incisions or irregularities in the ground or changes in the texture of the paint layer that do not correspond to the visible design.

A useful support to this technique can be the trans-illumination applied to painting on canvas. The light is transmitted through the object to investigate the presence of holes, tears or *craquelures* (Fig. 1.6.).

On the other hand, when the surface is particularly glossy, a single image in specularly reflected light allows a complete mapping (Fig. 1.7)



Fig. 1.7. E. Pazzini, *San Leo*, 1950's, oil on cardboard, private collection. a) Image a visible light, b) image of specularly reflected, corrected and straightened.

By observing and acquiring images under other types of radiation is possible to identify aspects otherwise invisible at human eye.

Illumination of paintings with ultraviolet light can induce some materials to exhibit fluorescence, possibly characteristic of that material.

Many aspects may be investigated in a qualitative fashion:

- Different types of varnish. An aged natural resin varnish, for example, shows often a greenish fluorescence.
- Areas of retouching. Recent brushstrokes of colors on top of the varnish usually do not show fluorescence. Therefore they appear darker under UV radiation. Recognizing them is important before any sampling operations because in retouching areas the material will be different than in original areas.
- Information on pigments. Sometimes it is possible to recognize the characteristic fluorescence of pigments or discriminate pigments that appear similar under visible light.

In figure 1.8 the comparison of visible and fluorescence image allows to see that the artist used two different green pigments for the leaves. Moreover, the pink of some petals was not obtained by a mixture of the same red and white pigments used for the other flowers.



Fig. 1.8. G. Nardozi, *Flowers*, 1889, tempera on paper, private collection. a) Image in visible light, b) image in UV fluorescence.

The imaging techniques allow us to obtain total images, useful to identify points of measurement in which spectroscopic techniques can be applied.

The information obtained by Image Diagnostics can be specialized using non-invasive local analysis like spectrophotometry and X-ray fluorescence (XRF), the definition of measurement points becoming easy using the image of UV fluorescence as a map.

XRF analysis is useful for the qualitative detection of atomic composition of materials.

A pigment is recognized by the detection of a high-atomic number element.

The XRF technique is useful to reveal pigment anachronism. For example, the titanium white enter in use after 1916, ancient paintings cannot contain this pigment, but may be plausible in retouching areas [6].

A limit of XRF application in the painting study is the impossibility to know in which layers the fluorescence radiation come from.

UV-VIS-NIR reflectance spectroscopy is a technique common to different bands of the electromagnetic spectrum.

It provides useful data the analysis of color and its variation on paintings. Although several variables may affect the reflectance spectrum acquired from a painting, Reflectance spectroscopy measurements provide, in most cases, information that permits recognition of the spectral features of pigments. This is possible using a spectrophotometer or optical fiber in contact on the painted surface.

Image spectroscopy can be considered both an imaging technique and a spectroscopic technique.

Because through image acquiring at different wavelength in visible range is possible to extract reflectance spectra in localized areas.

The advantage of this technique is the possibility to obtain reflectance spectra without contact with painting, which is not possible using a spectrophotometer. Therefore, in critical cases of surface deterioration or particularly protruding paintings, imaging spectroscopy is preferable.



UV radiation is useful to investigate the first layer of paintings, instead, the IR radiation is useful to investigate the slightly deeper layers.



Fig. 1.9. *Virgin and Child*, XIV century, tempera on wood, Church of Noale, Treviso. Courtesy of Soprintendenza del Veneto a) Image at visible light, b) IR reflectogram acquired by traditional device.

The IR reflectography is employed, in particular, to study underdrawings, the artist's preliminary sketch made before the application of paint layers. IR is also useful in revealing *pentimenti* and areas of damage and retouching.

In diagnostic protocol, paintings are always investigated by traditional device for IR Reflectography to check the effective presence of underdrawing.

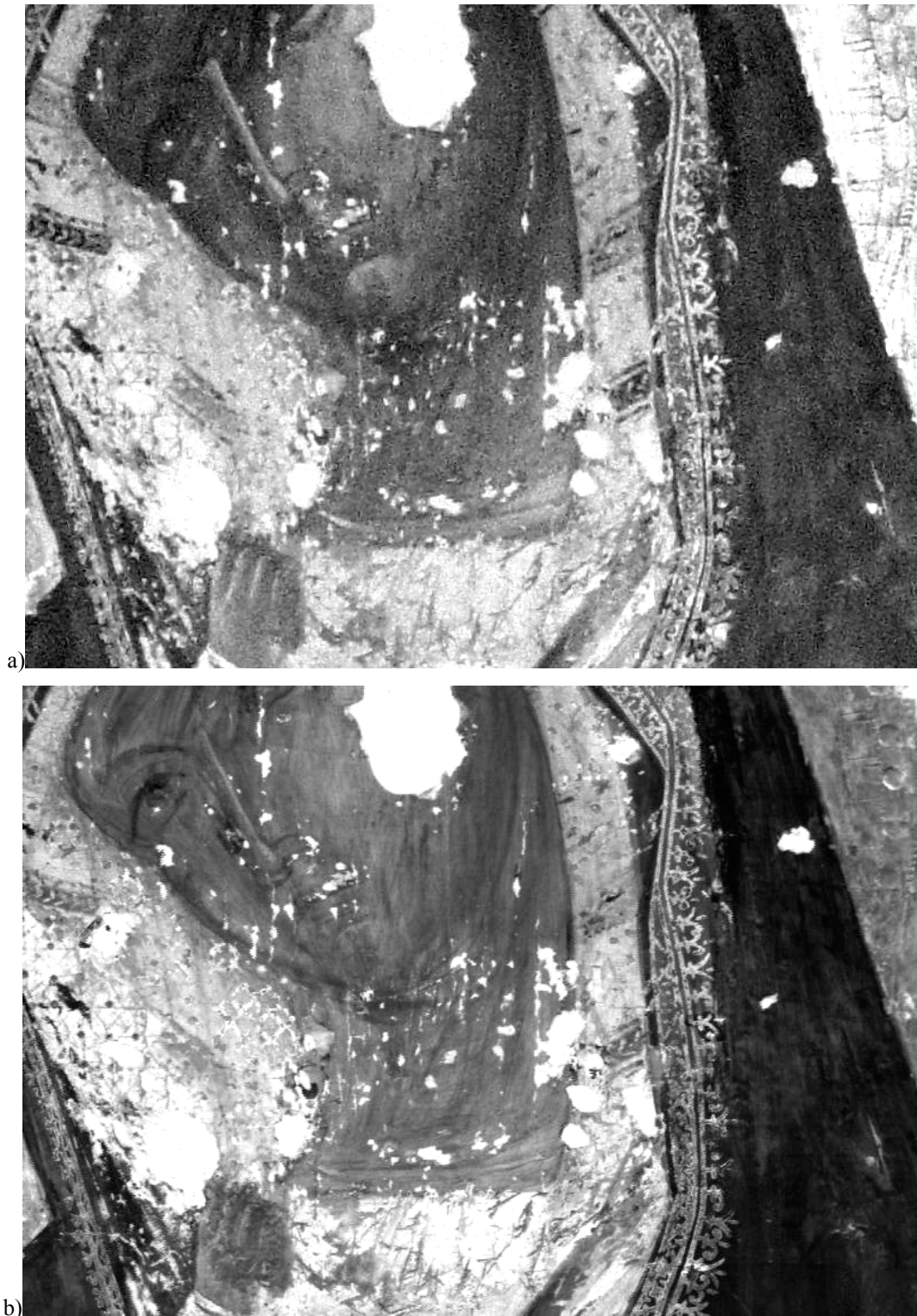


Fig. 1.10. *Virgin and Child*, XIV century, tempera on wood, Church of Noale, Treviso. Courtesy of Soprintendenza del Veneto. a) Detail of IR reflectogram acquired by traditional device, b) detail of wide band IR reflectogram.

Since the diffusion of commercial cameras based on Silicon detectors, the most common reflectography device is sensitive in the spectral range about 800 (depending on the optical filter used) up to 1100 nm. This spectral sensitivity is useful for most purposes.

But it is not always possible to see clearly all the line of the sketch under the pictorial film. The extension of spectral response to longer wavelength is possible using other semiconductor devices.

Moreover, comparing images at different wavelength in IR band can be a tool to gather additional information on the materials and to enhance the application of spectral analysis obtained with spectrophotometer and XRF.

The diagnostic study shown in figures 1.9. and 1.10. was made on a medieval painting during a recent restoration. It was subjected to several remaking over the centuries, aimed to recover the original features.

A comparison between two reflectograms acquired by traditional device and by wide band IR reflectography is given in figure 1.10.

The higher contrast of image b) improves the detection of details in Virgin Mary's face.

Among image diagnostics techniques, X-ray radiography can provide a wealth of information not obtainable with other techniques, for its capability to cross all layers of a painting.

In the radiography, paintings materials appear dark or light, according to their atomic constitution, density and thickness.

More absorptive materials, such a lead-containing pigments or the iron tacks used to pin canvas to stretcher, block the penetration of X-rays, and appear white on the radiography, when it is developed.

Due to the possibility of knowing the conservation status of pictorial film and preparation layer and, in particular, the morphology of support, the radiography becomes the favorite technique to investigate paintings on wood.



Fig. 1.10. *Virgin and Child*, XIV century. X-ray digital radiography acquired by the scanning device in Physics Department, Ferrara .

The X-ray radiography is somehow a complementary technique to IR reflectography. The high energy of radiation does not allow detection of an underdrawing, made with carbon-based material, but it can be particular useful to investigate pictorial *pentimenti* and hidden paintings.

The figure 1.10 shows X-ray radiography of the previous painting. The picture highlights the conservation status of the support and allows to recognize the original wiggly trait of the Virgin's figure.

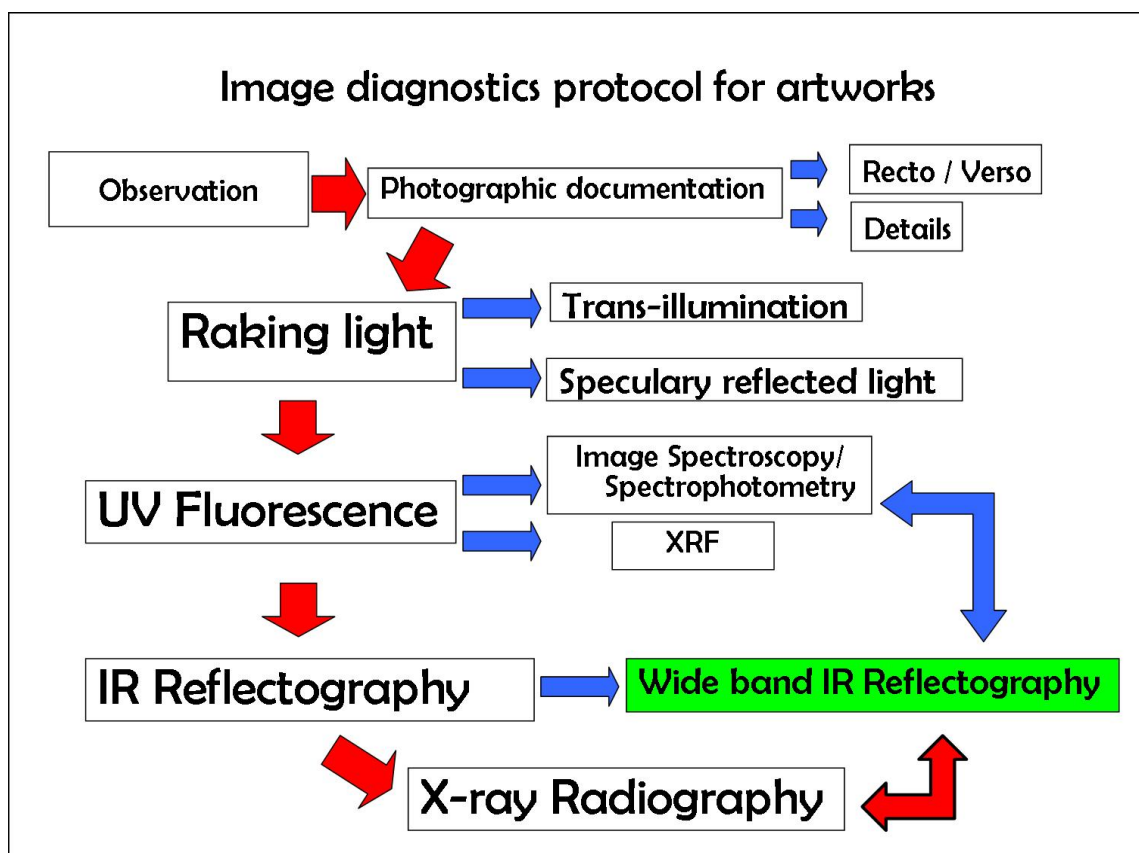


Fig. 1.11. Summary graph of image diagnostics protocol for artworks

The purpose of a diagnostic imaging protocol is to obtain knowledge on the state of conservation and materials of the artwork, considering the unique and specific needs that each artwork requires.

However, the conservation of artworks proceeds in two different but interconnected directions. On one side, laboratory tests to know the material properties. On the other side, monitoring to assess the risk in situ [11].

It has already been mentioned how important is the non-invasiveness in the field of works of art. In line with the rule of minimum intervention, preventive conservation is privileged over any other type of action on the artworks.

“Preserving” means to create around an artwork a suitable environment [12].

The control of microclimate parameters of the "container" where the artwork is exhibited - museum, galleries, churches, or showcases and storage boxes - allows to anticipate several problems, and a good management of the environment can be a tool to avoid restoration interventions.

## References

1. A. Frova, *luce colore visione*, Editori Riuniti, Roma 1984.
2. R. A. Serway, J. W. Jewett, *Principi di Fisica*, vol.1, II Edition, Edises, 1996, Napoli.
3. M. E. Wieseman, *A closer look: deceptions and discoveries*, National Gallery Company, distributed by Yale University Press, London, 2010.
4. C. Cucci, M. Picollo, M. Vervat, *Trans-illumination and trans-irradiation with digital cameras: Potentials and limits of two imaging techniques used for the diagnostic investigation of paintings*, Journal of Cultural Heritage, February 2011.
5. A. Aldrovandi, M. Picollo, *Metodi di documentazione e indagini non invasive sui dipinti*, Collana i Talenti, Il Prato, Padova, 2001.
6. M. Fratelli, *Beni Mobili: la movimentazione delle opere d'arte. Riflessioni, esperienze e progetti della Galleria d'Arte Moderna di Milano*, Collana i Talenti, Il Prato, Padova, 2001.
7. M. Matteini, A. Moles, *Scienza e restauro*, Nardini, 1985, Firenze
8. *Fotografia all'infrarosso, all'ultravioletto e della fluorescenza*, Pubblicazioni Kodak, 1973
9. A. Gilardoni, R. Ascani Orsini, *X-rays in art*, Mandello Lari, 1977, Como
10. F. Albertin, *K-edge radiography and applications to Cultural Heritage*, Ph.D. thesis, Università degli Studi di Ferrara, 2011.
11. D. Camuffo, R.H. Van Grieken, H. Busse, G. Sturaro, A. Valentino, A. Bernardi, N. Blades, D. Shooter, K. Gysels, F. Deutsc, M. Wieser, O. Kim, U. Ulrych, *Environmental monitoring in four European museum*, Atmospheric Environment, Volume 35, Supplement 1, , Pages S127-S140, 2001
12. A. Bernardi, *Conservare opera d'arte. Il microclima negli ambienti museali*, Il Prato, Padova, 2004.
13. <http://www.nationalgallery.org.u>

---

## CHAPTER 2

# WIDE BAND INFRARED REFLECTOGRAPHY

---





## 2.1 Results and improvements of IR Imaging of paintings

**I**R reflectography is a non-invasive image diagnostics technique to investigate paintings and other artworks.

IR radiation penetrates layers of pigments and surface alteration products, but are reflected back by slightly deeper layers; IR reflectography can therefore “see” below the surface and is particularly useful for discover the preparatory drawing of a painting.

The underdrawing is a guideline for the artist to make the subject of painting. It can be only sketched or very fine, rich of details and hatching of shadows, sometimes even using chiaroscuro. So the underdrawing becomes an artwork itself, evidence of the artist's creative process, destined to remain hidden forever, but, in some cases, made visible by this technique.

The study of underdrawings is of great interest for art historians because it reveals the author's hand in a direct way.

Other important information may be obtained by IR reflectography like “*pentimenti*”, inscriptions, or signatures. Sometimes it is possible to detect other paintings under the pictorial layer. In paintings since XIX century is frequent to find reused canvases previously painted.

In these cases, fundamental is the support of X-ray radiography, which can reveal details hidden in deeper layers of the painting. Conversely, IR can detect thin strokes of charcoal on the priming, which ignored by X-ray crossing.

In this way, IR reflectography and X-ray radiography can get complementary information.

The reflectographic technique got its best results on tempera paintings of XV century, with white gypsum preparation, black charcoal drawing and thin pictorial layers.

Since late sixteenth century, the artistic technique evolved to dark preparations and thicker paint layers. IR penetration is severely limited and reflectography becomes almost useless.

Extension of the spectral band to longer wavelengths is a valuable tool to improve reflectographic capability.

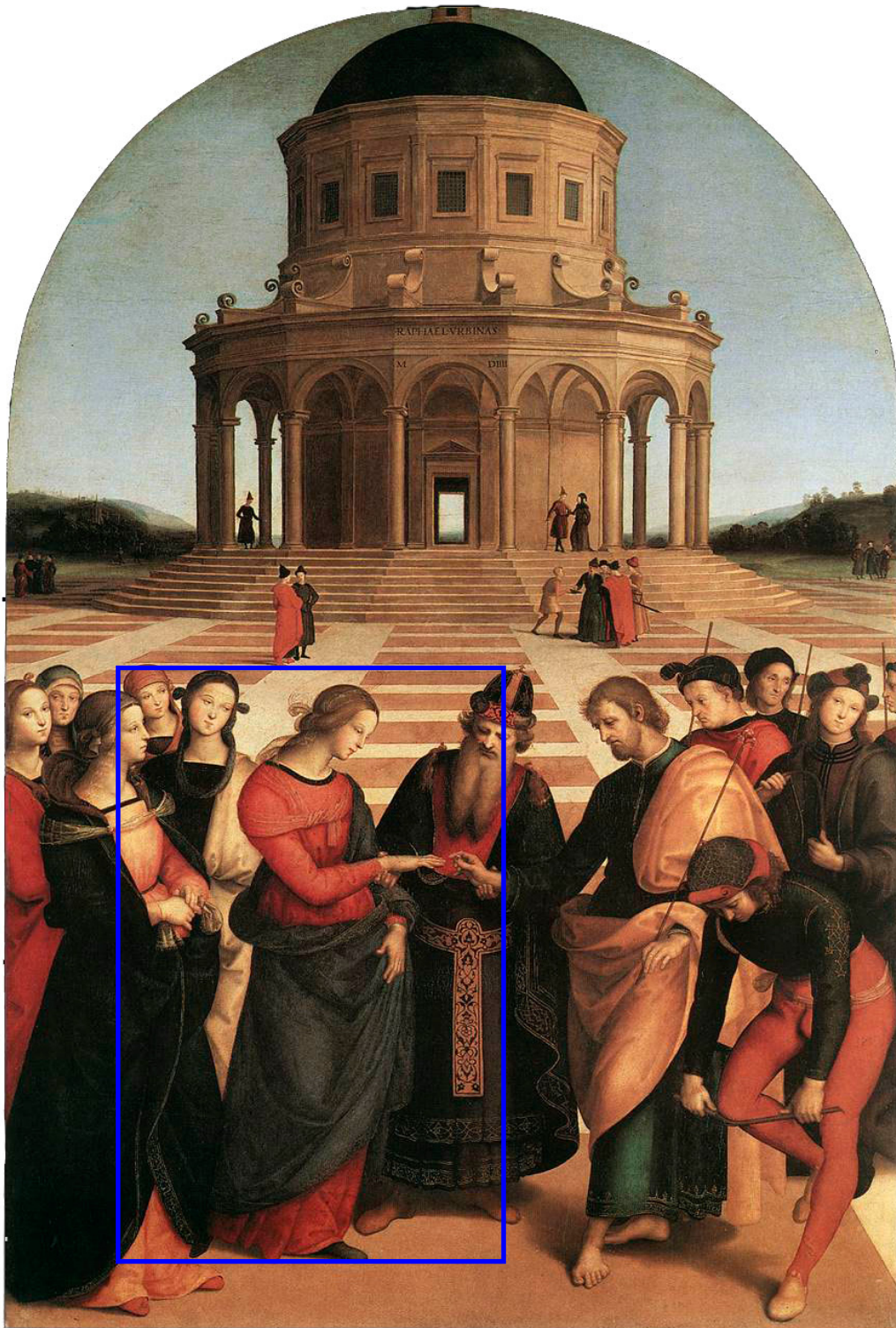


Fig. 2.1. Raffaello Sanzio, *“Marriage of the Virgin”*, 1504, oil on wood, 170 x 1,17  
Pinacoteca di Brera, Milan.



Fig. 2.2. Raffaello Sanzio, "*Marriage of the Virgin*", detail in visible light.



Fig. 2.3. Raffaello Sanzio, “*Marriage of the Virgin*”, detail of IR reflectography acquired by scanning device [1]

## 2.2 Traditional devices for IR Imaging

Several imaging systems have been used, over time, to make infrared images visible.

H. W. Vogel in the 1873 discover some dyes that, activating silver halide emulsion, could extend the spectral response of traditional photographic emulsions, but only in 1930 years the infrared photography was applied for the first time to cultural heritage.[4]

One of the first images in IR is of a papyrus, the *Liber Linteus Zagabriensis*, made in ivory black and cinnabar on linen. It is the longest Etruscan text existing.

Infrared allowed to reveal many details hidden to visible light. The photo was taken in 1935 by I. Plotnikov [14].



Fig. 2.4. IR photography of *Liber Linteus*, by Plotnikov, 1935.

Most commercial black and white infrared films had a spectral response from 700 nm up to 900 nm with a maximum approximately at 850 nm. For special emulsions the farthest spectral response was 1200 nm.

The first electronic system used to acquire infrared images was a thermographic camera (Barnes IR camera) modified for NIR with a PbS detector. This device was used by Van Asperen de Boer since 1964 [2].

In 1970 a Vidicon tube with a spectral response up to 2,2  $\mu\text{m}$  was marketed by Hamamatsu: the M214. These devices remained for at least 20 years the only choice for IR Reflectography.

The spectral response of Vidicon tube allowed a good detection of underdrawing, but it had low imaging performance.

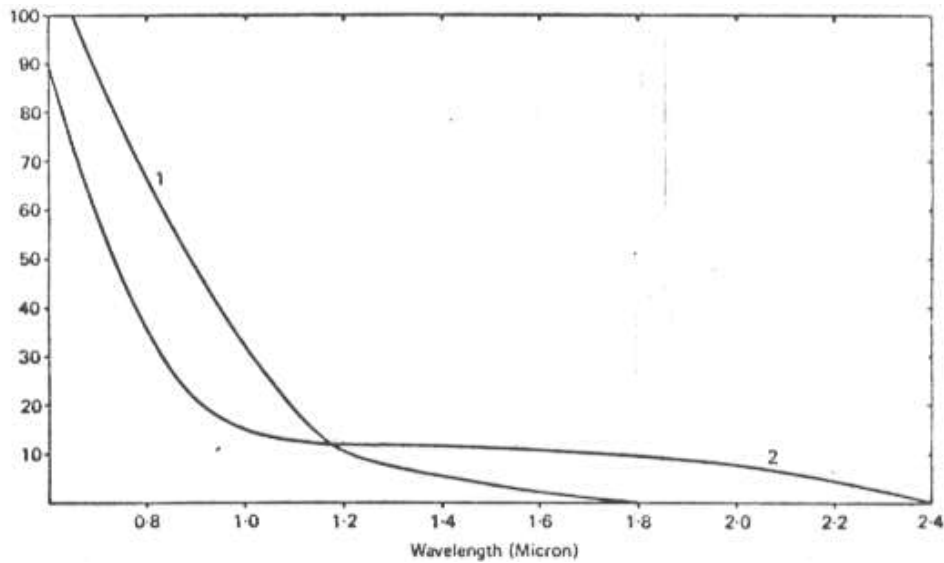


Fig. 2.5. (1) Curve of spectral sensitivity of Vidicon used by Van. Asperen De Boer (2) Curve of spectral sensitivity of Hamamatsu Vidicon [3].

The Vidicon tube had several drawbacks: low resolution, narrow range of grayscale and geometric aberrations that limited the quality of the image. Moreover: the high cost.

Therefore, during the 90's years, Vidicon tube was replaced by Silicon CCD infrared cameras with a spectral response limited at 1100 nm.

Images obtained by both devices needed to be printed; to get a reflectogram, with good resolution, of a whole painting the acquisition of several images was necessary.

For an accurate reading of the result, all images had to be printed and assembled in a mosaic.

In the 90's the spread of PC and computer graphics has facilitated these operations. Nowadays the stitching of images, the correction for uneven lighting and distortion is made by software.

In 1991, the first professional digital camera system (DCS) was released by Kodak.

The consumer digital cameras were developed to acquire digital photo in visible light.

The detector was a Silicon CCD equipped by a filter cutting IR. Removing that filter and replacing it with a visible light cutting, the camera could be adapted for IR reflectography.

In 2000, a digital camera provided of “NightShot” mode, for night view, was marketed by Sony: DSC-F717. It was the first camera line that allows to acquiring digital photos in both bands: NIR and visible light by a simple mechanical operation.

Nowadays, consumer digital cameras are affordable, transportable and have high spatial resolution. For these reasons, they are widely used in IR reflectography; but the detector is again a Silicon CCD with its limits of spectral response.

### 2.3 Advantages of scanning system

The need to obtain high-resolution aberration-free, IR images has lead to development of IR scanning devices.

In 1990, at National Institute of Optics in Florence, the first prototype of reflectographic scanning device became available. This consisted in a single indium gallium arsenic (InGaAs) semiconductor photodiode, which moved across the surface using motor-driven axis. A computer controlled the movement and acquired the data.

This system leaded several improvements to the reflectographic techniques. The advantage of a single photodiode advantage was the possibility to obtain a single image of extended area of the painting, and the simultaneous movement of the lighting system allowed a uniform brightness. The spatial resolution of 4 pixel/mm and high range grayscale (4096) allowed high quality images.

Another innovation of this device was the use of an InGaAs detector, characterized by low dark-noise high sensitivity and spectral response extended up to 1,7  $\mu\text{m}$ .

In this range of wavelength is possible to reveal several details of underdrawing not available with traditional CCD cameras.

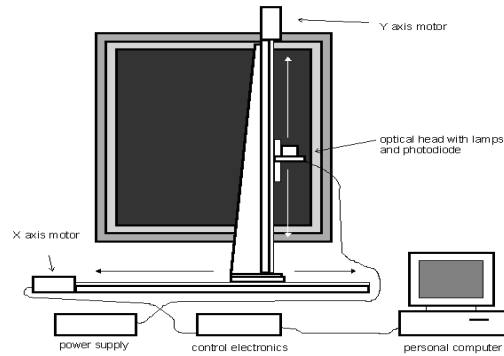


Fig. 2.6. Image and components scheme of reflectographic scanner system of INO, Florence. [14]

In the 2002 the scanning device was improved with a new optical system that allows the acquisition, in the same time, of two images, of same dimension, in the visible and IR band.

This is possible with the improvement of three fiber optics and three photomultipliers to obtain a RGB image. The two images can be perfectly superimposed, this make easier readability of the results obtained and the possibility to get a IR false-color image.

However, this apparatus was transportable, but complex mechanical setup and high weight prevented its use for a systematic inspection of paintings.

In 2004, at IFAC-CNR of Florence, the VIS - NIR iperspectral scanning device for high resolution image spectroscopy was developed.

Meanwhile, on the scanner device of INO-CNR further improvements were made and, in 2007, it became a hyper-spectral scanner in IR band up to  $2,2 \mu\text{m}$ .

In recent years, the scanner devices have got applications in several companies working in the field of diagnostics applied to cultural heritage and are required in the museums for extended measurement campaigns.



In 2009 the National Gallery of London was developed the Osiris camera.

It is a hybrid system, the detector is an InGaAs array (spectral band of 0,9 -1,7  $\mu\text{m}$ ), mounted on a scan system inside that allow to record images of much larger areas in one exposure.

In 2003, in Ferrara, has been started the project to develop a scanning device for wide band range IR reflectography, object of this work.

In this work, the development and applications of a new scanning prototype for wide band range IR reflectography with spectral response up to 2,5  $\mu\text{m}$  will be described.

## 2.4. Theory of IR reflectography

IR reflectography takes advantage of the property of NIR radiation to be less scattered by pictorial layers than shorter wavelengths and consequently to reach the deepest layers, hidden by superimposed colours.

This happens when scattering, in the main optical phenomena, prevents the propagation of light in the inhomogeneous mixture of pigment grains and organic medium.

If, on the contrary, a pigment is itself absorbing infrared, no advantage is obtained by infrared imaging.

The phenomena governing the propagation of NIR radiation into pigment layers are known. But the composition of these layers is irregular and inhomogeneous. So, any calculations based on ideal conditions, like propagation homogeneous in medium or scattering and absorption of incident radiation is approximate and rarely useful for practical applications.

Anyway, general features of the propagation of light in pictorial layers may be derived by an analytical theory based on a simplified model.

The theory of IR Reflectography as propagation of light in a scattering and absorbing medium was first treated by J. R. J. Van Asperen De Boer in the 70's years. He can be considered the founder of IR Reflectography applied to paintings.

De Boer used the Kubelka-Munk theory, developed in 40's, to explain the optical properties of pictorial layers under NIR radiation.

## 2.5. Kubelka-Munk diffusion theory

The Kubelka-Munk theory uses a simplified model of two diffuse light fluxes passing an elementary layer of infinitesimal thickness  $dx$ , one  $i$  proceeding from the top to the bottom of the paint film, the other  $j$  simultaneously upward.

$K$  and  $S$  are the fraction in both fluxes lost by absorption and scattering in the elementary layer. They are called the absorption and scattering coefficient of the paint layer.

The upward flux is reduced by absorption  $Kjdx$  and scattering  $Kjdx$ , but the amount of  $Sidx$  scattered from the downward flux is added

Therefore the upward  $dj$  flux is than

$$(1) \quad dj = -(S + K)jdx + Sidx$$

On the contrary, to the downward flux a  $Sjdx$  is added from the upward flux:

$$(2) \quad -di = (S + K)idx + Sjdx$$

$dj$  and  $di$  have different signs because the fluxes have different direction.

The two equations is the differential system of Kubelka-Munk.

$$(3) \quad \begin{cases} dj = -(S + K)jdx + Sidx \\ -di = (S + K)idx + Sjdx \end{cases}$$

In a Reflectography the reflectance is measured in each pixels of image, which is the ratio between the two fluxes.

Considering this ratio at the depth  $x$ , the reflectance can be obtained

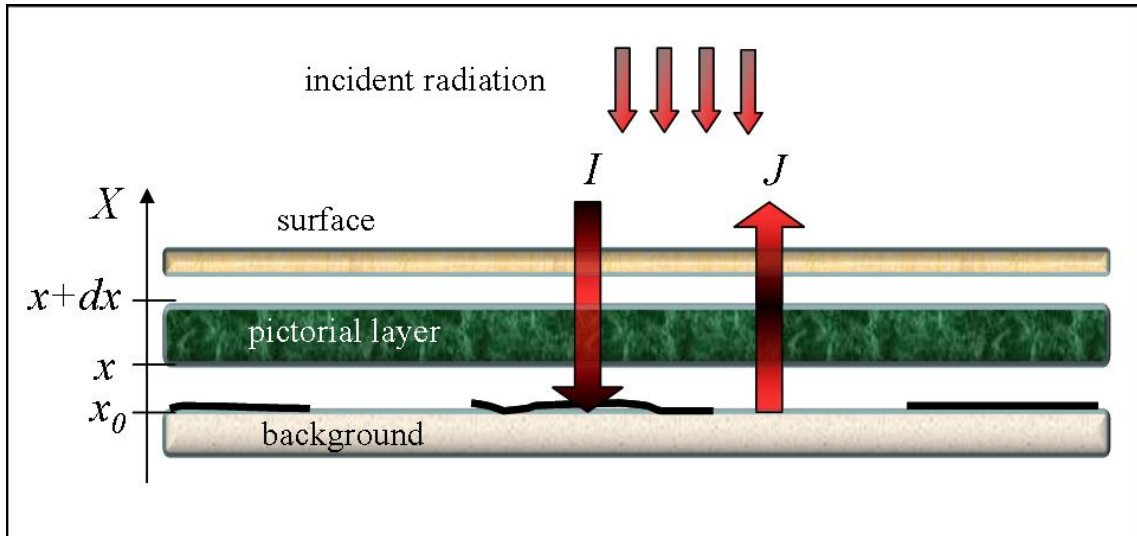


Fig. 2.7. Graphical representation of the two fluxes of Kubelka-Munk theory

The reflectance  $R_f$  of a uniform paint film of thickness  $x$  applied to a background of reflectance  $R_b$  is:

$$(4) \quad R_f = \frac{1 + R_b(a - b \coth bSX)}{a - R_b + b \coth bSX}$$

Where

$$(5) \quad a = \frac{K + S}{S}$$

$$(6) \quad b = \sqrt{a^2 - 1} = \sqrt{\frac{K^2 + 2SK}{S^2}}$$

When  $x \rightarrow \infty$  the function is independent by the reflectance of the background, then,  $R_\infty$ , the reflectance of an infinitely thick paint layer, turns out to be

$$(7) \quad R_\infty = \frac{1 + R_b(b - a)}{a + b - R_b} = \frac{K}{S} + 1 - \sqrt{\frac{K^2}{S^2} + 2\frac{K}{S}}$$

$R_\infty$  is dependent only by the K/S ratio. This relationship is named Kubelka-Munk function, and the behavior of  $R_\infty$  versus K/S is drawn in figure 2.8.

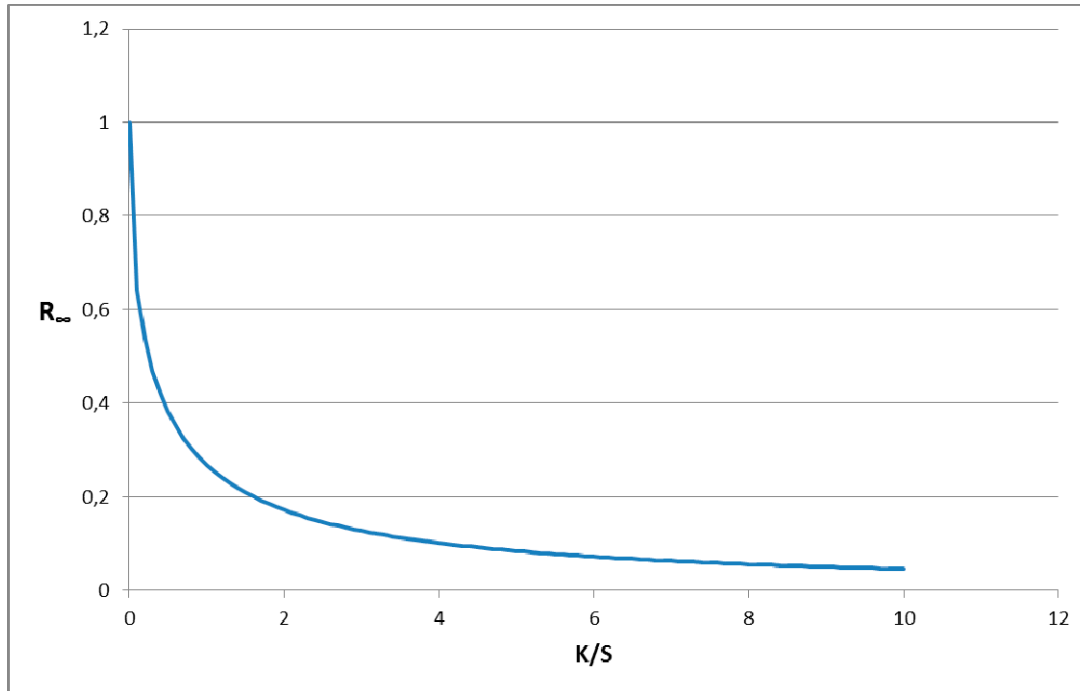


Fig. 2.8.  $R_\infty$  versus K/S

The simplified model of a painting consists of a single homogeneous layer of pigment on a background where the drawing is placed. Two different reflectances are involved,  $R_B$  and  $R_W$ , respectively the reflectance of the black line and of the white background, where  $R_B < R_W$ . Defining the contrast ratio  $k$  as:

$$(8) \quad k = \frac{R_B}{R_W}$$

It depends by the layer thickness  $X$  and it assumes values between 0 and 1. By this definition, high values of K refer to low contrast, between drawing and background.

In the figures 2.9 the trend of contrast on the variation of thickness on determinate values of  $R_W$  and  $R_B$ :

- Reflectance of white line with no layer is  $R_W(0) = 0,6$
- Reflectance of black line with no layer is  $R_B(0) = 0,1$
- So  $k = 0,17$  if no layer is superimposed

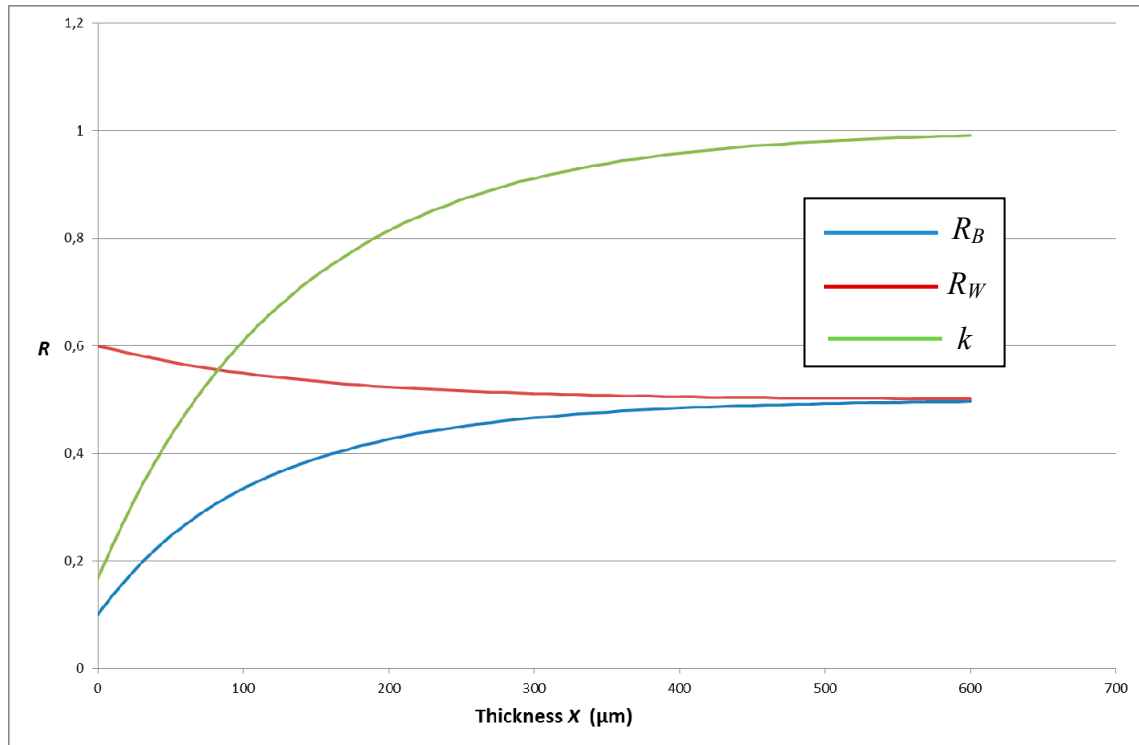


Fig. 2.9.  $k$  trend on reflectance versus thickness  $X$  for determinate values of  $R_W$  and  $R_B$ .

With the increasing of  $X$ , the reflectance values of  $R_W$  and  $R_B$  become coincident.

Here the value 1 of contrast corresponds to the same signal from two black and white points and the inability to distinguish them.

The value of contrast increases with increasing  $K$  and  $S$ . Therefore, high values of  $K$  and  $S$  inhibit reflectographic acquisition.

The detector sensitivity limits the contrast that can be made visible in the electronic image. This contrast limit,  $k_L$ , is reached when the layer thickness is  $X_0$ .

Substituting expression (4) in the definition (8):

$$(9) \quad k_L = \frac{1 + R_B(a - b \coth bSX_0)}{1 + R_W(a - b \coth bSX_0)} \cdot \frac{a - R_W + b \coth bSX_0}{a - R_B + b \coth bSX_0}$$

$X_0$  is the hiding thickness, the maximum thickness still allowing the detection of black/white lines, at the minimum detectable contrast.

The Kubelka-Munk theory is a tool to understand the phenomenon involved in the detection of a drawing under a pictorial layers. However the theory contains several simplifying approximations. First of all, it is one-dimension derivation, the whole consideration of 3D scattering being much more complex.

Besides, it take no into account the specular and internal reflectance of the paint layer and assumes that the refraction index of medium and air are the same.

The coefficient  $K$  and  $S$  have determinate values, assuming that are the same behavior trough the paint layers.

$S$  and  $K$  depend also from the pigment – medium ratio. The theory describes a simple paint layer made by dispersing a single pigment of uniform particle size homogeneously throughout the film, but it isn't a realistic model. In Medieval painting techniques several layers of pigments are frequent, with pigment mixtures and not uniform particle sizes [2].

This theory has been used to describe approximately the wavelength dependence of the hiding thickness  $X_0$ .

The figure 2.10 shows the hiding thickness plotted against the wavelength for different contrast ratios  $k$ , calculated for malachite at 20% concentration applied over a background  $R_B = 0,1$  and an infinitely thick chalk-animal glue ground with  $R_W = f(\lambda)$ . At these conditions the maximum is at 2  $\mu\text{m}$ .

Knowing the hiding thickness as a function on wavelength of the pigments can be a tool to anticipate the revelation of drawing under layers of several pigments.

The capability of drawing detection depends not only by the absorption of pigments superimposed, but also by the scattering coefficient and the thickness of pigment layer.

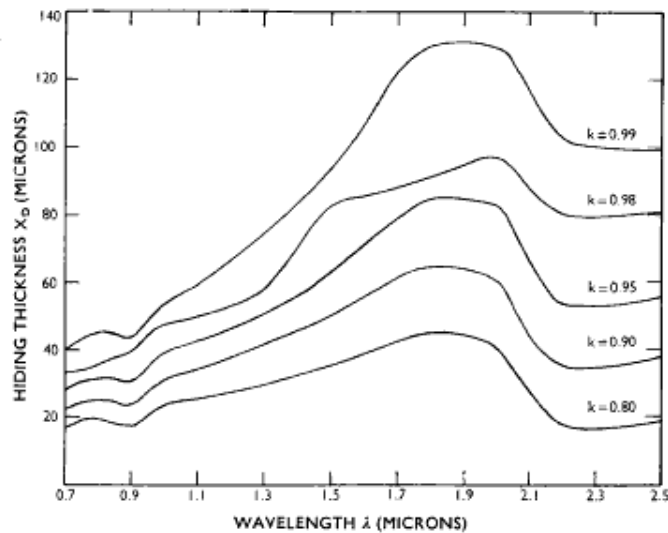


Fig. 2.10. The hiding thickness  $X_0$  plotted against the wavelength  $\lambda$  for various contrast ratios  $k$ , for paint of malachite in linseed oil, at concentration of 20%.

The interpretation of the plot in figure 2.10 is the following, if the optical system detects low-contrast drawing, say  $k = 0,99$  at  $\lambda=0,7 \mu\text{m}$ , a malachite layer  $40 \mu\text{m}$  thick is needed to prevent the visibility.

If the system detects drawing only with  $k=0,80$  contrast, a thickness of  $20 \mu\text{m}$  is sufficient to hide it. If the system maintains the same detection capability, at  $\lambda=1,9 \mu\text{m}$  it has some chances because the hiding thickness is doubled at that wavelength.

## 2.6 Wide band range

The reflectographic techniques have got significant improvements from the pioneering times of Van Asperen de Boer, in particular in the imaging performance.

At the Physics Department of Ferrara in 2003 has started a project to develop a scanning device for wide band IR reflectography.

The purpose was to extend the reflectographic capability in underdrawing detection on paintings since XVI century characterized by oil medium and dark background.

With oil medium thick pictorial films are allowed and  $X_0$  values tend to increase. Moreover, contrast tends to decrease due to dark background.

The detection of underdrawings in these paintings can be possible using an InGaAs detector with spectral response extended up to 2,5  $\mu\text{m}$ .

A painting to test the wide band capability has been based on the study of pictorial materials used by artists of XVI century (Caravaggio and caravaggeschi, Carracci, Pietro da Cortona, Lanfranco). It was designed in collaboration with G. Villa and G. Poldi of Bergamo University and realized by G. Scicolone restoration studio.

### 2.6.1 Test painting

The test painting is a framed canvas sized 25x30  $\text{cm}^2$ . It contains 12 insets, in which 6 pigments are applied oil medium by brush. Drawing (Fig. 2.13.c) was made by different ways: charcoal and brush with oil lamp black.

The canvas linen is prepared with a first layer of gypsum and animal glue and dark priming with burnt sienna earth.

The colors are applied in three layers to obtain three increasing thickness (Fig. 2.13.b).



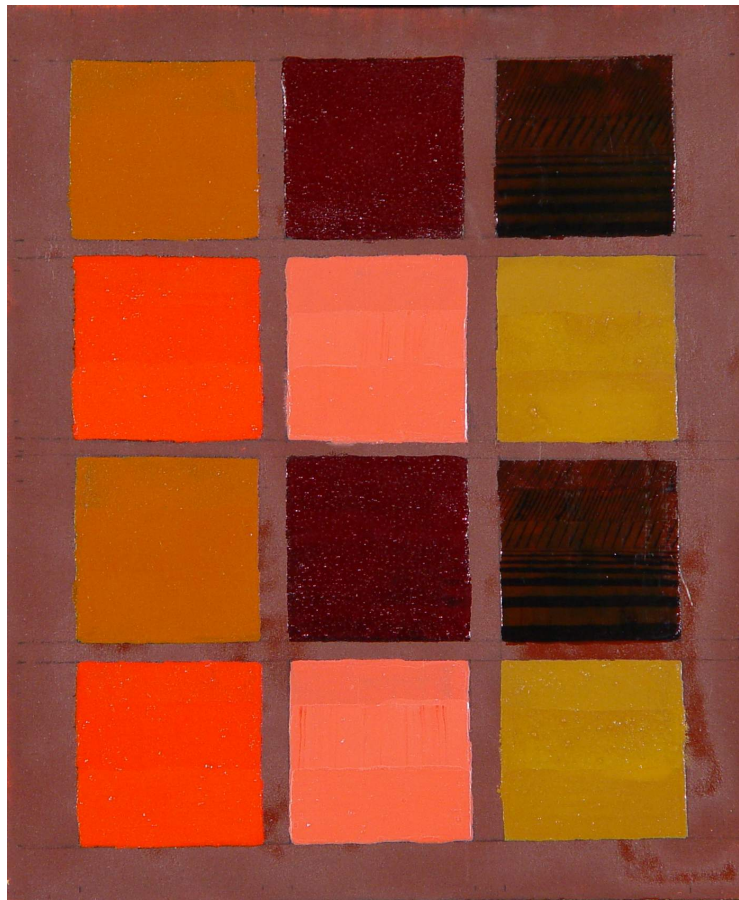


Fig. 2.11. Painting test.

Charcoal drawing	Yellow Ochre $\text{Fe}(\text{OH})_3$	Madder Lake $\text{C}_6\text{H}_4(\text{CO})_2\text{C}_6\text{H}_2(\text{OH})_2$	Copper Resinate $\text{Cu}(\text{CH}_3\text{CO})_2 \cdot 2\text{Cu}(\text{OH})_2$ $\cdot n\text{H}_2\text{O}$ $\text{Cr}_2\text{O}_7 \cdot n\text{H}_2\text{O}$
	Cinnabar $\text{HgS}$	Cinnabar 50% Lead White 50% $\text{HgS} + 2\text{PbCO}_3 \cdot \text{Pb}(\text{OH})_2$	Raw Sienna Earth $\text{Fe}_2\text{O}_3 \cdot n\text{H}_2\text{O} + \text{MnO}_2 +$ $\text{Al}_2\text{O}_3 \cdot \text{SiO}_2 \cdot 2(\text{H}_2\text{O})$
Black carbon and oil drawing	Yellow Ochre $\text{Fe}(\text{OH})_3$	Madder Lake $\text{C}_6\text{H}_4(\text{CO})_2\text{C}_6\text{H}_2(\text{OH})_2$	Copper Resinate $\text{Cu}(\text{CH}_3\text{CO})_2 \cdot 2\text{Cu}(\text{OH})_2$ $\cdot n\text{H}_2\text{O}$ $\text{Cr}_2\text{O}_7 \cdot n\text{H}_2\text{O}$
	Cinnabar $\text{HgS}$	Cinnabar 50% Lead White 50% $\text{HgS} + 2\text{PbCO}_3 \cdot \text{Pb}(\text{OH})_2$	Raw Sienna Earth $\text{Fe}_2\text{O}_3 \cdot n\text{H}_2\text{O} + \text{MnO}_2 +$ $\text{Al}_2\text{O}_3 \cdot \text{SiO}_2 \cdot 2(\text{H}_2\text{O})$

Fig. 2.12. Summary table of pigments.

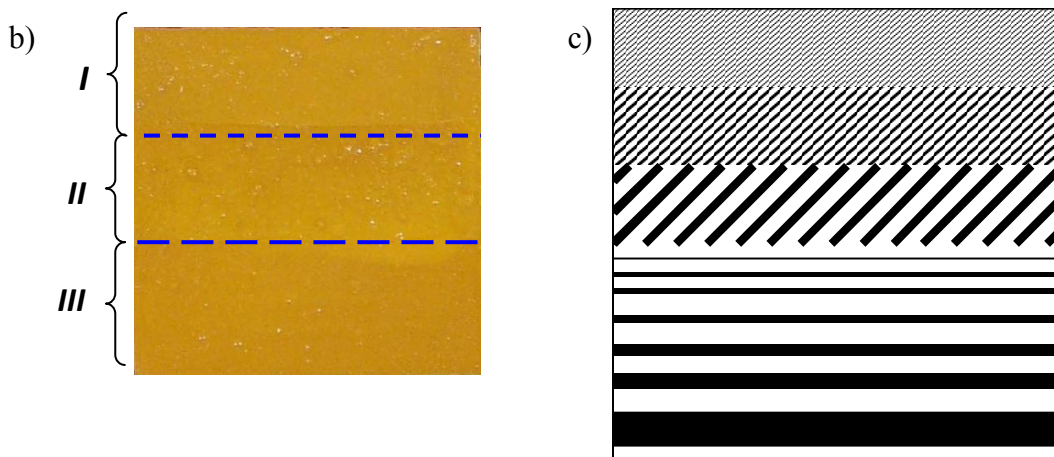
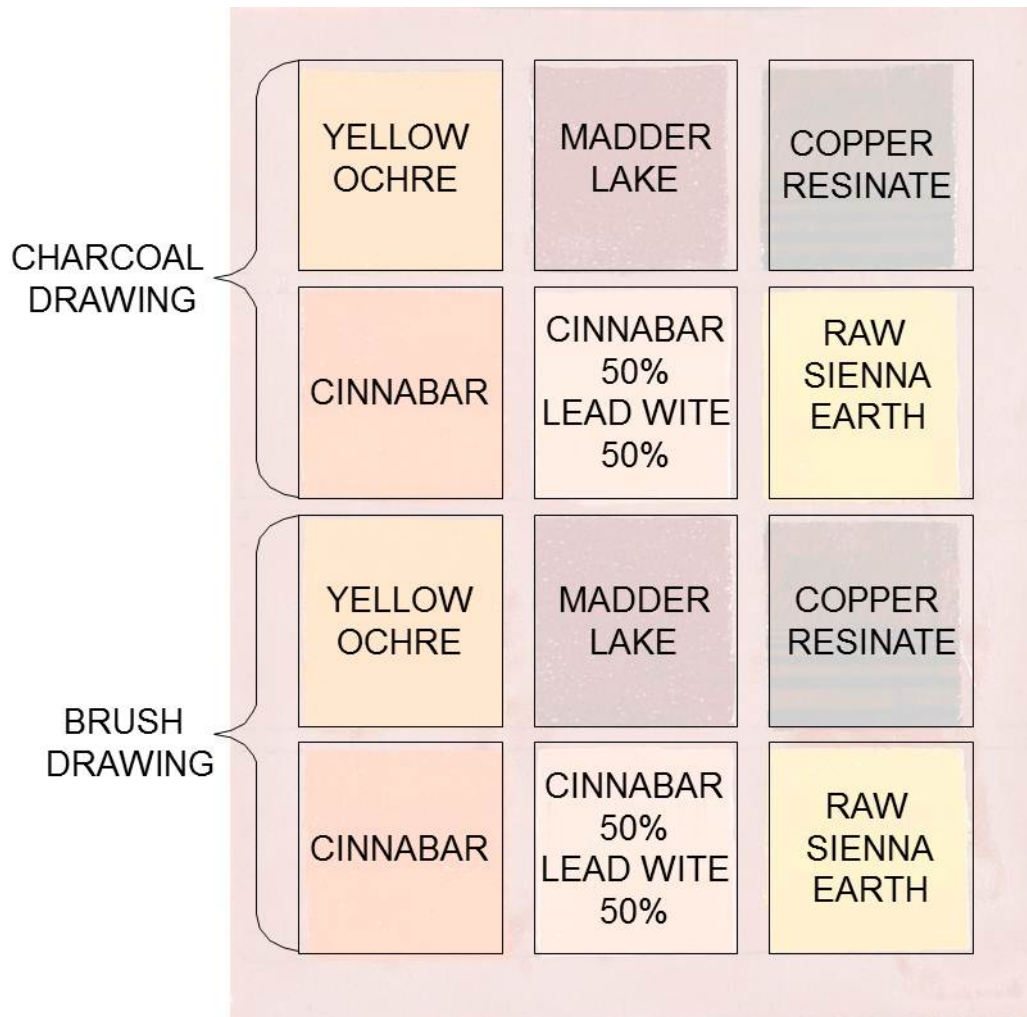


Fig. 2.13. Painting test, a) scheme of pigments, b) scheme of different layers thickness, c) scheme of underdrawings.

## 2.6.2 Results

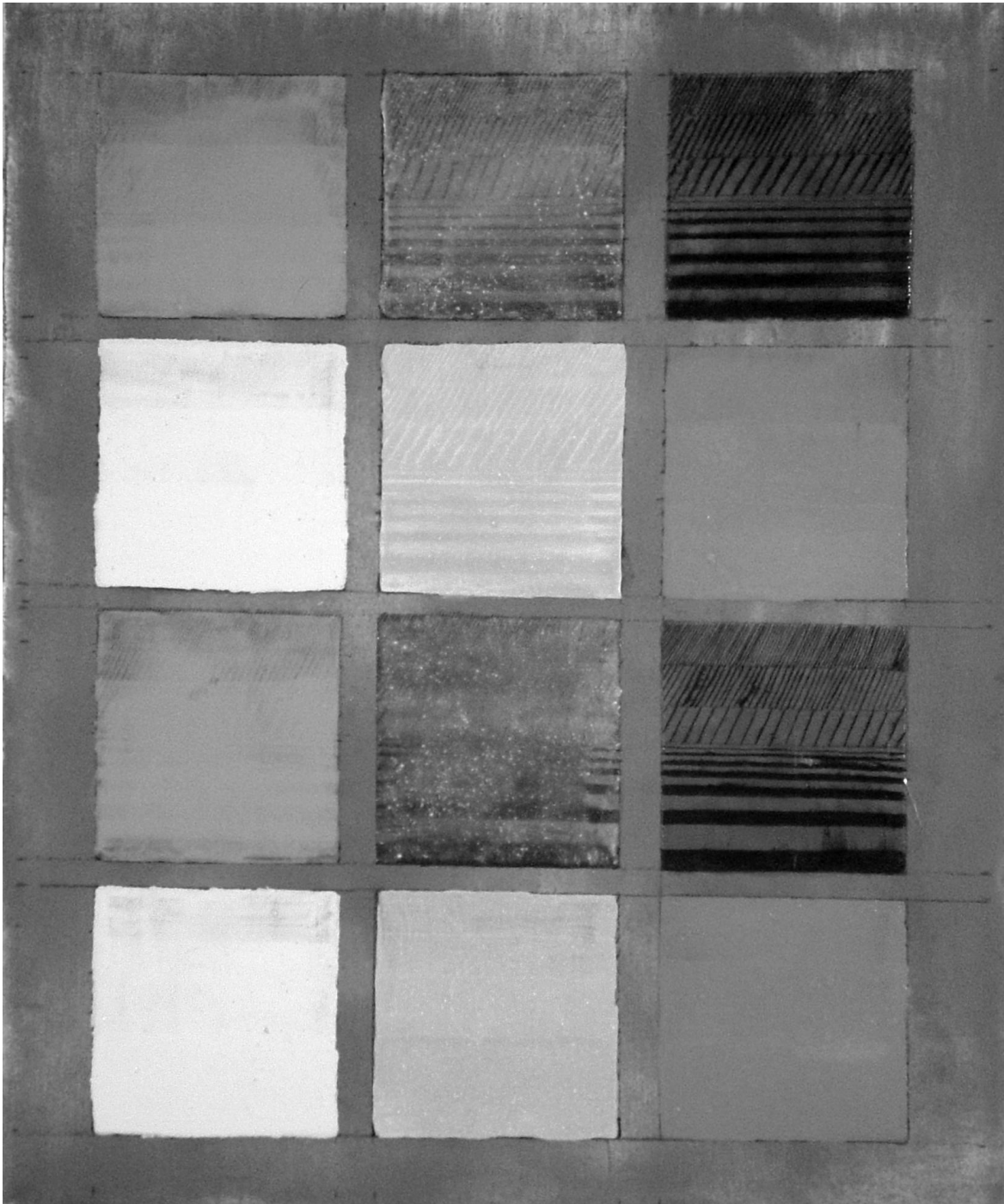


Fig. 2.14. Infrared reflectogram acquired by Sony camera with Silicon CCD and Schott filters RG-950

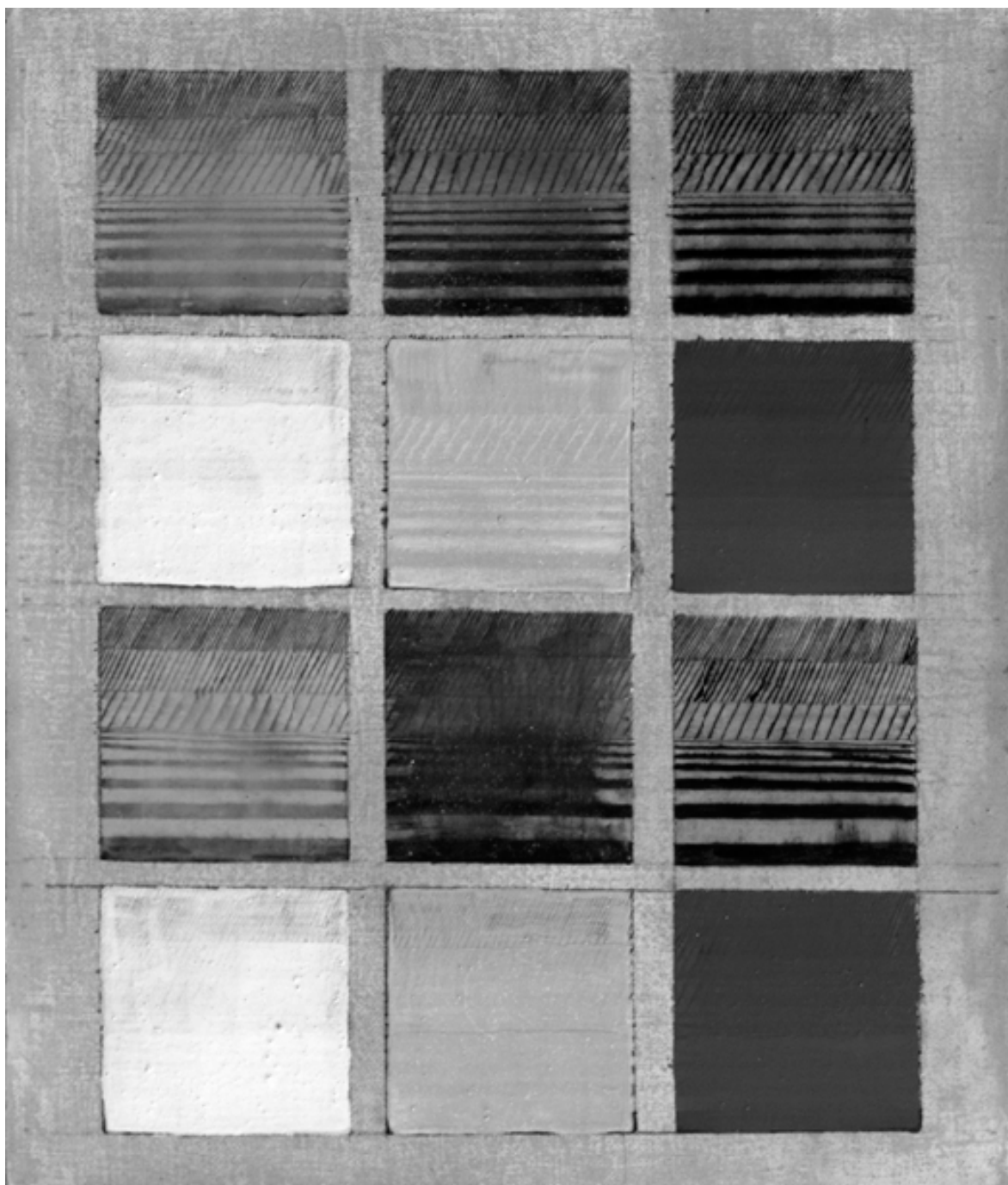


Fig. 2.15. Infrared reflectogram acquired by the scanning devices for wide band IR reflectography using InGaAs detector.

The reflectographic images have been acquired by Sony Digital Camera DSC-F717, with Schott glass filter RG-950 and by the scanning device for wide band IR reflectography using InGaAs detector with no filter.

Comparing the two images is possible to observe interesting results.

The priming of burnt sienna Earth appear more light in image acquired by InGaAs increasing background contrast and an increase in contrast can increase the  $X_0$  values and hiding thickness of pigments (Fig. 2.11.).

Madder lake is an organic pigment, for its high viscosity is not possible to make three marked layers of thickness.

In the Sony image the drawing is visible but the reflections avoid a good detection.

In particular, in the inset with drawing by brush, the detection is limited by the high thickness due at the concentration of paint in the central area.

In the second image with InGaAs detector the drawing is more visible because the high contrast of detector has increased the value of  $X_0$ .

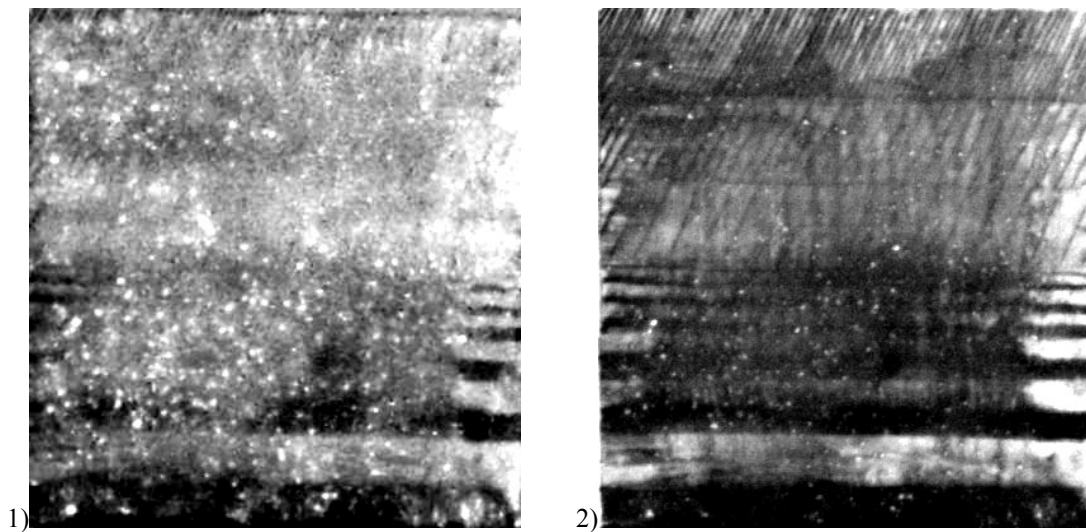


Fig. 2.16. comparison of Madder Lake inset with drawing by brush with incremented contrast 1) Image acquired by Sony camera. 2) Image acquired by InGaAs detector.

The drawing under Yellow Ochre is hardly visible by Silicon detector (Fig. 2.17.1). On the contrary it is well imaged by InGaAs (Fig. 2.17.2).

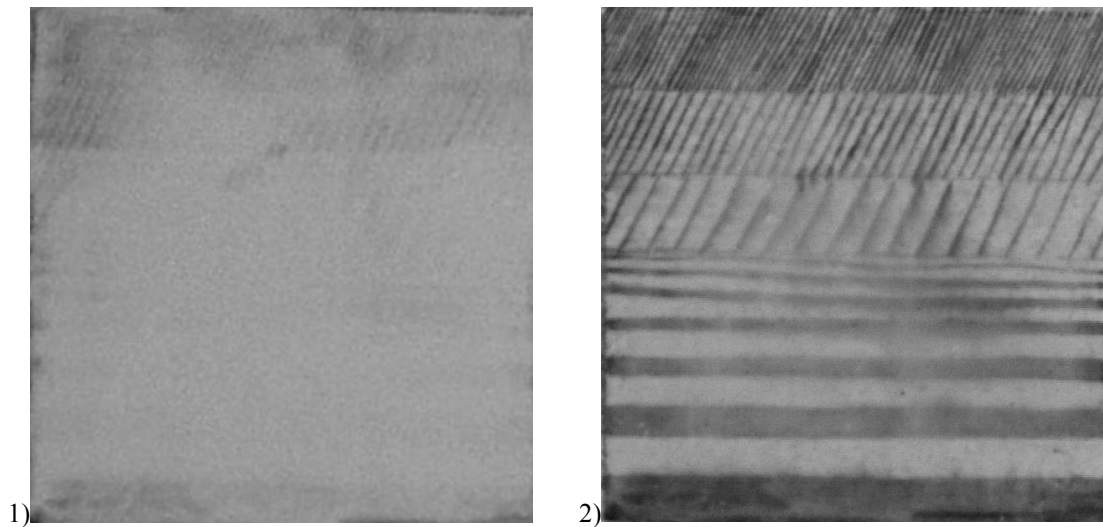


Fig.2.17. comparison of Yellow Ochre inset with drawing by brush 1) Image acquired by Sony camera. 2) Image acquired by InGaAs detector.

In both images by Si and InGaAs, Cinnabar covers the drawing.

In the IFAC-CNR database reflectance spectra acquired by FORS techniques, in the bands of UV-VIS-NIR up to 2500 nm of several ancient and modern pigments, are available.

The samples are made with oil medium, thin pictorial layers on canvas support and kaolin and titanium dioxide of preparation [13].

Observing the reflectance spectrum of Cinnabar (Fig. 2.18.a) is possible to see that it has high reflectance in almost the whole spectrum. This is due to high value of S coefficient that inhibits the detection of underdrawing.

In the thin paint layer is possible to observe the reduction of hiding thickness, and through InGaAs detector is possible to recognize the texture at more tight lines (Fig. 2.19.).

In the inset of Cinnabar and Lead White 50% the effect is similar.

Both reflectance spectra of pigments show high reflectance, but beyond 1200 nm, Lead White presents most deep absorptions, probably also due of background, that decreases the value of S coefficient and facilitates the detection of the drawing, in particular in two more thin layers.

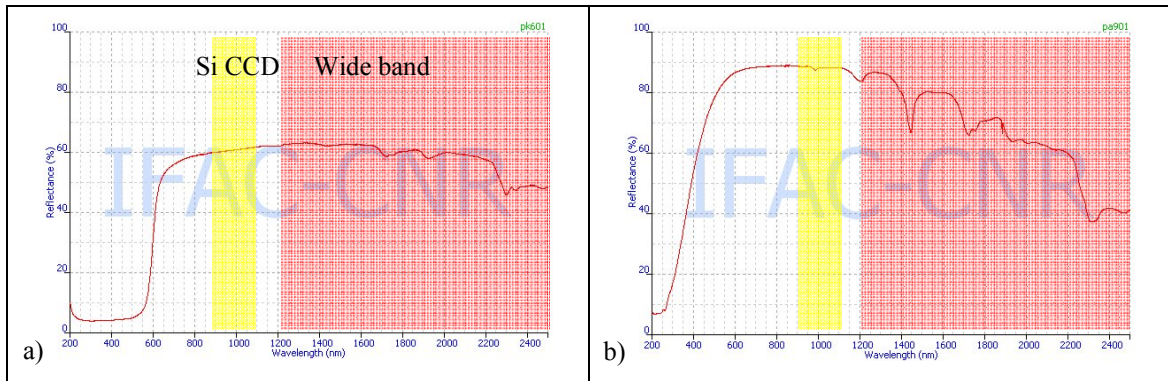


Fig. 2.18. Reflectance spectra. a) Cinnabar, b) Lead White.

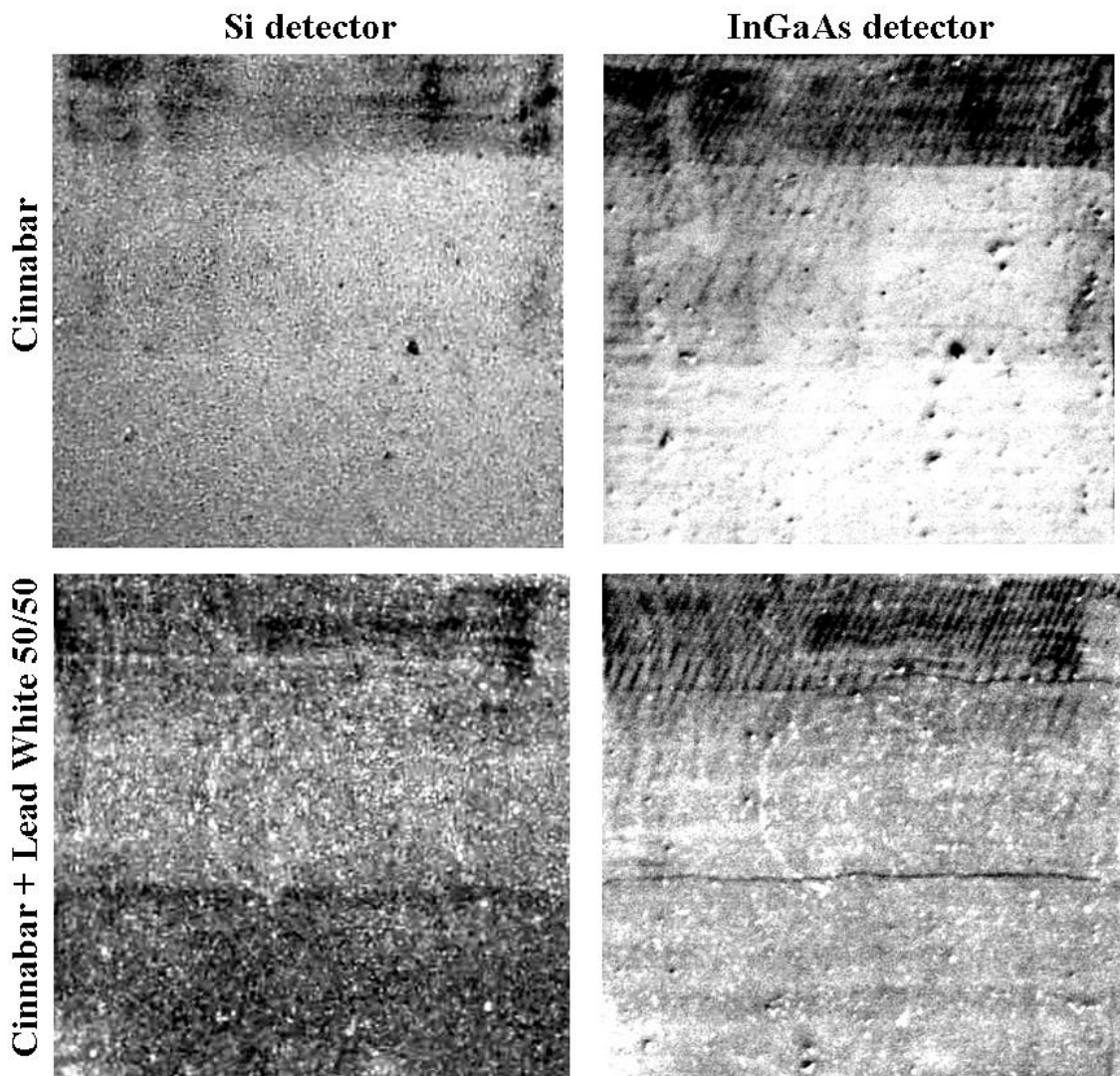


Fig. 2.19. comparison of Cinnabar and Cinnabar and Lead White inset with drawing by brush (incremented contrast).

Raw Sienna Earth shows low reflectance in the image acquiring by InGaAs, in this case, the increase of K coefficient inhibits a good detection of underdrawing (Fig. 2.15.), however, the lines are recognizable about the borders and in the thin layers (Fig. 2.20.). In the image acquired by silicon CCD the drawings is visible just a bit in the inset with charcoal drawing in the first thin layer.

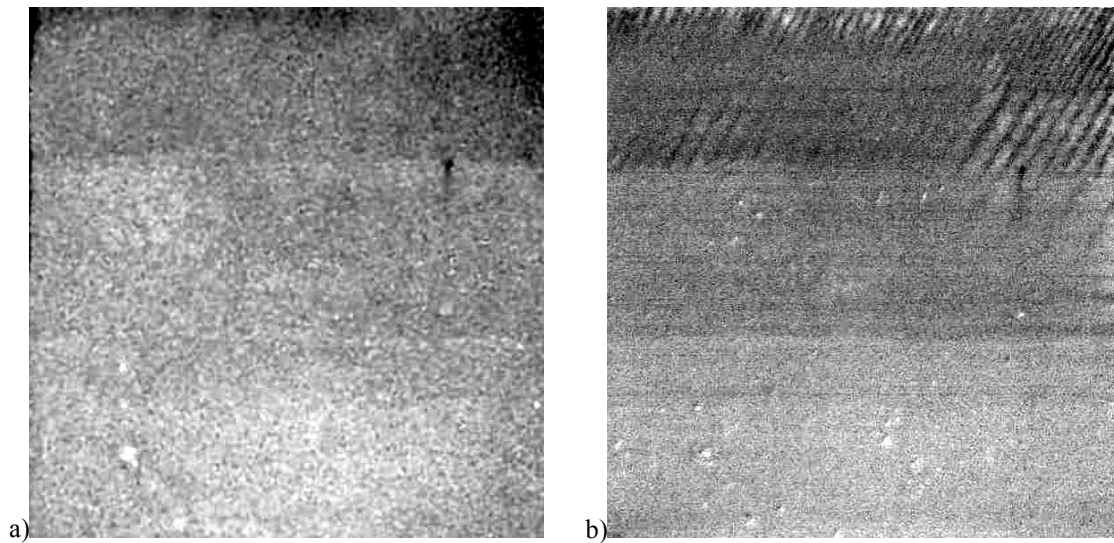


Fig. 2.20. comparison of Madder Lake inset with drawing by brush with exaggerate contrast 1) Image acquired by Sony camera. 2) Image acquired by InGaAs detector.

### 2.6.3 Discussion

The measurements on test painting have shown that InGaAs detector is more efficient in the detection of underdrawing than silicon CCD, validating the wide-band choice.

Observing a reflectance spectra of pigments used is possible to draw several considerations.

- Several brown pigments used in dark priming (Burnt Umber Earth, Van Dike Brown), above 1000 nm, show an increase of reflectance [13], this carries to increase the contrast background, so tends to decrease the hiding thickness of pigments.
- High values of reflectance, in detection band, inhibit capability to discover underdrawing, like in cinnabar case. The same is for high absorption (high K value), like in Raw Sienna Earth case.



- A good compromise for detection of underdrawing may be medium-low values of reflectance, about 30%, like in Yellow ochre case.

However, the detection of underdrawing depends by many factors: the concentration of pigments in the medium, contrast of background, thickness of pictorial layers, the presence of various pigments and the interaction between the optical properties of these. That makes very difficult a real anticipation of underdrawing detection in a painting.

Beyond 2,5  $\mu\text{m}$  the reflectance decreases due to O-H and C-H vibration of oil and proteins present in the paint medium and varnishes that absorb IR radiation about 2,9  $\mu\text{m}$  and 3,3  $\mu\text{m}$ .

In the range of middle infrared, the radiation emitted from the painting itself becomes more important and overwhelms the faint reflected radiation. However, the possibility to use detectors with spectral response beyond 2,5  $\mu\text{m}$  is not excluded, using, for example, MCT detector and a narrow band illumination.

## References

1. R. Bellucci, D. Bertani, M. Ceriana, E Daffra, A. Di Lorenzo, C. Frosinini, C. Gallazzi, L. Lodi, M. Milazzo, A. Natali, M. Olivari, M. Signorini, *Oltre il visibile: indagini riflettografiche*, Università degli Studi di Milano, 2001, Limited Edition.
2. J.R.J van Asperen de Boer, *Infrared Reflectography, Method for the Examination of Paintings*, Applied Optics 7, 1711-1714, 1968.
3. J.R.J van Asperen de Boer, *Reflectography of Paintings using an Infrared Vidicon Television System*, Studies in Conservation, 1969, pp 96-118.
4. R. A Lyon, *Infrared radiation aid examination of painting*, in: *Technical Studies in the Field of the Fine Arts* 2, 1934, pp 203-212.
5. C. Robimarga, *Aspetti fondamentali della propagazione della radiazione infrarossa negli starti pittorici. Applicazioni alla riflettografia IR e alle misure di riflettanza*, Thesis in Physics, University of Milan, A.A. 1992-1993.
6. P. Kubelka, *New Contributions to the Optics of Intensely Light-Scattering Materials. Part I*, Journal of the optical Society of America, Vol. 38, 448-448, 1948.
7. G. Poldi, *Messa a punto di un metodo non invasivo applicabile in situ per riconoscere i pigmenti e la loro successione nello strato pittorico*, Ph.D. thesis, Università degli Studi di Firenze, 2006.
8. N. Bevilacqua, L. Borgioli, I. Adrover Gracia, *I pigmenti nell'arte dalla preistoria alla rivoluzione industriale*, Collana i Talenti, Il Prato, Padova, 2010.
9. C.F. Bohren, D. R. Huffman, *Absorption and scattering of light by small particles*, J. Wiley & Sons, 1983.
10. L.E. McNeil, R. H. French, *Light scattering from red pigment particles: multiple scattering in a strongly adsorbing system*, Journal of Applied Physics, Vol. 89 N.1, pp 283-293, 2001.
11. D. Bertani, M. Cetica, P. Poggi, G. Puccioni, E. Buzzegoli, D. Kunzelman, S. Cecchi, *A scanning device for infrared reflectography*, Studies in Conservation, Vol. 35, London, 1990, pp 313-117
12. M. Gargano, N. Ludwig, G. Poldi. *A new methodology for comparing IR reflectographic system*, Infrared Physics & Technology, 49, 2007, pp 249 - 253.

13. <http://xp9.ifac.cnr.it>  
M. Picollo, G. Basilissi, C. Cucci, L. Stefani, M. Tsukada, *Ultraviolet, Visible and Near Infrared Reflectance Spectra of Modern Pictorial Materials in the 200-2500 nm range*,
14. <http://www.brera.unimi.it>
15. <http://arte.ino.it>

---

## CHAPTER 3

# SCANNING DEVICE

---



### 3.1 Project for a scanning device for wide band IR Reflectography

The project has been started in 2003, and foresaw the development of a scanning device for Wide Band IR Reflectography to extend the spectral response up to 3,5  $\mu\text{m}$ .

The project focused on an optical system capable to support single photodiode IR detectors of different types.

Actually the system mounts a Two-color K3413-08 detector by Hamamatsu. It is composed by two single photodiode Si and InGaAs and is equipped by a thermoelectric cooling. The combination of different semiconductors covers a wavelength range from 0,3 up to 2,5  $\mu\text{m}$ .

The improvement of spectral response in the MIR, up to about 3,5  $\mu\text{m}$  is foreseen using an MCT detector.

The main sections of the scanning device are:

- Mechanical structure and positioning system
- Optical system and lighting
- Detector
- Control PC and Data Acquisition Software

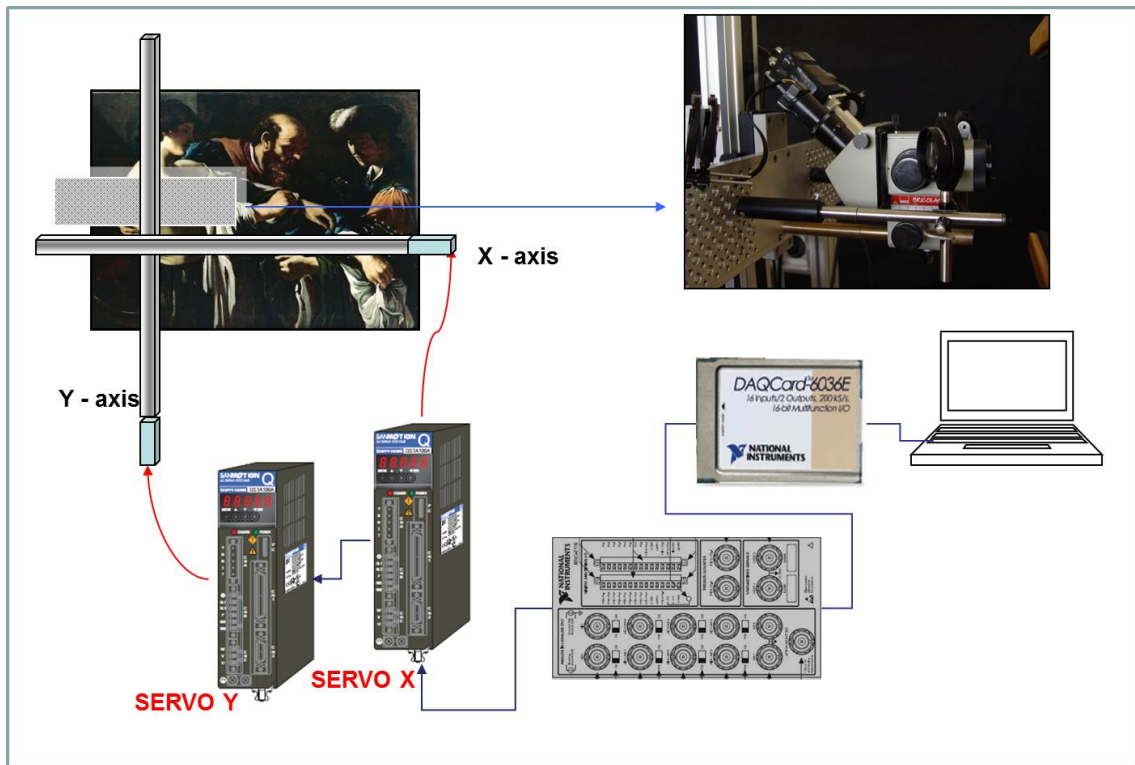


Fig. 3.1. summary diagram of the components of the scanning system.

A short description of handling scanning system basics and the specifications of all components will follow

### 3.2 Scanning system

A typical scan starts with a horizontal movement, along a whole line, left to right.

At the end of each horizontal line the mobile support moves vertical by one step, and then moves again horizontally in the reverse direction, from right to left (Fig. 3.2).

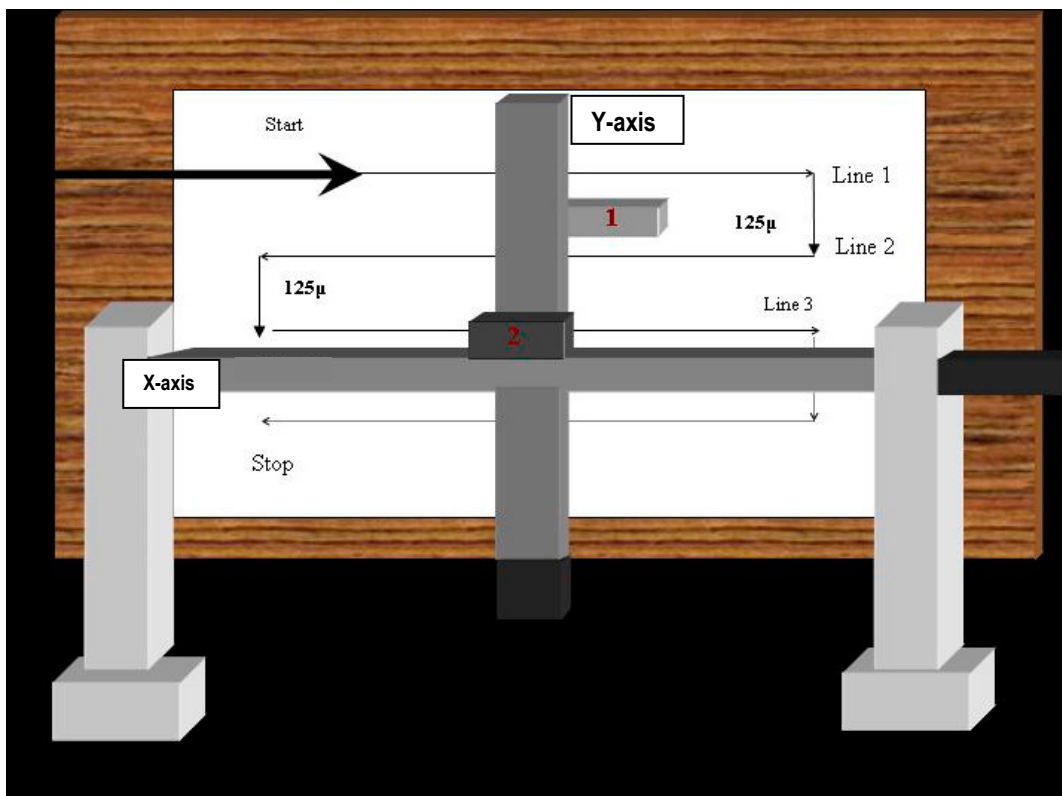


Fig. 3.2. Scheme of the scanning system.

During movements, signals from IR detectors are acquired synchronously with horizontal axis position for each scan line.

Vertical step size, horizontal scan lines are selectable by user, via software. The scan area can cover 90 x 90 cm<sup>2</sup> maximum.

### 3.3 Mechanical system

The mechanical support has been designed and developed by the services of Mechanics, Electronics and Computing of the Department of Physics and INFN Section of Ferrara.

It was designed with the following specific goals:

- Reduced vibrations
- Easy to assembled and transport
- Quick and practical system management.

The scanning device is composed by two motorized linear guides, supported by a structure of aluminum bars profiles.

The structure consists of two supports for the rails and two lateral supports, with leveling feet, to be used on any floor (Fig. 3.3).

The vertical axis (Y-axis guide) is attached to horizontal axis (X-axis guide). Y-axis guide is transported by X-axis for each horizontal scan line.

Both guides are equipped with limit switches to stop movement in case of overrun fault. The movement is provided by two servo motors controlled by two servo drivers (P30B08075DCS00M by SANYO DENKY Inc.). Drivers are AC powered (220VAC, 750W max).

Each servo unit commands from a control PC using a serial interface. Control PC can start, run, stop the motors and gets position/status of each axis.

Axis position is measured using incremental encoder mounted on motor shaft (Fig. 3.4.). The encoder sends the angular position signals to the motor drive. On X-axis, encoder signals are also used as clock signal for data acquisition, with a resolution of 1000 P/R, adapted to the resolution of the acquisition devices.

When X-axis motor moves, the encoder generates a set of pulses related to motor shaft angular position. The acquisition is synchronized on these pulses. By this way, the acquisition takes place at precise angular positions, no matter which speed is actually turning the rotor. Motor angular positions corresponds to linear translational positions in a fixed way (ball-screw mechanical transmission) so acquired data are associated to precise horizontal scan points.

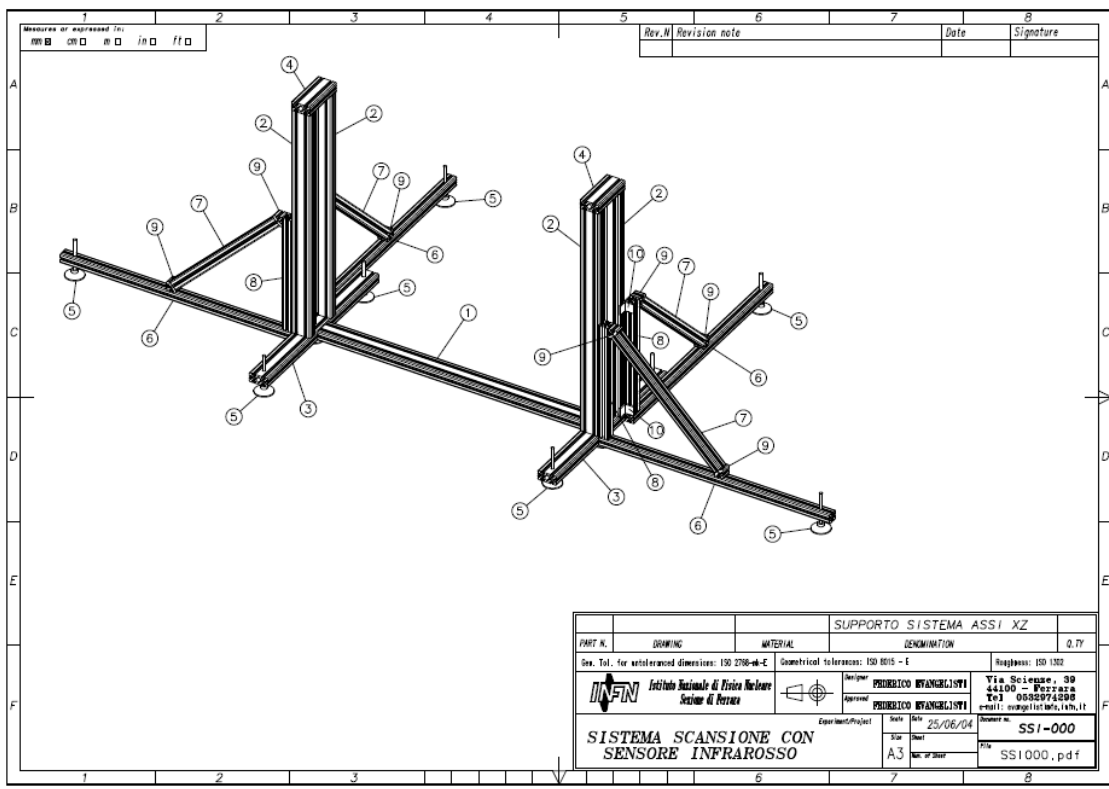


Fig. 3.3. Drawing of the mechanical support

### 3.4 Acquisition device

The image sampling is acquired during the horizontal movement, 0.90 cm wide, performed at 0,2 m/sec mean speed. The distance and frequency of acquisition are defined by the engine system. Signals from the photodiode are acquired with a horizontal pitch of 5  $\mu\text{m}$ , at 12 bit/pixel. The acquisition pitch is independent from the speed.



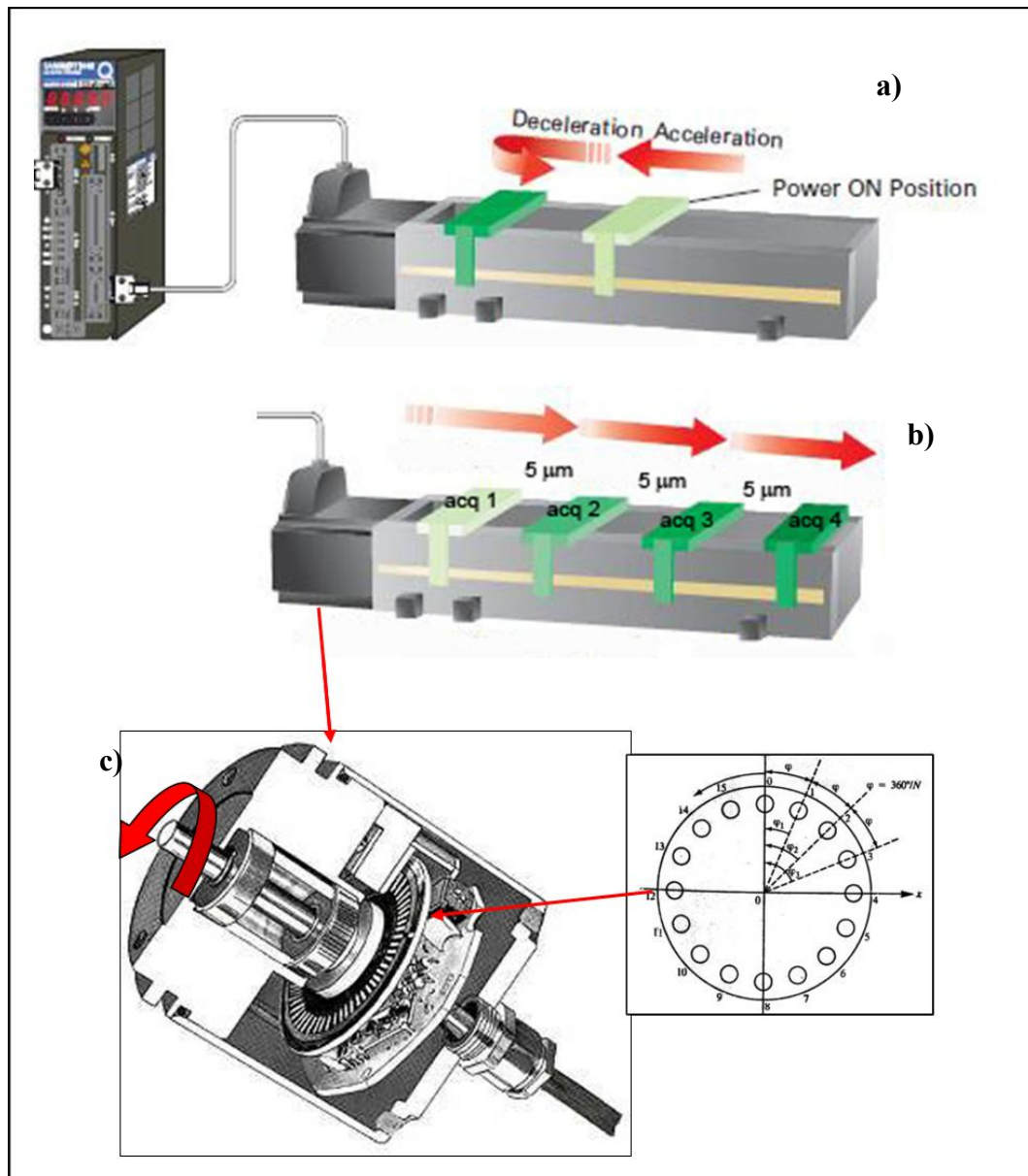


Fig. 3.4. Scheme of Acquisition system. a) Movement of scan with representation of acceleration ramp; b) Scheme of acquisition; [4] c) section of a motor with incremental encoder.

The control PC is a Notebook working with Microsoft Windows XP operating system. Control PC motion commands are transmitted to motor drives via serial line RS232. Signals from detectors are digitized and acquired by a DAQ Card-6062E by National Instruments Corporation, with dedicated software drivers, connected to the notebook with PCMCIA interface.

The acquisition device samples analog signal at 12 bit with a maximum sample frequency of 40 kHz. The DAQ board receives detector and trigger signals via the BNC-2110 interface.

The detector outputs are connected to BNC inputs AIN0/1, the encoder output signal is connected to PFI/0 trigger port (Fig. 3.5).

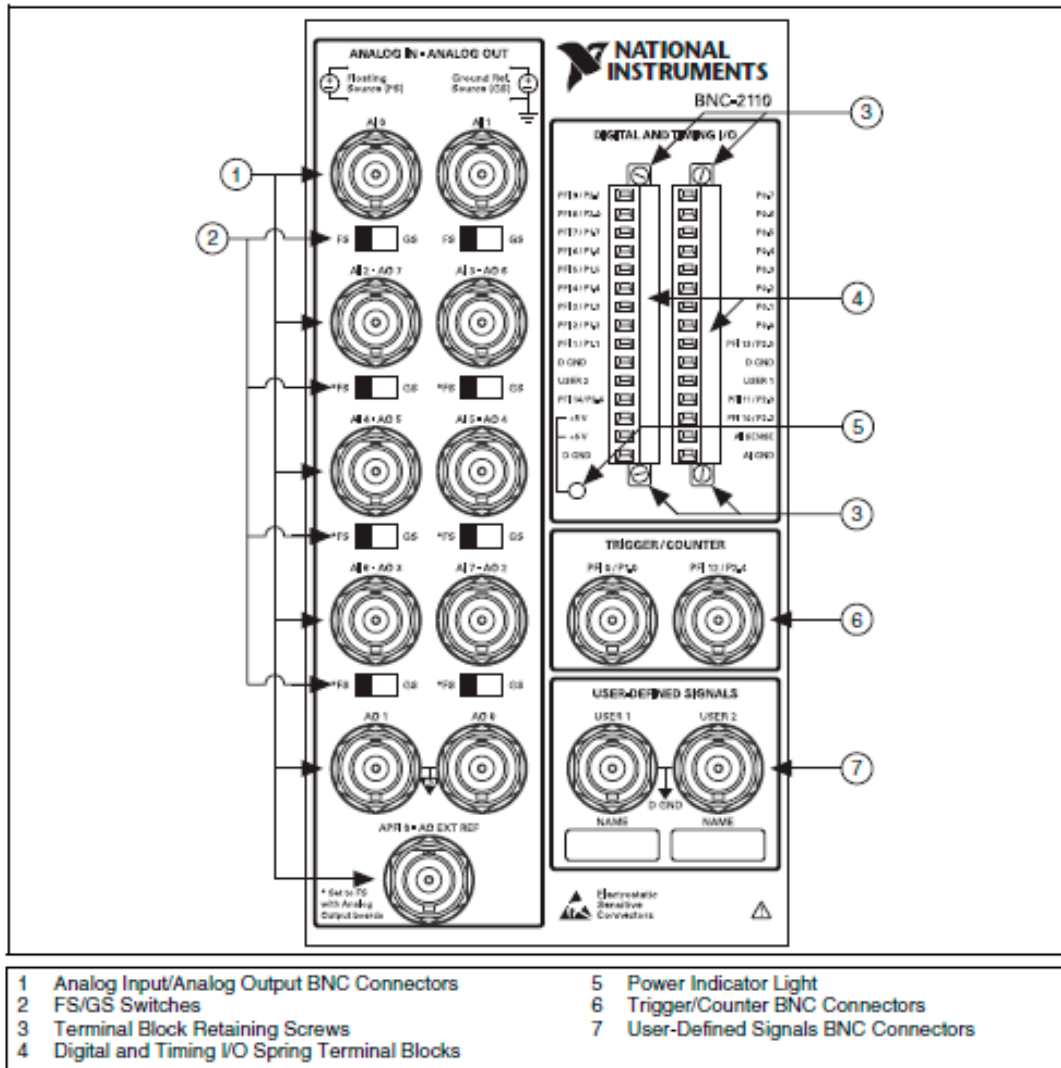


Fig. 3.5. drawing of BNC-2110 [5].

### 3.5 Safety System

During the scan, if any fault occurs during movement of the engine system, the operation is stopped and an alarm is issued. In this case scan can be always resumed and restarted using software commands.

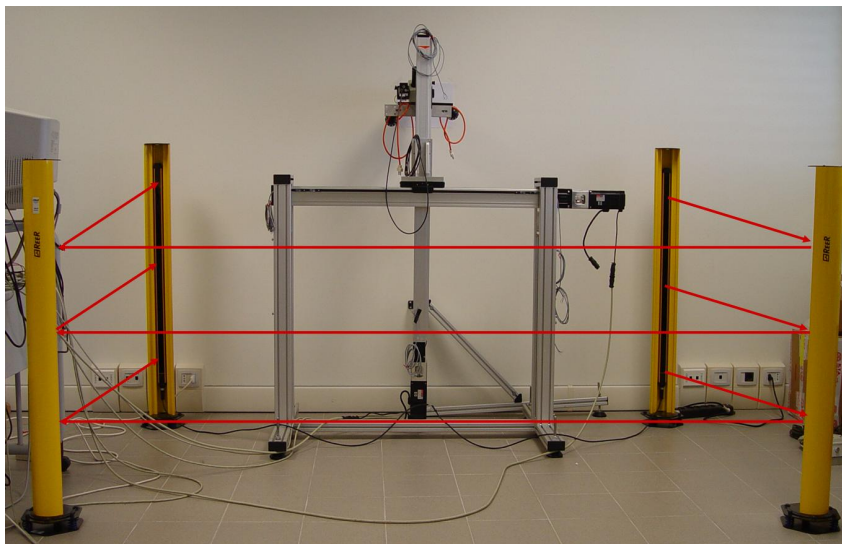
Moreover, to prevent risks arising from the movement the presence of fast moving parts, the whole is surrounded by an infrared safety barrier.

It consists of an optical barrier (model Vision VX Fmc-3B by REER S.p.a. Torino), provided of three IR beams. The particular application of this system is the protection of arms and legs from fast moving parts.

The security system is composed by three parts: an emitter, a receiver and three mirrors. The emitter produces a light ray that, through the mirrors, strikes the receiver.

Through this system is possible to enclose the working area of device. Any attempt to cross the barrier blocks the movement.

The mirrors allow to isolate a rather large area. For application in museums and galleries it will be possible to perform scans safely even in presence of unauthorized personnel.



a)



b)

Type	VX Fmc 3B
Number of ray	3
Ray distance mm	400
Response speed ms	6
length of Barrier m	1

c)

Fig. 3.6. Safety system. a) Graphical representation of system operation. b) Components: 1. Emitter; 2. Receiver; 3. Mirror. c) Table of specifications [6]

### 3.6 Optical system

The optical system is a binocular microscope head MVS 10 mounted on a Y-axis, provided by a revolver with selectable magnification steps: 0,6 x – 1 x – 2 x – 4 x – 7 x. In place of one microscope eyepiece there is the detector, while a camera for positioning and focusing purposes is placed at the second eyepiece.

This monitoring camera is MTC 1100 (by MAC-TVCC) is a mini-camera B/N provided of CCD 1/4" with fixed focal length connected to a LCD Monitor Dikom (Fig. 3.7.).

The focal planes of the detector and the camera have been adjusted to coincide.

The choice of the microscope is justified by the following features.

- Enlarge the area focused on the detector to cover the active area of photodiode.
- Guarantee a working distance of about 10 cm, suitable to avoid damage to the painting,
- Allow a depth of field of about 0,5 cm, compatible with the roughness of pictorial surfaces.

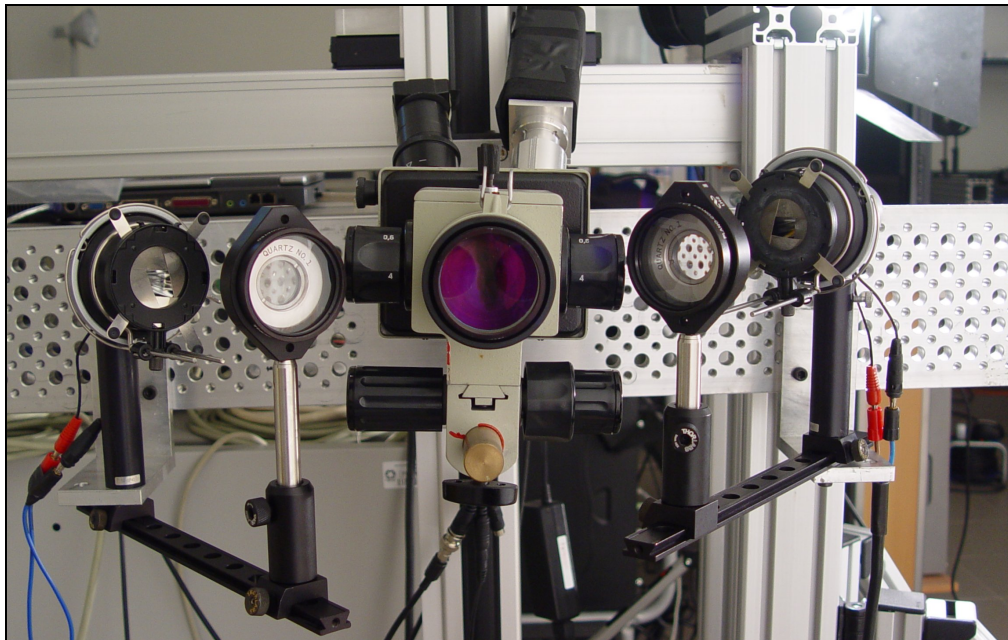


Fig. 3.7. Optical system.

The lighting system is mounted on a steel plate with threaded holes, which moves together with the optical system to maintain the same lighting conditions constant throughout the scanning.

Two light (Pollux by Erco) placed at  $45^\circ$  from the painting and equipped by halogen lamps of 50W are employed. They are stabilized by an external power supply adjusting the voltage up to 12V.

To reduce the effect of overheating, the lamps are equipped by:

- diaphragms to reduce quantity of the light;
- silicon plates, cutting wavelengths shorter than 1100 nm, (used only for the applications with InGaAs detector).

A quartz lens ( $f = 850$  mm) is concentrating light on the target area.

All elements are mounted on a rails system to allow adjustments (Fig. 3.8.).

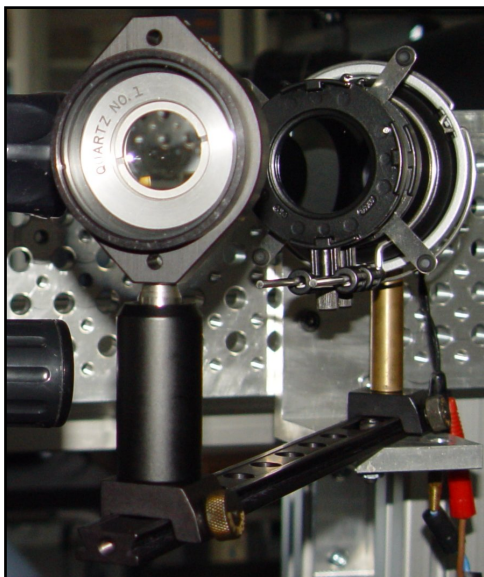
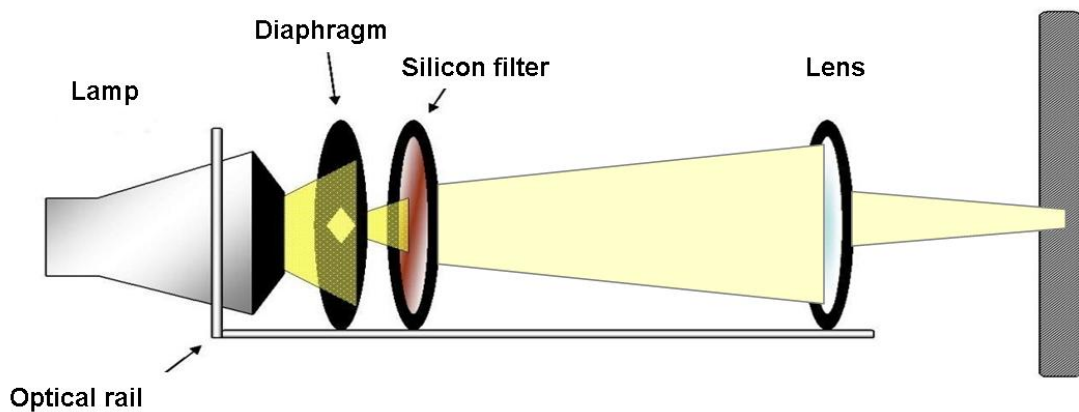


Fig. 3.8. Scheme of lamp filtration and photo of a lamp and lens mounted on the rail system.

### 3.7 Detectors

The selection of infrared detectors has been based mainly on the wavelength region and peak sensitivity wavelength

For the requirements of IR reflectographic imaging, quantum detectors are more suitable than bolometric and pyroelectric.

Quantum detectors offer high detection performance and a faster response speed. In general, quantum detectors must be cooled for accurate measurement except for detectors used in the near infrared region.

Typical spectral response characteristics of infrared detectors are shown in figures 3.9

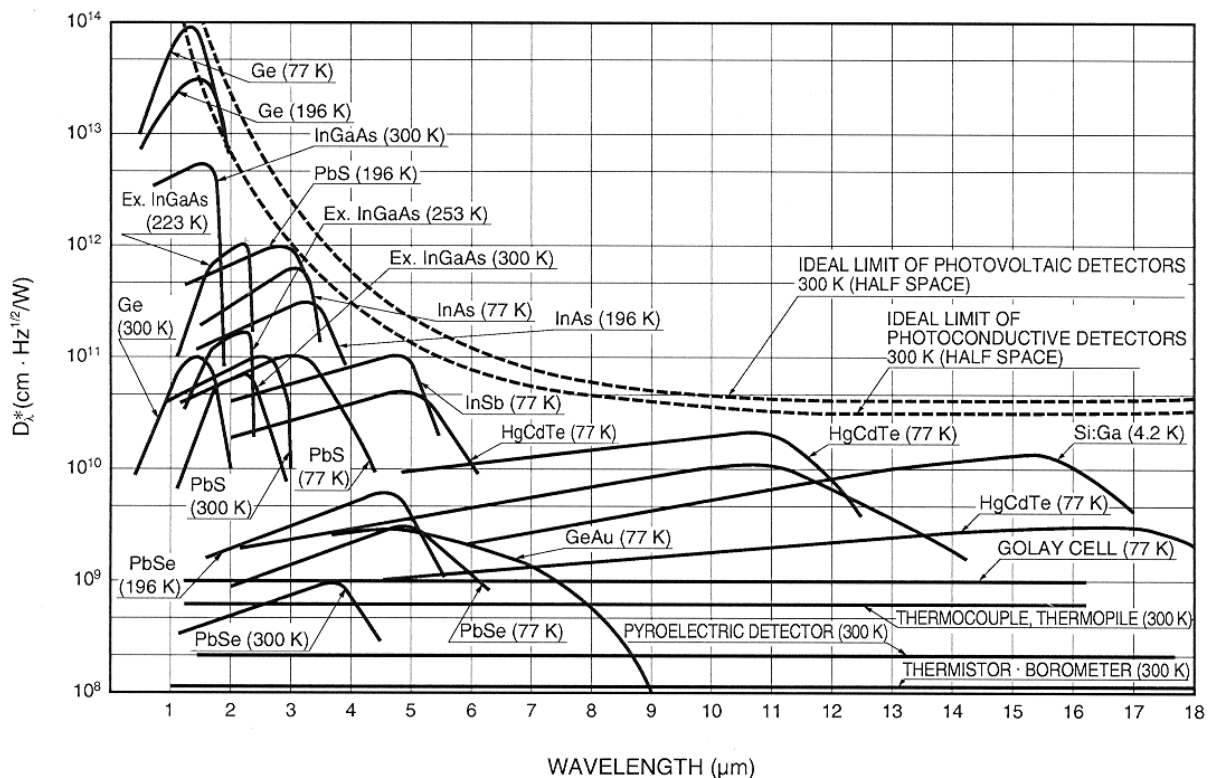


Fig. 3.9. Comparison among spectral responses of various infrared detector of Hamamatsu [7].

The choice of detectors to extend the spectral band wide is gone on two different types of quantum detectors: a photovoltaic InGaAs and a photoconductive MCT (HgCdTe).

### 3.7.1. Two-color detector

The detector selected for the scanning device for Wide band IR Reflectography is a Two-color K3413-08 detector manufactured by Hamamatsu Photonics K.K. (Fig. 3.10).

This is a hybrid detector containing, in this particular type, a Si photodiode mounted over an InGaAs PIN photodiode, along the same optical axis.

Due to transparency of Silicon at wavelength over 1100 nm, this detector delivers the possibility of acquiring two images simultaneously in different spectral bands.

This Si-InGaAs combination covers a wide spectral response range from 0,25  $\mu\text{m}$  to 2,5  $\mu\text{m}$ .

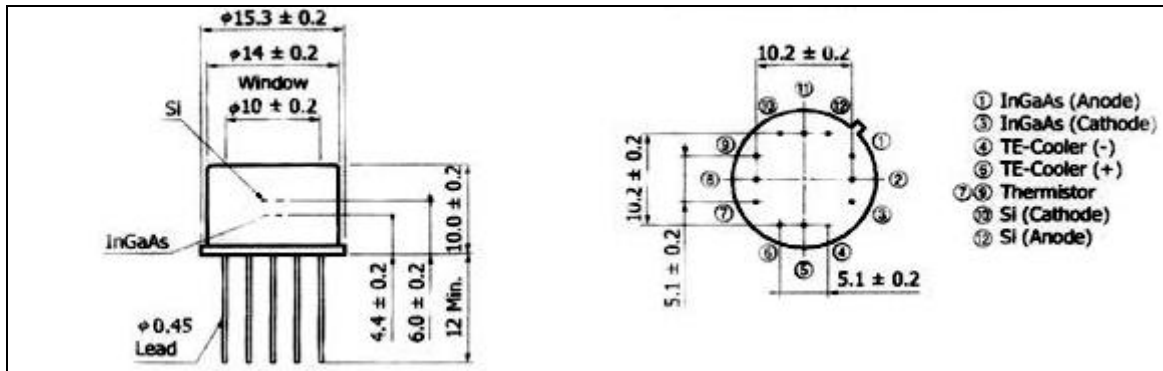


Fig. 3.10. Drawing of Two-color K3413-08 detector by Hamamatsu Photonics K.K. [7].

### 3.7.2 Si photodiode

Type	K3413-08	
Spectral range	$\mu\text{m}$	0,27 - 1,1
Peak sensitivity $\lambda$	$\mu\text{m}$	0,94
Active area	mm	2,4 x 2,4

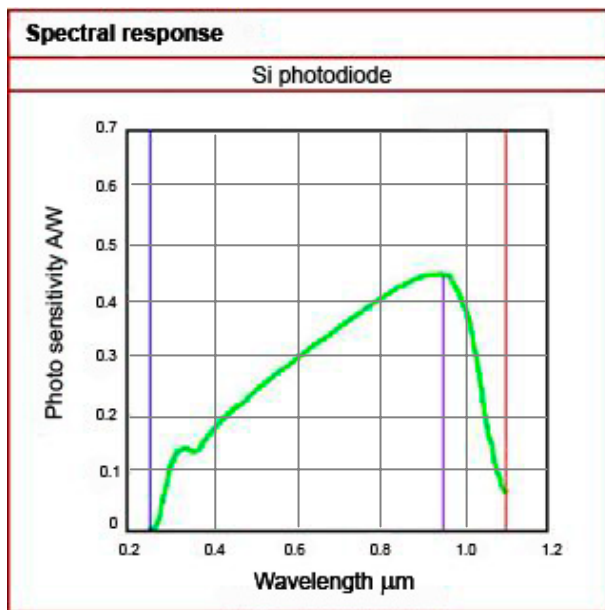


Fig. 3.11. Specification and spectral response of Si photodiode [7].

The Si photodiode is placed under the InGaAs and the active area of sensitivity has square form.

In reflectography applications, the Si photodiode is shielded with a high-pass filter, cutting off wavelengths below 0.85  $\mu\text{m}$ , and the Si plates used to filter the lamps are removed.

The use of Si is limited to applications where the comparison of different spectral bands is useful. For wide band reflectography the InGaAs photodiode is preferred.



### 3.7.3 InGaAs PIN photodiode

Changing the composition ratio, of this semiconductor, it is possible to vary the spectral response.

Standard type of InGaAs photodiodes ( $x=0,53$  in the ternary composition of  $\text{In}_x\text{Ga}_{1-x}\text{As}$ ) have a threshold wavelength of  $1,7 \mu\text{m}$  as the band gap is  $0,73 \text{ eV}$  at room temperature. InGaAs with  $x=0,82$  offer a threshold wavelength extended up to  $2,6 \mu\text{m}$  as the band gap is lowered to  $0,48 \text{ eV}$  at room temperature. This is the semiconductor used in the Two-color K3413-08 detector.

Type	K3413-08	
Spectral range	$\mu\text{m}$	0,94 - 2,57
Peak sensitivity $\lambda$	$\mu\text{m}$	2,3
Active area	mm	1 $\emptyset$

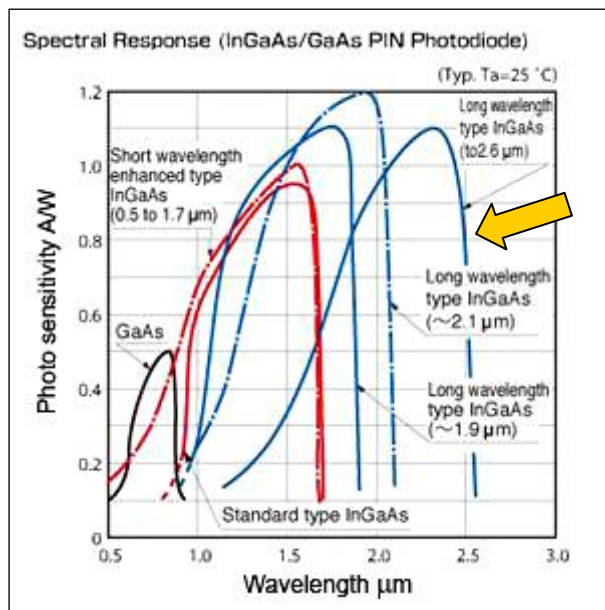


Fig. 3.12. Specification of InGaAs photodiode and comparison among spectral responses of various InGaAs photodiodes by Hamamatsu [7]. The yellow arrow indicates the response of model K3413-08 employed in the scanning system.

The InGaAs PIN photodiode is placed over the Si and the active area of sensitivity is circular.

### 3.7.4 MCT detector

The band gap of HgCdTe crystals depends on the composition ratio of between HgTe and CdTe.

Changing the composition allows infrared detector with maximum sensitivity at different wavelength.

For this reason and for superior sensitivity at long wavelengths, MCT is the most flexible semiconductor for application in the mean-IR.

Type	P4631	
Spectral range	$\mu\text{m}$	2 - 4,3
Peak sensitivity $\lambda$	$\mu\text{m}$	3,6
Active area	mm	1 $\emptyset$

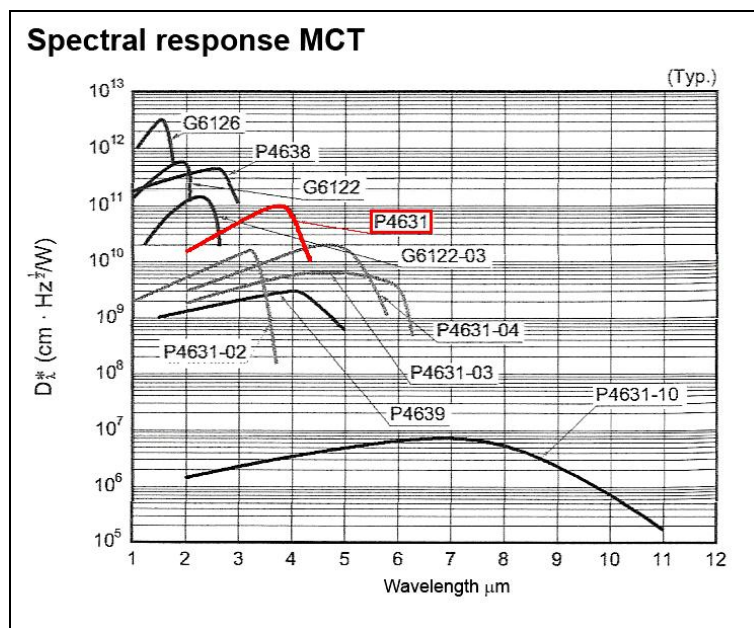


Fig. 3.13. Specification of MCT detector and comparison among spectral responses of various MCT detectors of Hamamatsu [7]. The red line indicates the model P4631.

At this time, the MCT detector has not yet been used in the scanner for reflectographic applications.

In fact, the use of MCT is impaired by the considerable thermal emission of the painting at room temperature, in the same range of sensitivity of this detector.

Further tests will be performed.

### 3.7.5 Thermoelectric cooler

The cooling system is a key feature that influenced the selection of the detector. A liquid nitrogen cooling system could limit the portability of the instrument.

The detector selected employs a thermoelectric cooling based on Peltier effects, reaching a minimum temperature of ~30 K under the environment

## 3.8 Software

The information in binary code obtained during the conversion is stored on computer memory in the format of raw data.

The resulting image is obtained by software able to convert the raw data in an image format.

In the final image, each information obtained by horizontal acquisition corresponds to the gray level of a pixel, and the number of lines scanned corresponds to the vertical dimension.

Control of scanning and acquisition takes place through the computer.

Two special programs have been developed by the electronic service INFN Ferrara, written in Visual Basic on Windows environment:

- Control (Ctrl)
- Scale 2

An open source software is used for opening –processing-saving-images:

- ImageJ.

By the Ctrl software is possible to set the scan area and check the progress of the scanning and acquisition

The scan area is set by the user and includes the length of the run, the vertical pitch and the number of lines to scan.

The unit of measurement used to the motion is the qstep. A qstep corresponds to one motor revolution.

During the scan is possible to check the coordinates of position and the engine status given by control software (Fig. 3.14-4)

Each scanned line scan is saved as a raw format file (.dat) named in sequential numerical order (line0001.dat, line 0002.dat, etc...).

Each .dat file corresponds to one line of pixels of the final image. At the end of the scan all file are stored in the PC hard drive.

The program Scale 2 joins all the scan lines in a single matrix, named lineall.dat, correcting the aspect ratio (Fig. 3.15).

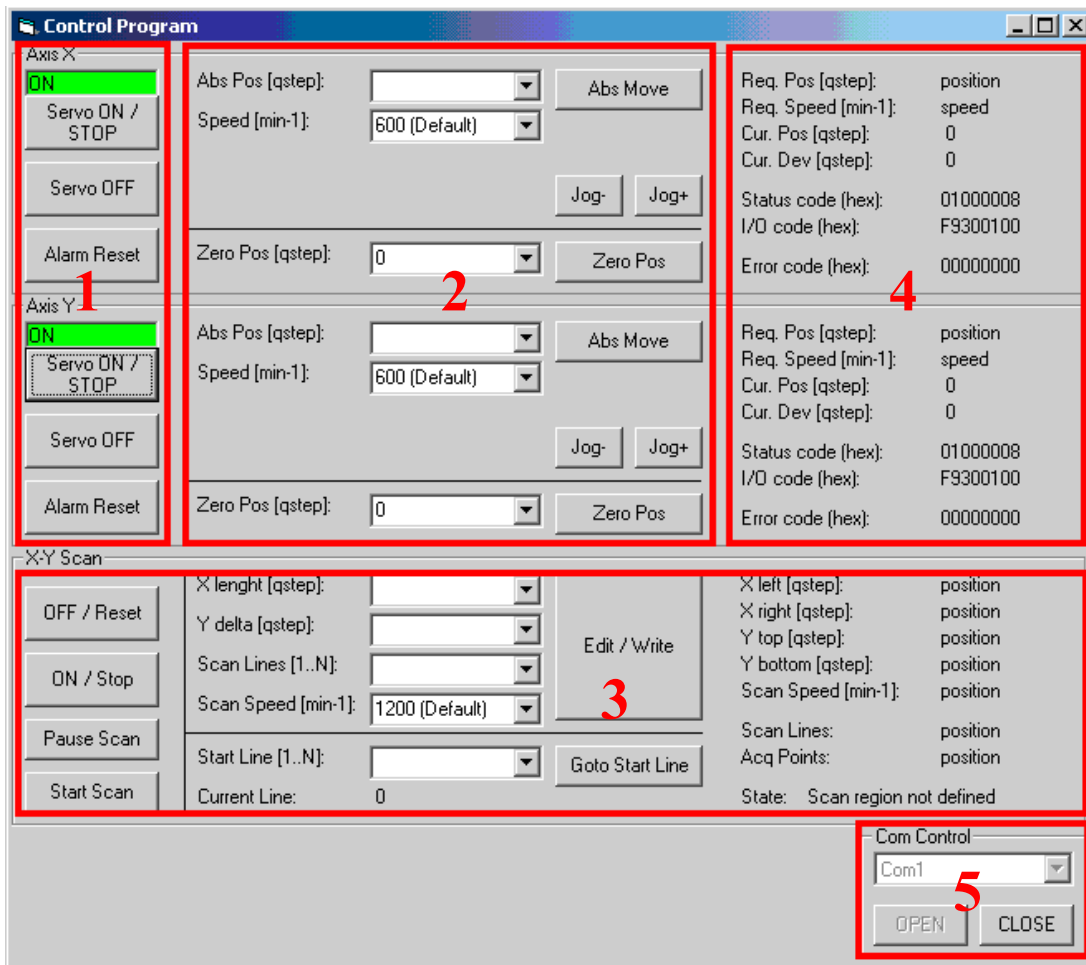


Fig. 3.14. Interface of Ctrl software, 1) Servomotors management; 2) Position settings; 3) Setting of scanning area; 4) coordinates of actual position and engine status; 5) Control of COM-port.

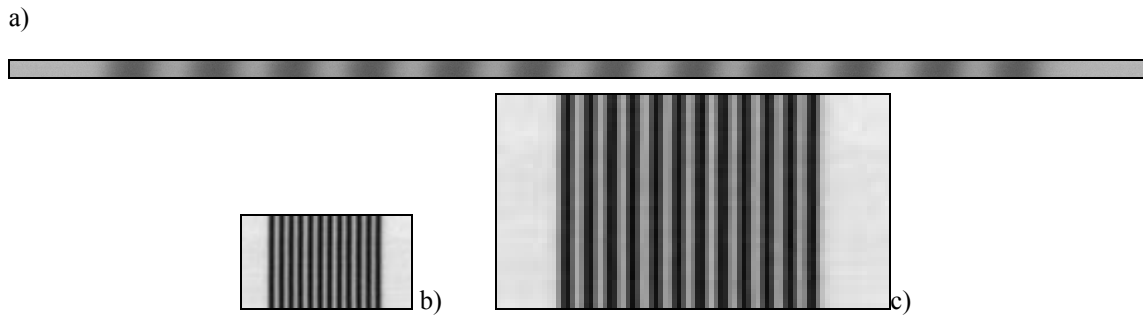


Fig. 3.15. Scan of an optical target 600/600  $\mu\text{m}$ ; a) Image 4000x50 pixel with no scaling; b) Real size image, 80x50 pixel. X-scaling 1:50; c) magnification of b 200x125.

The horizontal acquisition pitch is 5  $\mu\text{m}$ . On the other hand, the vertical sampling is set by user, from 100  $\mu\text{m}$  up. Thus the resulting raw image has a wrong aspect ratio, magnified at least 20 times in the horizontal dimension. Setting this sampling ratio, Scale 2 corrects image size taking the average of the oversampled points.

The raw image obtained is then converted by ImageJ software to other suitable graphic formats.

## References

1. D. Bertani, M. Cetica, P. Poggi, G. Puccioni, E. Buzzegoli, D. Kunzelman, S. Cecchi. *A Scanning Device for Infrared Reflectography*. Studies in Conservation, Vol. 35, 1990, p.113.
2. L. Consolandi, D. Bertani. *A prototype for high resolution infrared reflectography of paintings*, Infrared Physics & Technology, 49, 2007, pp 232 - 242.
3. P. Carcagni, A. Della Patria, R. Fontana, M. Greco, M. Mastroianni, M. Materazzi, E. Pampolini, L. Pezzati. *Multispectral imaging of paintings by optical scanning*; Optics and Lasers in Engineering, vol.45, 2007, pp360-367
4. <http://www.sanyo-denki.com>
5. <http://www.ni.com/>
6. <http://www.reer.it/>
7. <http://www.hamamatsu.com>



---

---

## CHAPTER 4

# SYSTEM OPTIMIZATION

---

---





## 4.1 Optical Target

**A**n optical target has been designed to test the spatial resolution of the scanning system.

The target was drawn by the vector program Adobe Illustrator CS2 and printed by plotter in A3 format on a transparent film. This to avoid the imprecision due to the capillary absorption by paper in the ink jet prints.

In addition, because the ink used in commercial printers is often transparent to infrared, different printing methods have been tested.

The optical target is composed of six series of lines b/w and seven lines of different width.

Series b/w			Lines width $\mu\text{m}$
b/w $\mu\text{m}$	n°lines	lp/mm	
140/140	36	3,57	140
150/150	33	3,30	150
250/250	20	2,00	250
300/300	16	1,60	300
350/350	14	1,42	350
600/600	8	0,83	600
			1000

Tab. 4.1 summary table of series and line present on the optical target

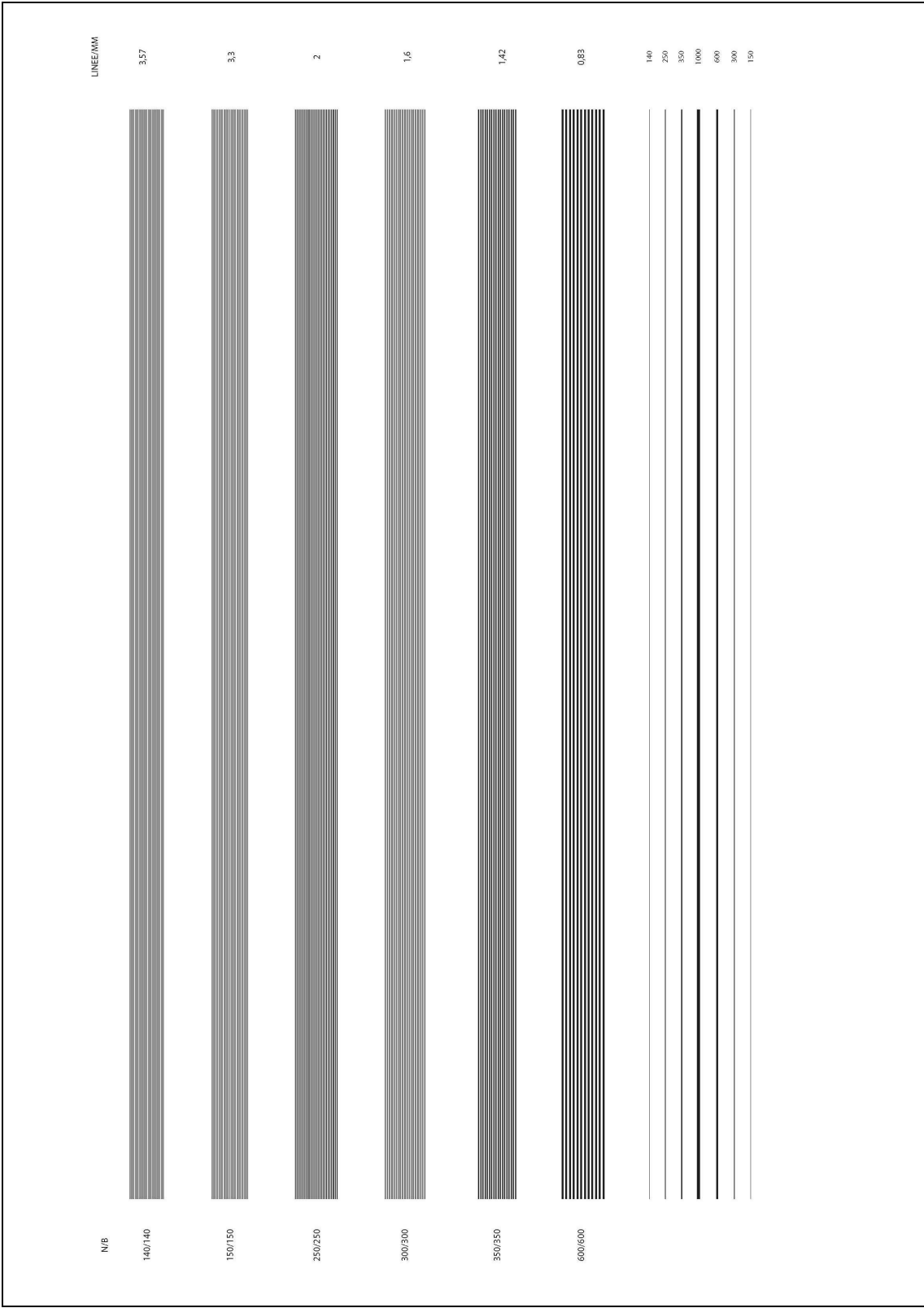


Fig. 4.2. Optical target

## 4.2 Spatial resolution

The spatial resolution has been optimized exploiting the magnification of the binocular microscope.

The two photodiodes employed, Si and InGaAs, have different sizes. Through the magnification of microscope is possible to project different areas of the subject on the photodiode in order to fill the entire size of the active area.

Photodiode	Active area size	Magnification			
		1x	2x	4x	7x
InGaAs	1000	500	250	140	
Si	2400	1200	600	340	
	$\mu\text{m}$	$\mu\text{m}$	$\mu\text{m}$	$\mu\text{m}$	

Tab. 4.3 Dimension of an object projected on the active areas of photodiodes using the magnifications.



Tab. 4.4. Image scanning on the optical target to test the spatial resolution of the scanning system.

The contrast is the minimum distance between two objects close together, which can be viewed as separate by an instrument.

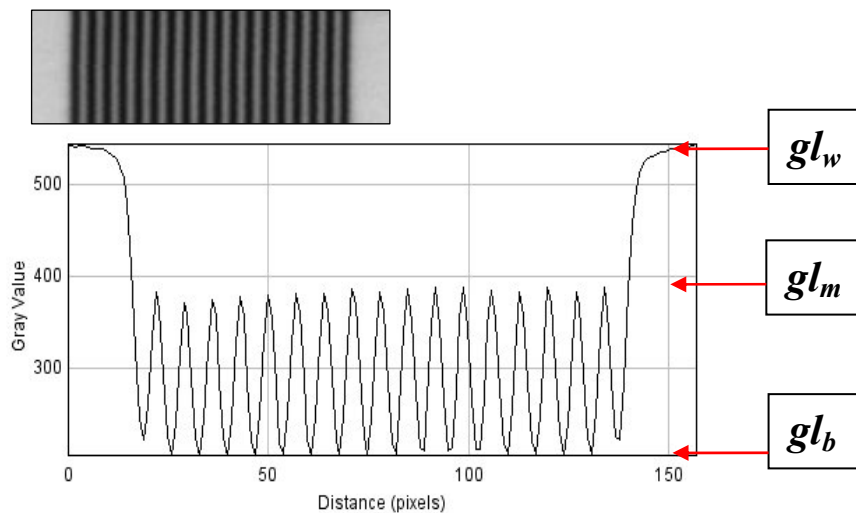
The spatial resolution has been determined by the contrast calculated on grey level values of the image of the line series.

- Gray level of white background ( $gl_w$ ).
- Gray level of black line ( $gl_b$ )
- Middle gray level of a white line ( $gl_m$ )

In this case the contrast definition of Weber is used.

$$C = \frac{\Delta I}{I_B} = \frac{(gl_m - gl_b)}{(gl_w - gl_b)}$$

With  $I$  and  $I_B$  representing, respectively, the luminance of the features and the background luminance. Weber definition of contrast is used to measure the local contrast of a single target of uniform luminance seen against a uniform background [3].



Tab. 4.5. The  $gl$  values are obtained from a plot profile of the series b/w.

The following tables are presented a summary of the results obtained for the single photodiodes InGaAs and Si.

A contrast of about 30% is considered enough to the aim of underdrawing detection.

InGaAs photodiode has an active area smaller than the Si photodiode; it has reached a resolution of 2lp/mm using 4x magnification.

The 7x magnification does not increase considerably the spatial resolution of InGaAs detector because it limits the passage of IR reflected reducing the  $gl$  range. According to

table 4.3 the photodiode distinguishes a series of 140/140  $\mu\text{m}$  using 7x magnification but the contrast is very low, thus it is not useful. The images is available in figure 4.8 Si photodiode has larger active area rather large of 2,4 mm. The 7x magnification is necessary to reach a resolution comparable to InGaAs photodiode (Fig. 4.9). On the contrary its spread of  $gl$  values is larger than that of InGaAs.

InGaAs									
Active area size	1 mm $\varnothing$								
magnification		4x				7x			
b/w $\mu\text{m}$	lp/mm	$gl_w$	$gl_b$	$gl_m$	C %	$gl_w$	$gl_b$	$gl_m$	C %
140/140	3,57	Not detectable				Not detectable			
150/150	3,30	Not detectable				Not detectable			
250/250	2,00	529	222	320	<b>32</b>	390	226	277	<b>31</b>
300/300	1,60	543	212	353	<b>42</b>	395	226	283	<b>33</b>
350/350	1,42	529	200	384	<b>55</b>	397	218	308	<b>50</b>
600/600	0,83	540	177	455	<b>76</b>	397	196	357	<b>80</b>

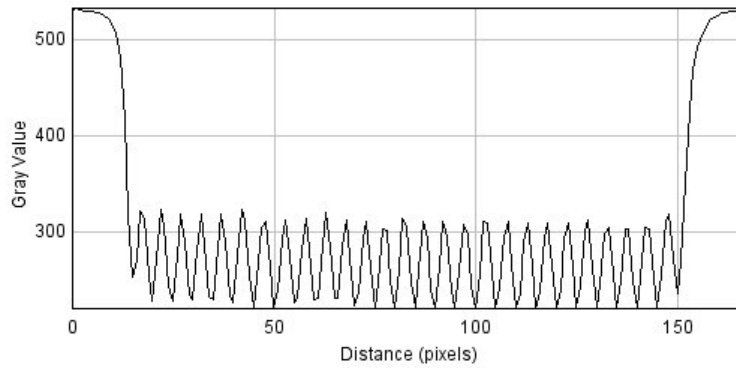
Tab. 4.6. Results for InGaAs photodiode.

Si									
Active area size	240x240 mm								
magnification		4x				7x			
b/w $\mu\text{m}$	lp/mm	$gl_w$	$gl_b$	$gl_m$	C %	$gl_w$	$gl_b$	$gl_m$	C %
140/140	3,57	Not detectable				Not detectable			
150/150	3,30	Not detectable				Not detectable			
250/250	2,00	Not detectable				615	232	340	<b>28</b>
300/300	1,60	Not detectable				624	206	379	<b>41</b>
350/350	1,42	Not detectable				627	181	416	<b>52</b>
600/600	0,83	1122	285	830	<b>65</b>	629	139	545	<b>82</b>

Tab. 4.7. Results for Si photodiode.

## InGaAs

4x

250/250  $\mu\text{m}$ 

7x

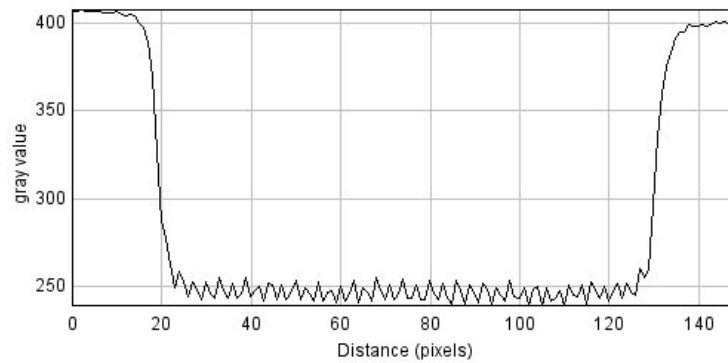
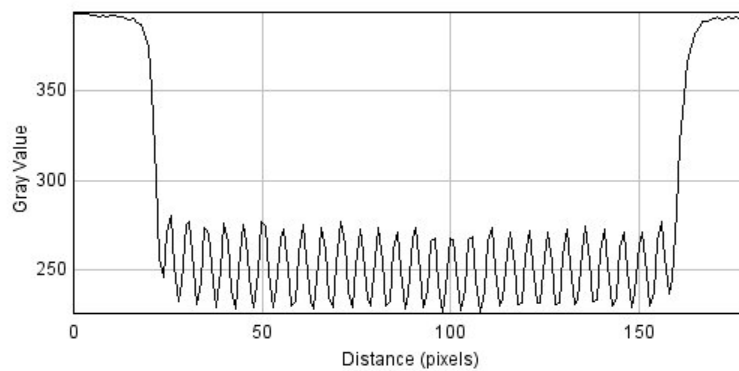
140/140  $\mu\text{m}$ 250/250  $\mu\text{m}$ 

Fig. 4.8. The images and respectively plots for the main results of InGaAs photodiode.

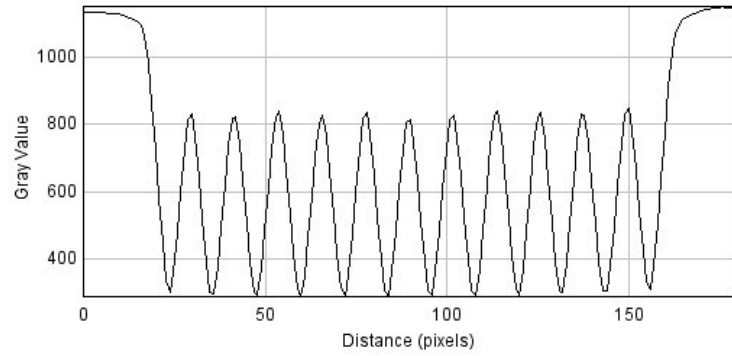
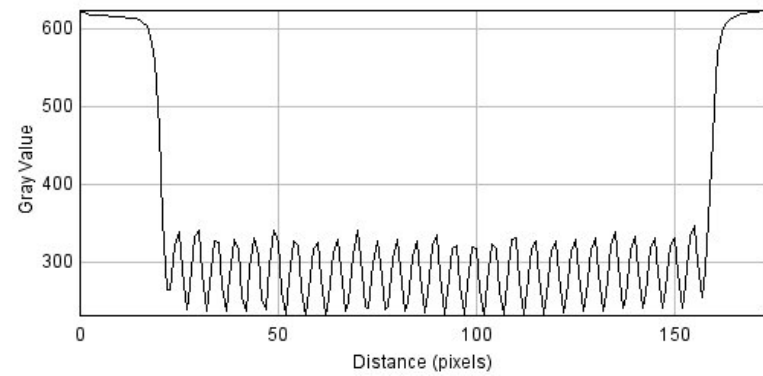
**Si****4x**600/600  $\mu\text{m}$ **7x**250/250  $\mu\text{m}$ 

Fig. 4.9. The images and respectively plots for the main results of Si photodiode.

### 4.3 Overheating reduction

In the Chapter 3 has been introduced the filtration of the lamps to avoid the overheating of the painting (Fig. 3.8.).

The overheating effect was due to the prolonged illumination of the object with halogen lamps. These, even if they move with the optical system, illuminate a wide area of the painting. This causes the overheating of the painting with subsequent thermal emission from this, in addition to the IR reflection detected.

In the resulting image, the thermal emission causes an increase in brightness as the scan proceeds.

The filtration of the lamps using: a diaphragm, a silicon plates and a quartz lens, had carried to a reduction of this effect.

The overheating effect was found in the first applications on painting with dark background.

#### 4.3.1 *“Return of Prodigal Son”*

The artwork, belonging to a private collection, is probably contemporary copy of a painting by Guercino in 1619 conserved in the *Kunsthistorisches Museum* in Vienna, depicting the return of the prodigal son.

The wide band IR Reflectography has been performed with the aim to verify if there was an underdrawing. There, it is reported concerning the overheating effect.

The painting, of relatively large size (80x130 cm), was scanned in seven sections (Fig. 4.11.).

Each image scanned shows the overheating effect. An example is in figure 4.12, the plot profile shows the increasing of gray level values in a uniform region, from 20 up to 60. Particularly evident is, in figure 4.13, the presence of different bands due to repeated stops of the scan.

The images have been adjusted and stitched by software obtaining a fairly good result (Fig. 4.14).





Fig. 4.10. Attributed to Guercino, “Return of the Prodigal Son”, oil on canvas, XVII century, private collection



Fig. 4.11. Reflectographic images acquired by scanning device illuminating with lamps and no filters. Each image corresponds to one scan.

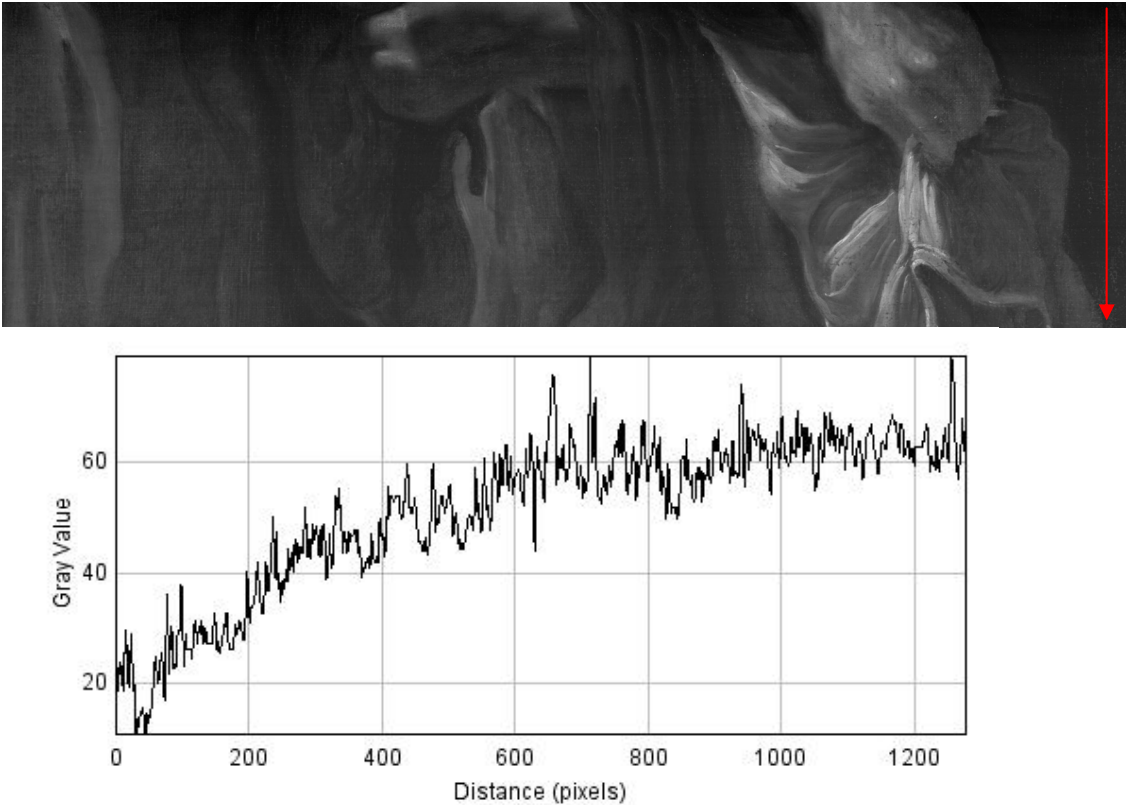


Fig. 4.12. Reflectographic image and plot profile of pixels along the red arrow.

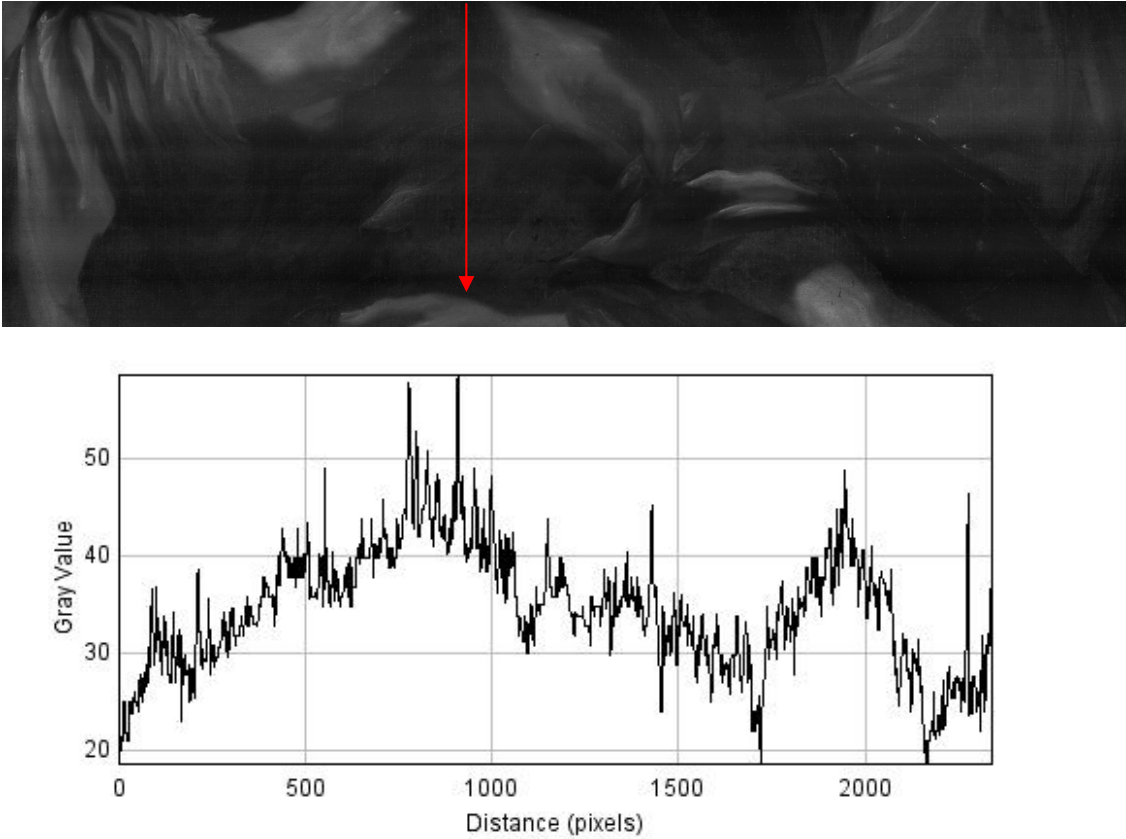


Fig. 4.13. Reflectographic image and plot profile of pixels along the red arrow.



Fig. 4.14. Correction and stitching of reflectographic images scanned.



Fig. 4.15. Detail of IR reflectography with incremented contrast compared to visible. Some lines of underdrawing are recognizable along the nose, mouth and chin.

The reflectographic image highlights the texture of the canvas and in the profile of the son is possible to recognize some lines that may correspond to an underdrawing (Fig. 4.15.).

### 4.3.2 “*Maddalena penitente*”

Another example of a painting of dark background and large dimension (125x95 cm), where the overheating effect has been found, is “*Maddalena penitente*”. It is oil painting on canvas of 16th century recently restored. The old damages have been highlighted by the image diagnostics.

In the image acquired with no filter of the lamps shows an evident thermal emission proceeding downwards, in the sense of the scan (Fig. 4.17).

The plot profile highlights a stop after 850 lines scanned. The scan was restart after an enough time to allow a small drop in temperature such as to slightly decrease the values of the gray levels. However, the brightness resumes growing, assuming a difference of gray level values of about 140.

The first part of curve in the plot profile is similar to the emission curve of black-body, with a sudden rise, after the start, and a subsequent *plateau*.

After 1600 scanned lines was necessary to stop the scanning.

A second test has been performed with the filtration of the lamps. The thermal emission is more reduced. Comparison the plots profile is possible to observe that the thermal emission has been reduced obtaining a difference of gray level values of 30 (Fig. 4.18).

The reduction of overheating effect had allowed the entirely scanning of the painting with no stop. The reflectographyc image highlights the retouch on the surface (Fig. 4.19).



Fig. 4.16. *Maddalena penitente*, 16<sup>th</sup> century, oil on canvas, private collection

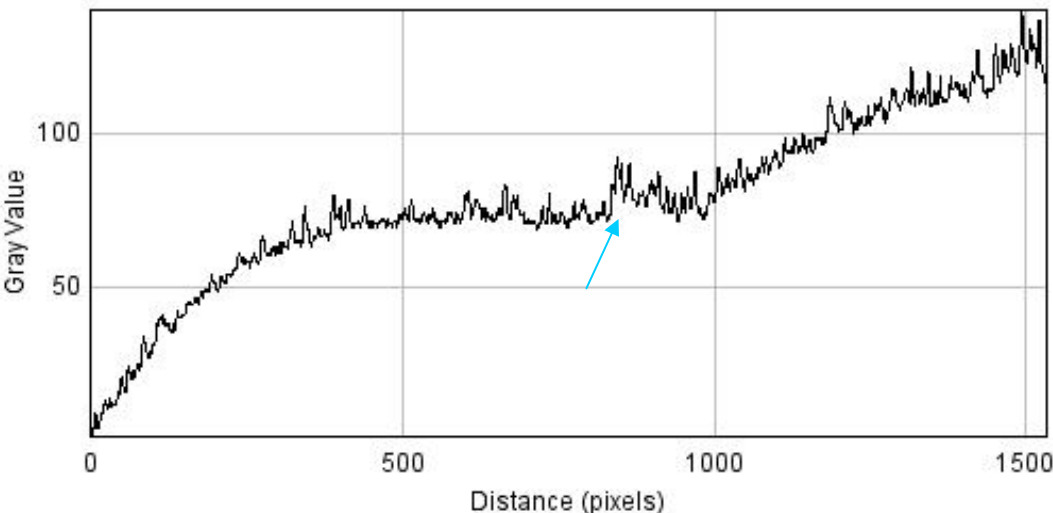


Fig. 4.17. Reflectographic images acquired by scanning device with InGaAs detector with lamps no filter. The plot profile corresponds to the line of pixels along the red arrow. The blue arrow indicates the stop and restart of the scanning.

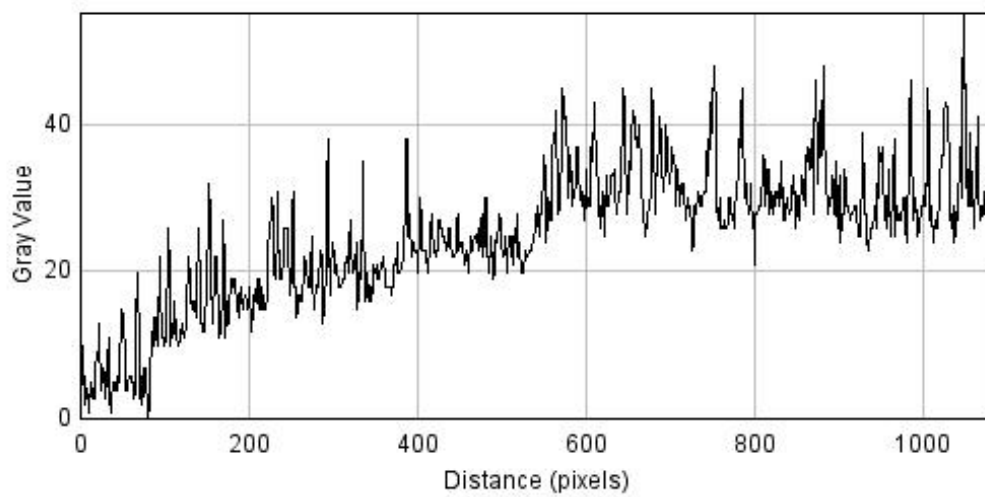


Fig. 4.18. Reflectographic images acquired by scanning device with InGaAs detector with filtered lamps. The plot profile corresponds to the line of pixels along the red arrow.

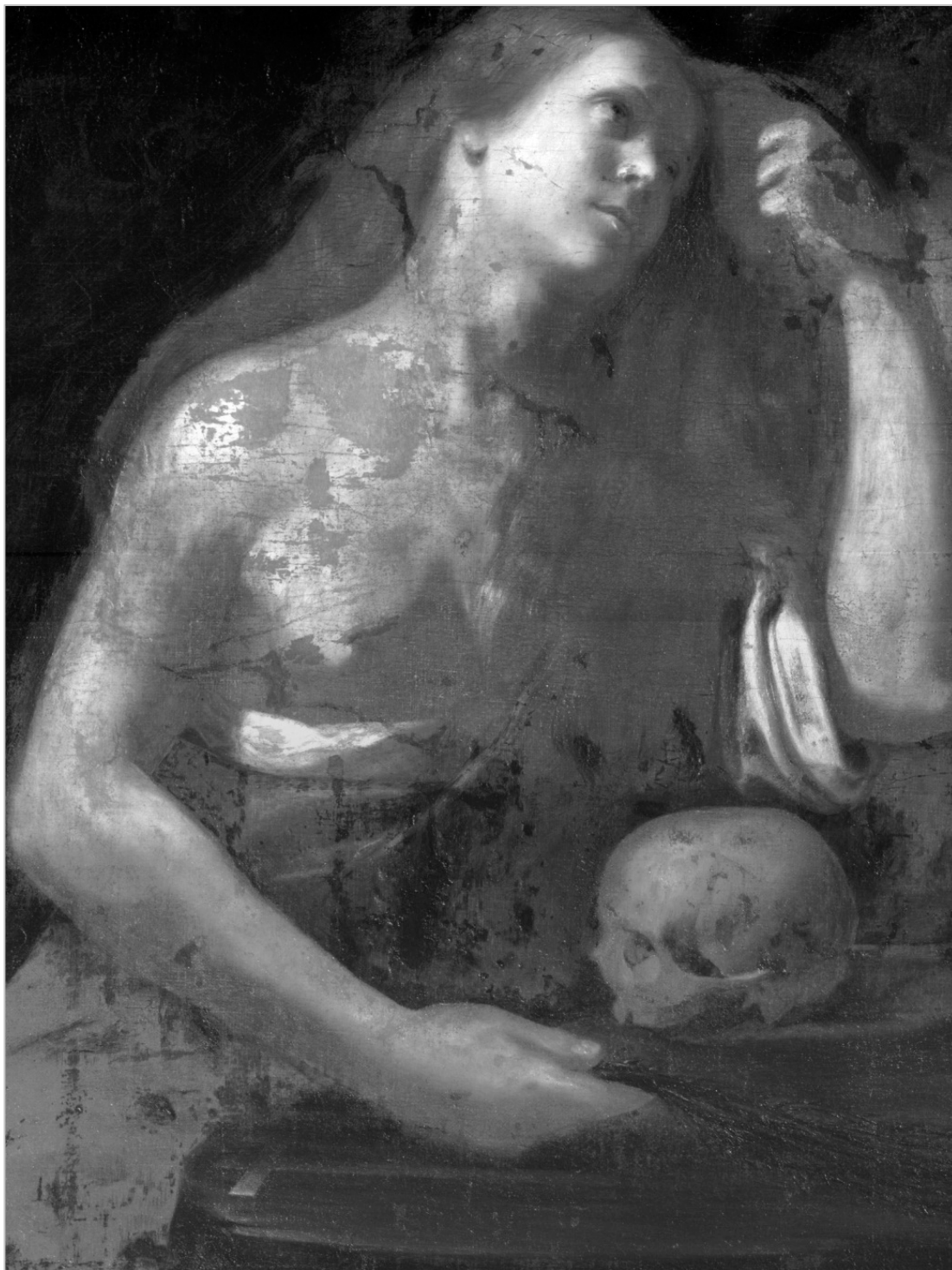


Fig. 4.19. Reflectographic scanning with InGaAs detector with filtered lamps. It was acquired in a one scanning with no stop.



**References**

1. B. Jähn. *Image processing for scientific applications*. CRC Press, New York, 1997.
2. S. W. Smith. *The Scientist and Engineer's Guide to Digital Signal Processing*, California Technical Pub, 1999.
3. E. Peli, R. B. Goldstein, *Contrast in images*, in Visual Communication and Image Processing '88, T.R. Hsing, ed., Proc. Soc. Photo-Opt. Instrum. Eng. 1001, 521-528, 1988.
4. X. P.V: Maldague. *Theory & practice of infrared technology for non-destructive testing*. Wiley, 2001



---

---

**CHAPTER 5**

**APPLICATIONS**

---

---



## 5.1 Virgin with Child and Saints

Artist: Giovanni da Mel

Period: about 1530

Technique: tempera on wood

Size: 270x160 cm

Location: Church of St. Mary, Mel, Belluno

Diagnostics requested by the conservator in charge of the restoration by the *Soprintendenza del Veneto*

### ***Purpose***

The painting depicting the enthroned Virgin and Child with Saint Roch and Saint Sebastian, was subjected to several restorations and remaking over the centuries.

The purpose of the diagnostics stage was to distinguish the original remains. To this aim, the X-ray digital radiography was the first requested.

The work was made before restoration.

The painting showed a poor conservation status. Pieces of Japanese paper covered several areas of surface to avoid detachments. A wood structure was superimposed to the panel for transport safety.

The application of wide band IR reflectography has been proposed to, the following aims.

- Investigating the underdrawings in the more interesting areas: Virgin and Musicians. Probably original areas.
- Possibly integrating RX results.
- Testing the capability to investigate the painting under the patches of Japanese paper.

Due to the large size of painting, the scan was made on a limited portion to be consistent with the time available. In this case, about eight hours.

**Results**

The X-ray radiography had shown several layers of painting made by different material with different X-ray absorptions. The interpretation was made more hardly due to the poor state of original pictorial film and the superposition of many restoration layers.

Clear islands of paint film in the radiography are the original painting (Fig. 5.5.d).

In the wide band IR reflectography these areas appear darker (Fig. 5.5.b).

Here the white areas correspond to the more superficial layer that is the more recent.

Figure 5.3 shows that from the lighter areas to darker areas there are intermediate gray levels. This means that several layers superimposed are present.

The wide information, dept, due to 12 bit acquisition, allows to clear the patches of Japanese paper using the editing software Photoshop (Fig.5 .2 and 5.4)

In the patch areas has been subtracted a value of grey level obtained by the average of an adjacent area. By this way the reading continuity of the result is preserved.

The same adjustment has been made on the radiography to delete the wooden crosspieces mounted on the backside.

The presence of underdrawing has been detected in some details: in the reflectographic image of musicians, in figure 5.5, is possible to recognize some line of unedrrawing in the face of righter figure end in its cloth.



Fig. 5.1. G. Da Mel, *Virgin with Child and Saints*, XIV century, tempera on wood Courtesy of Soprintendenza del Veneto



Fig. 5.2. a) Reflectographic scanning with InGaAs detector; b) Detail in visible light; c) Detail of reflectography; d) Detail corrected by software with removal of the patch.



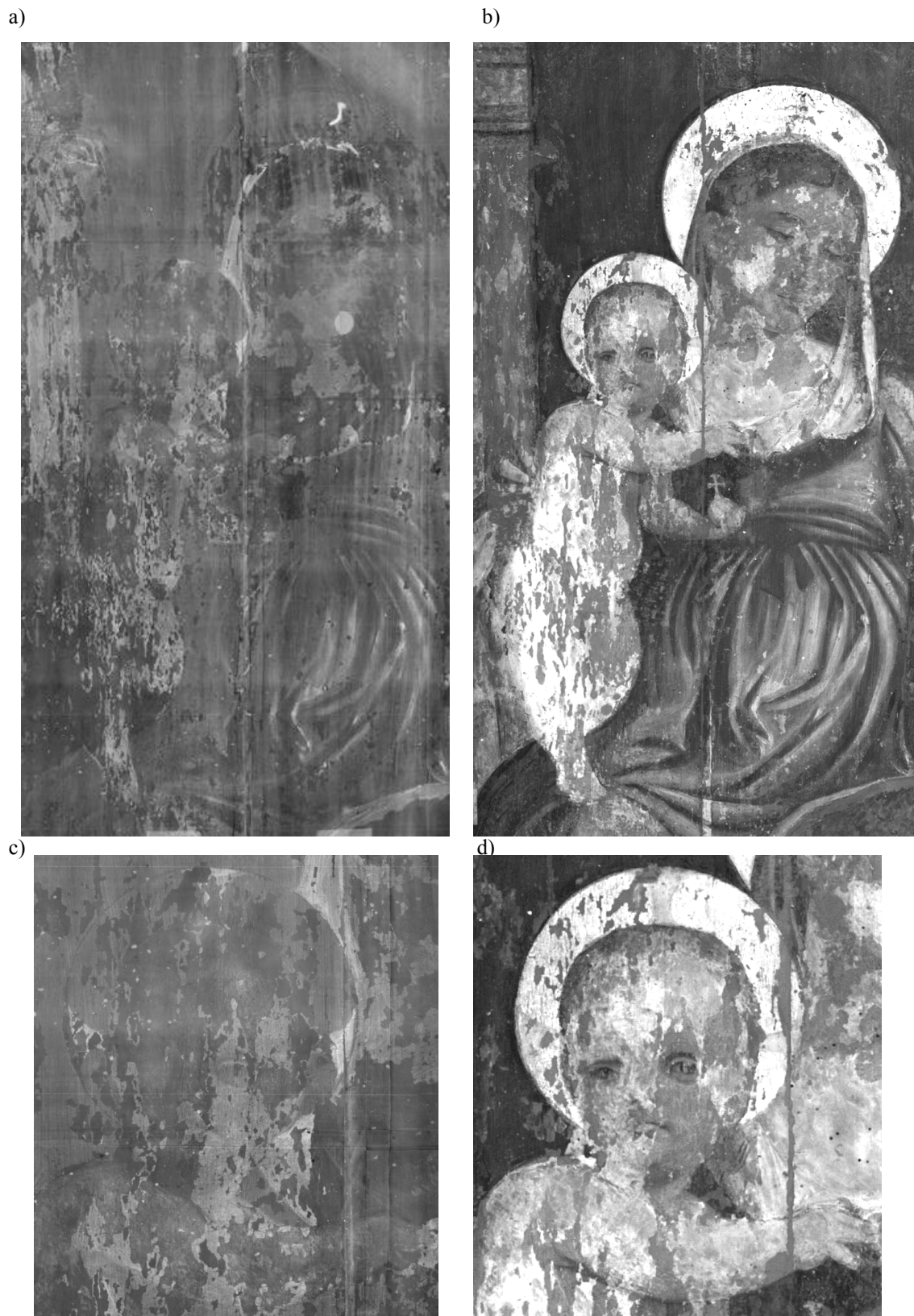


Fig. 5.3. a) Detail of X-ray radiography; b) IR reflectography corrected by software with removal of the patch; c) Radiographic detail of the child; d) IR reflectography of the detail (c).

a)



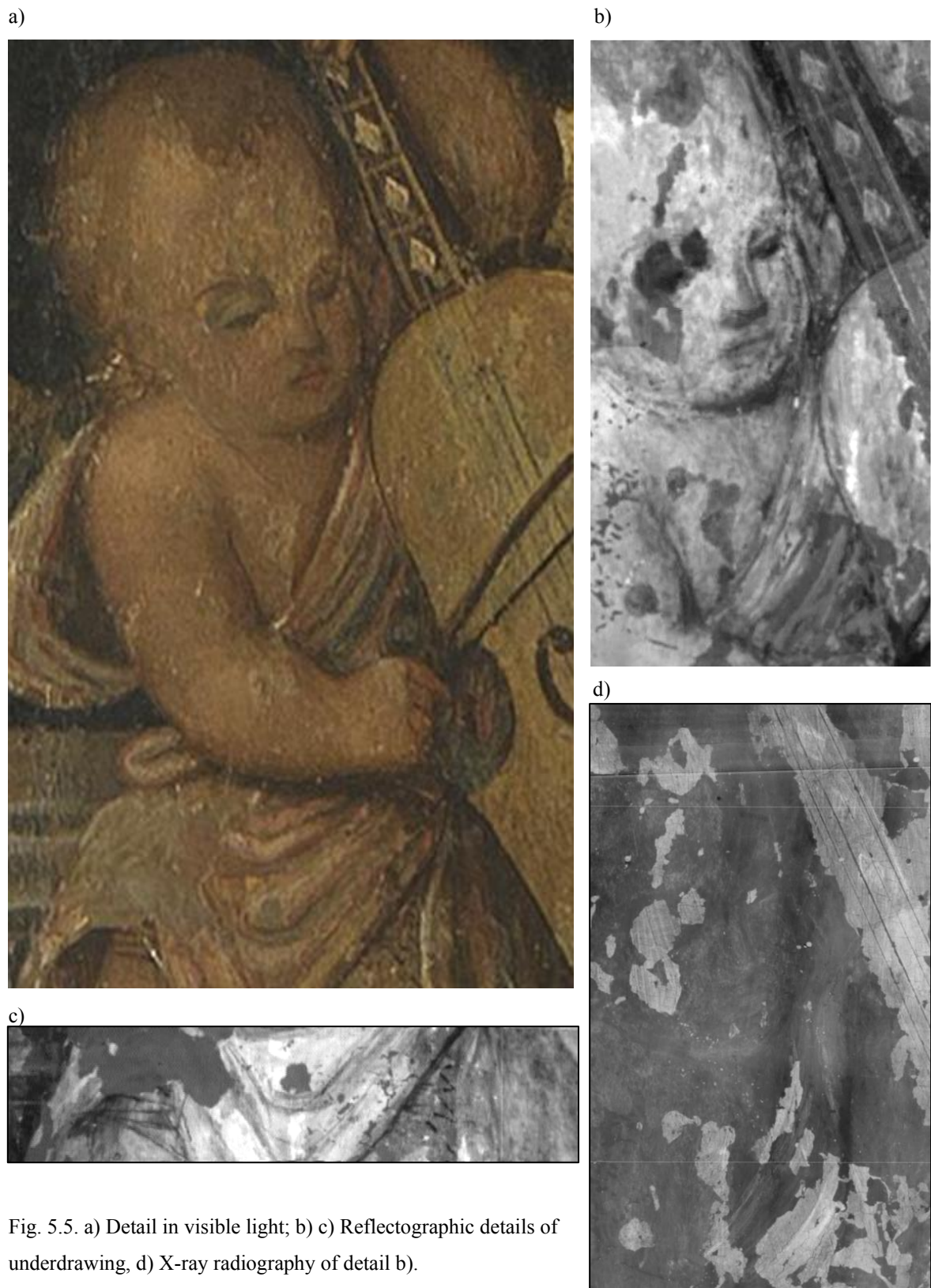
b)



c)



Fig. 5.4. a) Detail in visible light; b) Reflectographic scanning with InGaAs detector; c) Detail corrected by software with removal of the patch.



## 5.2 Portrait of Cardinal Mazzarino

Artist: unknown

Period: 17th century

Technique: oil on canvas

Size: 80x60

Location: private collection

### *Purpose*

The painting, with dark background, is a three-quarter portrait of Cardinal Mazarin. Behind the figure there are inscriptions relative to the character portrayed.

It has been repainted and relined, probably in the 20<sup>th</sup> century.

The diagnostic protocol has been applied to investigate the conservation status.

Infrared Reflectography with Silicon CCD got interesting results, carrying different consideration on the original features.

The wide band IR Reflectography has been applied to clarify how the most recent over-painting has influenced the current aspect of the subject.

### *Results*

The IR Reflectography by Si CCD in figure 5.7 had showed (Fig. 5.7.):

- the upturned mustache are posterior to the first version of the portrait;
- an insert of canvas is present in the upper part of the painting, due to relining.

The scanning with InGaAs detector shows that the insert is constituted by a different type of canvas (Fig. 5.8. a). Moreover, the guidelines draw under the inscription on background are clearly visible (Fig. 5.8. b).

The underdrawing is present also on the insert of canvas, as well as the skullcap of the cardinal.

Upturned mustache, skullcap and inscription on the background are identifying characteristics of the character to Cardinal Mazzarino. Thus is possible to conclude that the person portrayed was probably another character that assumed the features of Cardinal Mazarin after the restoration.

Following the diagnostics study, the original portrait was recovered by removing the over-painting by laser cleaning.



Fig. 5.6. *Portrait of Cardinal Mazzarino*, 17<sup>th</sup> century, oil on canvas, private collection.



Fig. 5.7. Detail of IR Reflectography with Si CCD

a)



b)

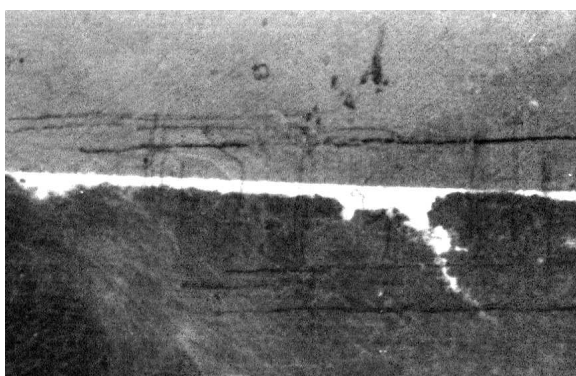


Fig. 5.8. a) Reflectographic scanning with InGaAs detector; b) detail of the drawing under the inscription in the upper right

### 5.3 Landscape by Guglielmo Ciardi

Technique: oil on wooden panel

Artist: Guglielmo Ciardi, signed

Period: second half of 19th century

Size: 20x15 cm

Location: private collection

#### *Purpose*

The painting is a small table representing a country landscape characterized by thin pictorial film.

The purpose of the diagnostics session was obtaining information on the art materials by non-invasive techniques.

For this aim, Image Spectroscopy<sup>1</sup> has been applied and wide band IR Reflectography has been used to observe the behaviour of pigments in the wavelength range of 1 - 2,5  $\mu\text{m}$ .

#### *Results*

The Image Spectroscopy showed all details of underdrawing at 790 nm (Fig. 5.10.). Thus, the wide band could not add anything more to the detection of this.

However, the infrared image in a different spectral band (Fig. 5.11.) allows different consideration.

The blue pigment of the mountains appears transparent in the sensitivity range of silicon, while appear darker in the wide band range.

---

<sup>1</sup> The Image Spectroscopy device has a spectral range from 410 up to 910 nm and is equipped with interferential filters 10nm wide.



The reflectance spectrum obtained by Image Spectroscopy shows a peak about 480-500 nm and high reflectance from 690 nm. As suggested by wide band reflectography, the diffuse reflectance should drop between 1 and 2,5  $\mu\text{m}$ .

Comparing these results with the reference spectra of IFAC-CNR database [4] it turns out that this behaviour may be compatible to a cobalt-based blue pigment (Fig. 5.13.).



Fig. 5.9. G. Ciardi, landscape, 19th century, oil on wood, private collection.



Fig. 5.10. Image acquired by Image Spectroscopy device at 790 nm, with indication of the measurement point of the spectrum.



Fig. 5.11. Wide band IR Reflectography with InGaAs detector.

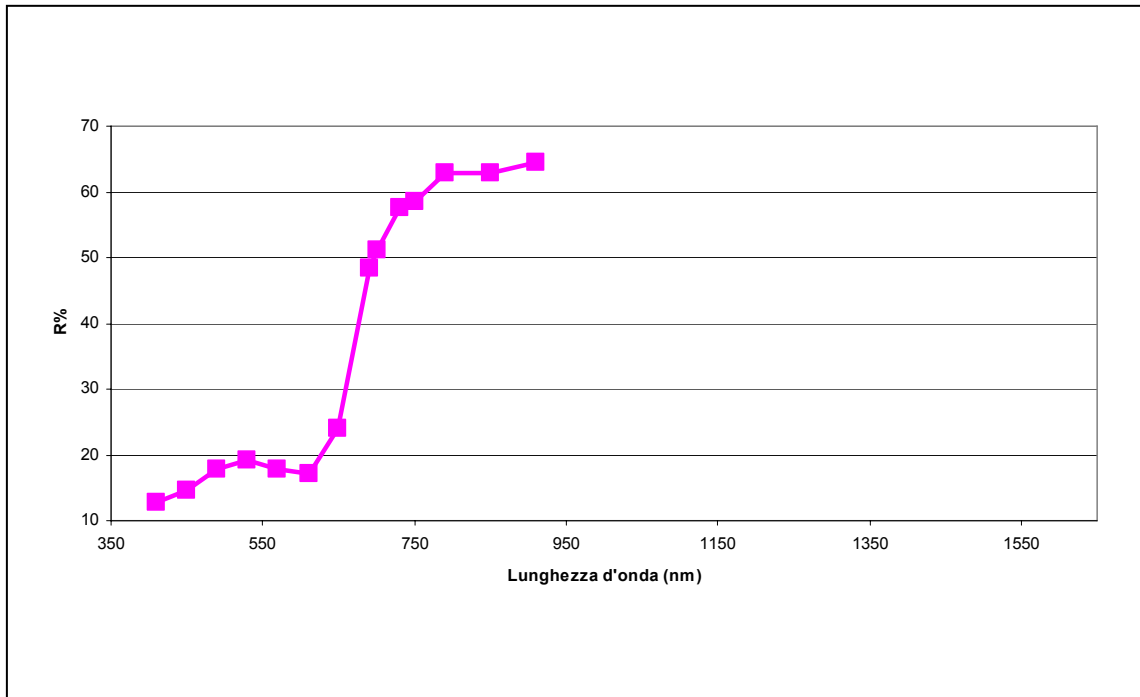


Fig. 5.12. Spectrum obtained by Image Spectroscopy on the blue pigment of the mountains.

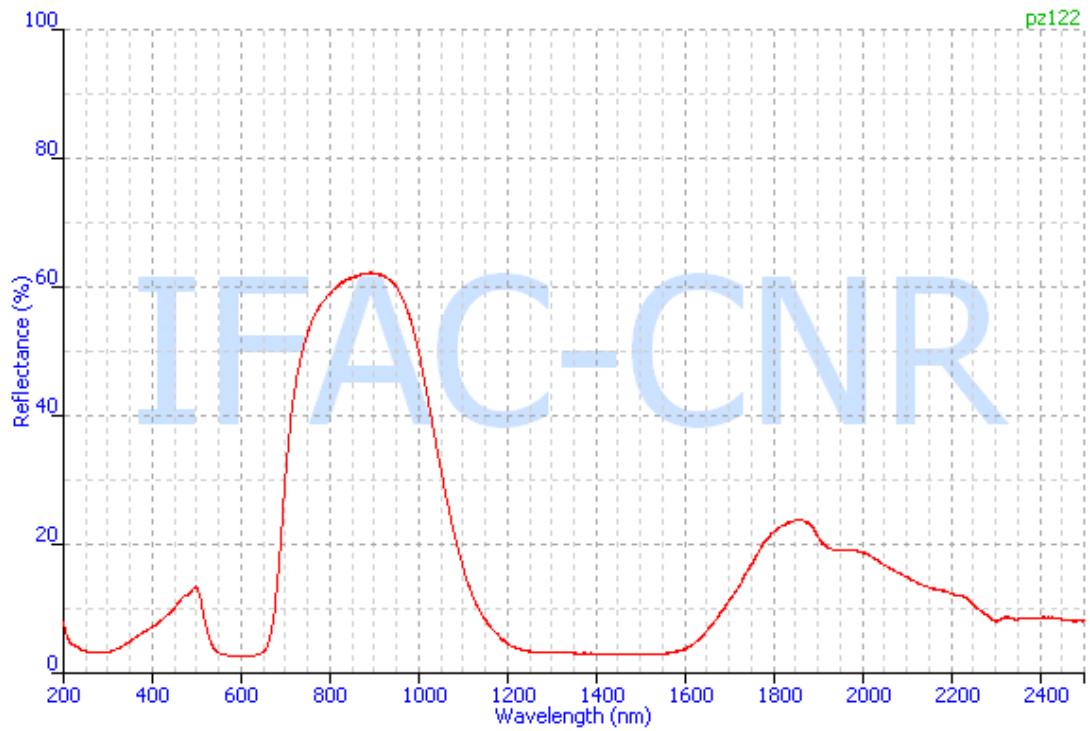


Fig. 5.13. Spectrum of Cobalt Blue available in IFAC-CNR database [4].

## 5.4 Flowers

Technique: oil on paper

Artist: Gabriella Nardozi, signed

Period: 1889, dated: “18 settembre 1889”

Size: 38x 29 cm

Location: private collection

### *Purpose*

The artist reproduces the flowers in a very realistic way, like in a herbarium.

This painting of academic features is characterized by very fine technique. The paint is made by thin and uniform layer on not treated paper.

The purpose was to investigate the underdrawing with IR Reflectography.

### *Results*

The infrared Reflectography with Silicon CCD detected the underdrawing in several part of the painting: along the edge of the white petals, where the paint layer is thinner, and under the light green of the leafs (Fig. 5.17.a).

On the contrary, the dark green appears in the sensitivity range of Si more adsorptive, preventing the detection of underdrawing.

The wide band IR Reflectography has been applied to improve the results obtained with Si CCD.

In the image acquired by InGaAs detector, both green pigments, have shown the underdrawing (Fig. 5.16.). Moreover, the drawing under the white pigment, hardly recognizable by Silicon detector, appears here well clear (Fig. 5.17.)



Fig. 5.14. G. Nardozi, Flowers, 1889, oil on paper, private collection.



Fig. 5.15. Reflectographic image acquired by Si CCD.



Fig. 5.16. Reflectographic image acquired by scanning device with InGaAs detector.

a)



b)



Fig. 5.17. Comparison of a detail. a) IR Reflectography acquired by Si CCD; b) IR Reflectography acquired by InGaAs detector.

## 5.5 Landscape 20<sup>th</sup> century

Technique: oil on round wooden panel

Artist: unknown

Period: first half of 20<sup>th</sup> century

Size: Ø 35 cm

Location: private collection

### *Purpose*

The painting depicts a country landscape. It has a particular round structure. The wooden support consists of a cask cover with a thin strip of leather along the edge. On the verso a thick layer of paper is glued on wood (Fig. 5.18.b).

The diagnostic study was made to investigate the conservation status and the structure of the support. Thus, the completely image diagnostics protocol has been applied.

### *Results*

The IR reflectography using Silicon CCD shows nothing more than visible to the eye (Fig. 5.19.). In the image acquired by scanner with InGaAs detector is possible to see several rectangular inserts under the pictorial layer. Moreover, an anomalous white cloud appears in the sky. In this area the pictorial layer has a higher reflectance in the range 1000-2500 nm (Fig. 5.20.).

The digital X-ray radiography revealed that the white cloud was the headgear of the portrait of a lady, covered by a complete overpainting of the workpiece (Fig. 5.21.).

In the X-ray radiography the rectangular inserts aren't detected, probably because they are pieces of paper used to obtain a uniform background. Instead, the radiography reveals the presence of a canvas under the pictorial layer.

Also in this case, the wide band IR reflectography has detected details not visible to the Si CCD and, at the same time has obtained information complementary to the X-ray radiography



a)



b)



Fig. 5.18. Landscape, oil on wood, private collection, a) recto, b) verso.



Fig. 5.19. Reflectographic image acquired by Si CCD.

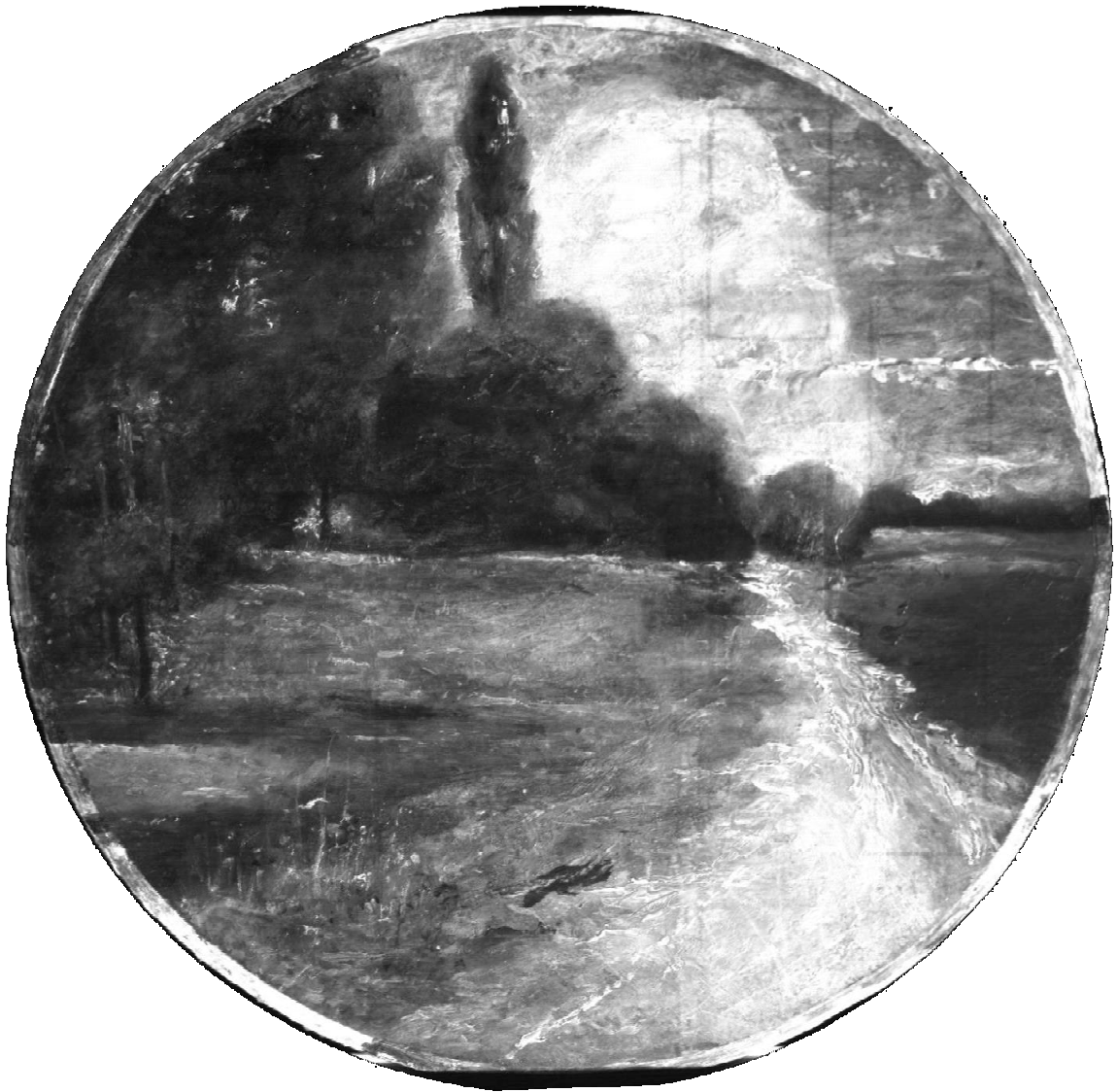


Fig. 5.20. Reflectographic image acquired by scanning device with InGaAs detector.



Fig. 5.21. Digital X-ray radiography.

## 5.6 Five paintings by the same artist: Edoardo Pazzini

Edoardo Pazzini was born in 1887 in Verrucchio (Rimini) and died in Rimini in 1967. He was a landscape painter that has portrayed the most evocative places all around his birthplace.

Five paintings have been studied to investigate the evolution of execution technique on his artworks. The results of wide band IR Reflectography will be discussed.

The pastel dated 1926 depicts a landscape of San Marino (Fig. 5.22.). It is a painting of the early period of Pazzini.

The vivid colors conceal the sketch created by the gray, used also to write the date in the lower left.

In the reflectographic image the gray crayon appears dark, highlighting the drawing that outlines the contour of the houses and the branches of trees (Fig. 5.23.).

*“Lungo la strada a Padullio con donna e anitre”* is a oil on cardboard (Fig. 5.24.).

In this painting the stains of color describe the landscape. People and animals are represented with the fluid color. In particular, two central animals are recognizable only in the reflectographic image because, in visible light, they tend to be confused with the gray of the road.

The artist used to write notes on the backs of his paintings, made more readable by IR reflectography by InGaAs detector even under the framing paper (Fig. 5.26.). This painting on the back is full of information, including the date 12/12/43, written under the title (Fig. 5.26. b) and 12.11 *“terminato prima seduta”*.

Moreover, the InGaAs detector reveals that under the framing tape some lines of squaring are present (Fig. 5.26. d).

In this case the lines are present on the backside, in *“L’azzurra vision di San Marino”* (Fig. 5.27.) are on the recto.

In this oil on cardboard the lines of squaring are visible in the reflectographic image in the lower area. On the contrary the signature disappears, due the transparence at IR of the red pigment (Fig. 5.28.).

Also in this case the backside is full of writing, but the readability is made more difficult by the texture of the covering paper. The reflectographic image reveals several inscriptions by pencil not visible in the figure 5.29. On the contrary the ink on the label and of the stamp disappears.

“*San Leo*” and “*Oxen*” are paintings of the artist's maturity. In these paintings the brushstroke became the main feature to outline the forms.

The squaring of space remains visible along the edges, profiting of the superimposition of frame without the need to observe the IR reflectography.

Observing the relectographic image is possible to see the fluid brushstrokes of “*San Leo*” (Fig. 5.32) opposed to those, brief and sharp, of “*Oxen*” (Fig. 5.34).

These fleeting considerations do not want to be an exhaustive description of the artistic technique of Edoardo Pazzini. They are aimed to giving an overview of the potential of wide band IR reflectography, not only to investigate the underdrawing, but to deepen the execution techniques of a contemporary artist.



Fig. 5.22. E. Pazzini, *Landscape of San Marino*, 1926, crayon on paper, 40x30 cm private collection.



Fig. 5.23. Reflectographic image acquired by InGaAs detector.



Fig. 5.24. E. Pazzini, *Lungo la strada a Padullio con donna e anitre*, 1943, oil on cardboard, 20x30 cm, private collection.



Fig. 5.25. Reflectographic image acquired by InGaAs detector.



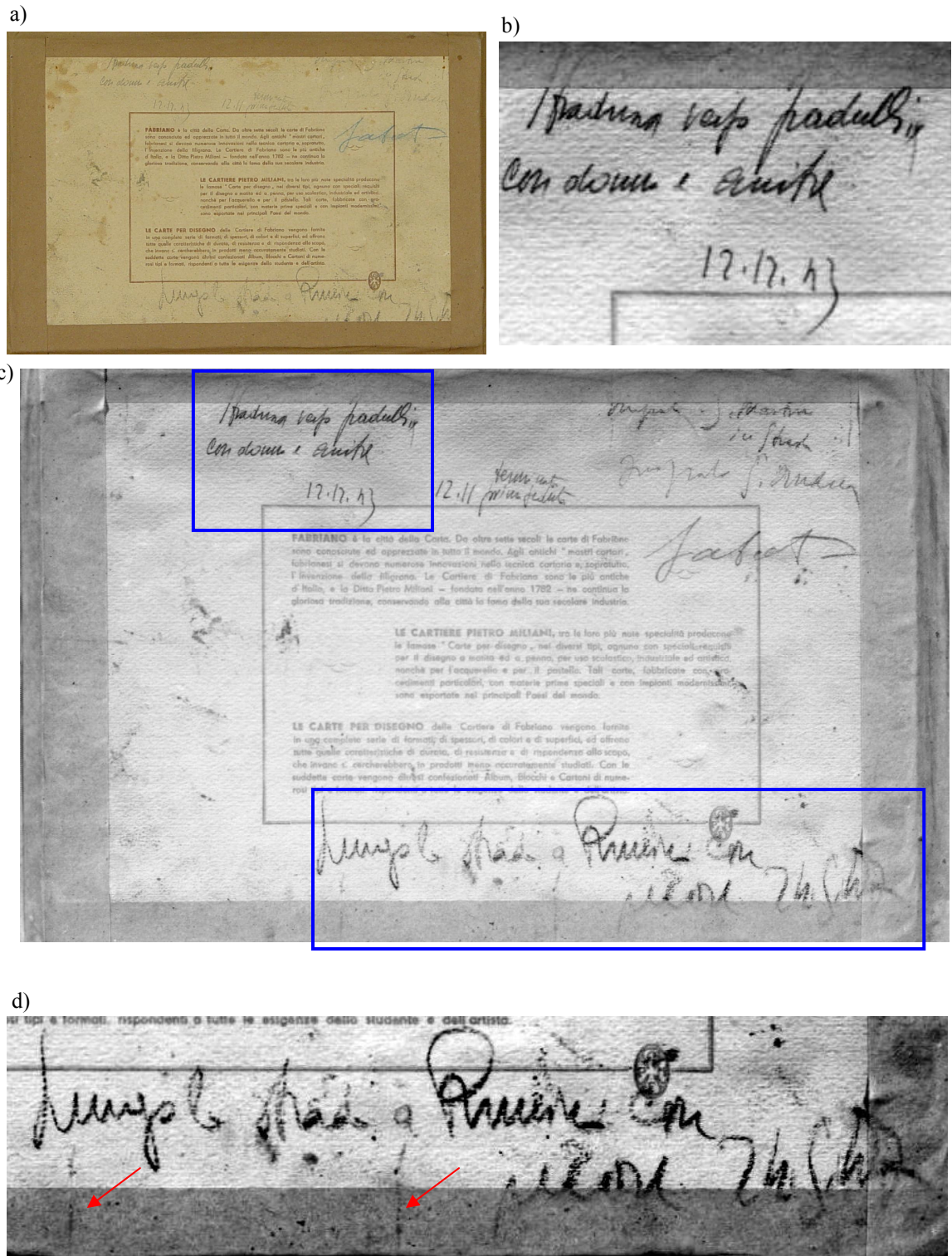


Fig. 5.26. Lungo la strada a Padullio con donna e anitre, Verso. a) Image at visible light, b) detail of IR reflectography; c) Reflectographic image acquired by InGaAs detector with indication of details; d) detail of IR Reflectography with indication of the squaring;



Fig. 5.27. E. Pazzini, *L'azzurra vision di San Marino*, 40s years, oil on cardboard, 40x30 cm, private collection.



Fig. 5.28. Reflectographic image acquired by InGaAs detector, the rectangle shows the lines of squaring.

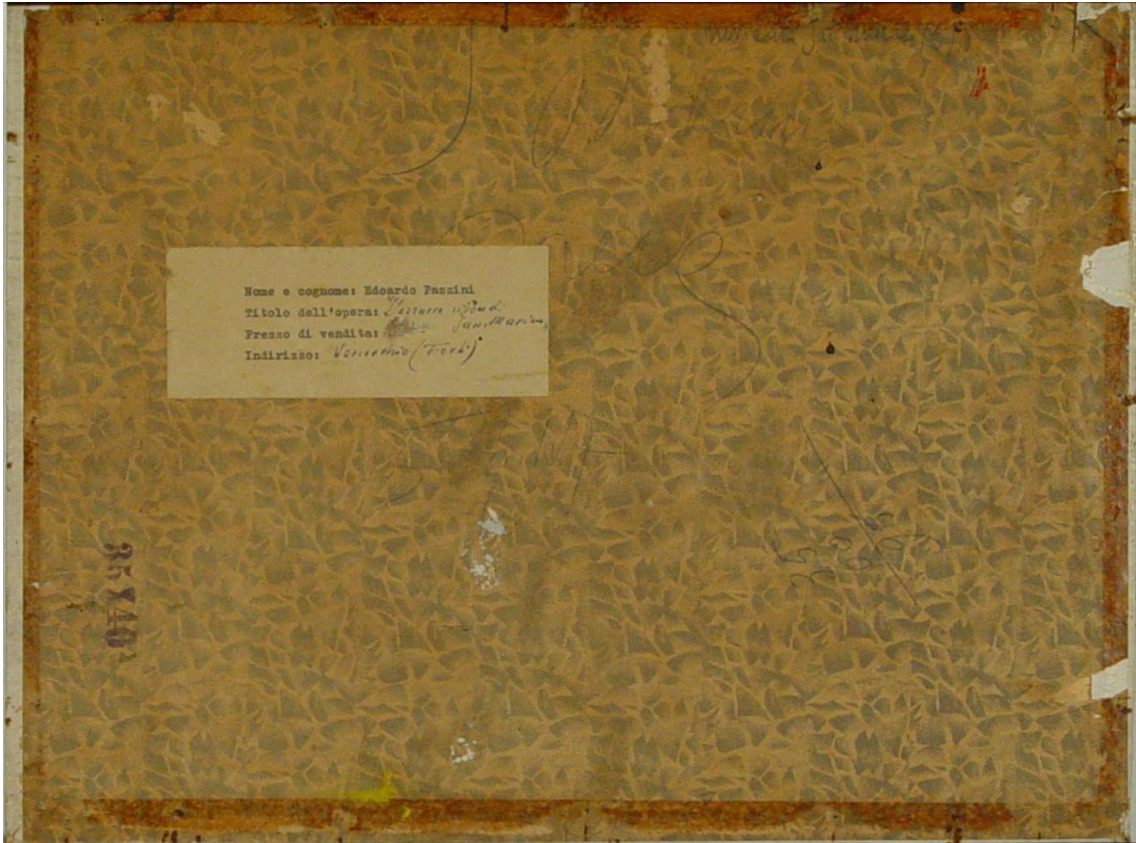


Fig. 5.29. E. Pazzini, *L'azzurra vision di San Marino*, verso.

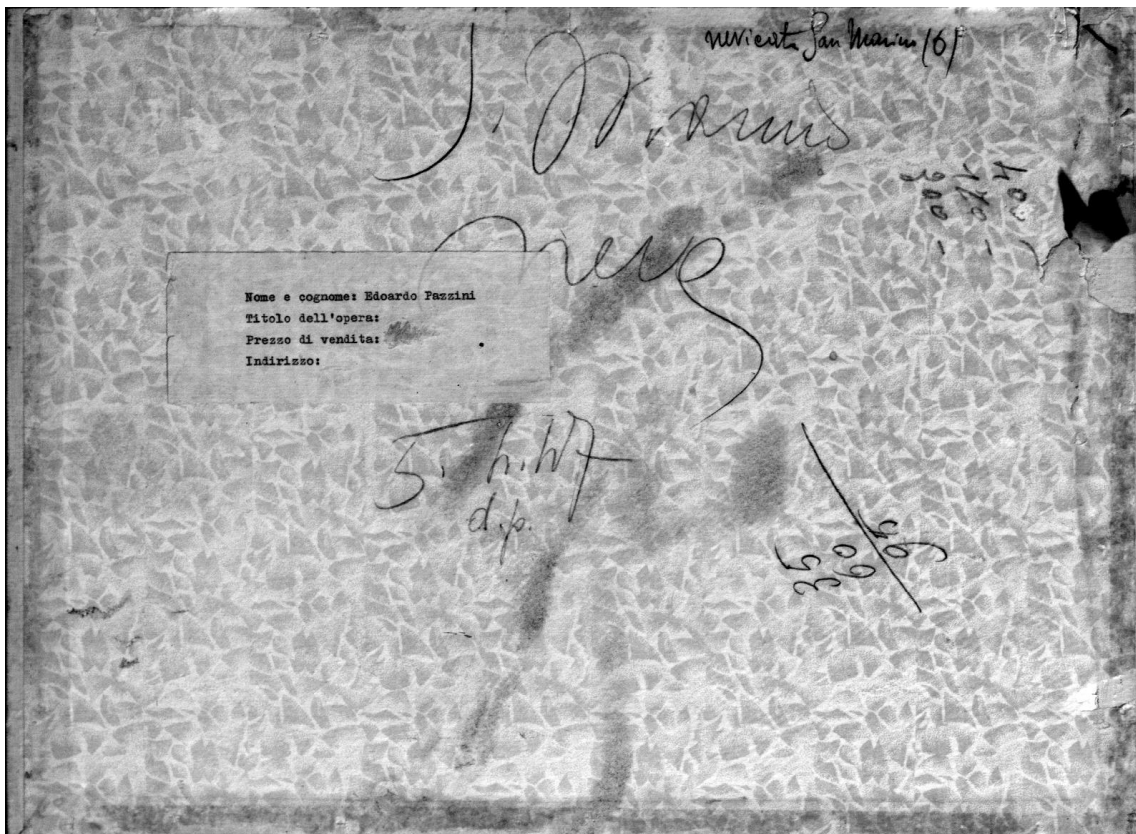


Fig. 5.30. Reflectographic image acquired by InGaAs detector



Fig. 5.31. E. Pazzini, *San Leo*, 50s years, oil on plywood, 50x60 cm, private collection.



Fig. 5.32. Reflectographic image acquired by InGaAs detector



Fig. 5.33. E. Pazzini, *Oxen*, 50s years, oil on plywood, 50x60 cm, private collection.

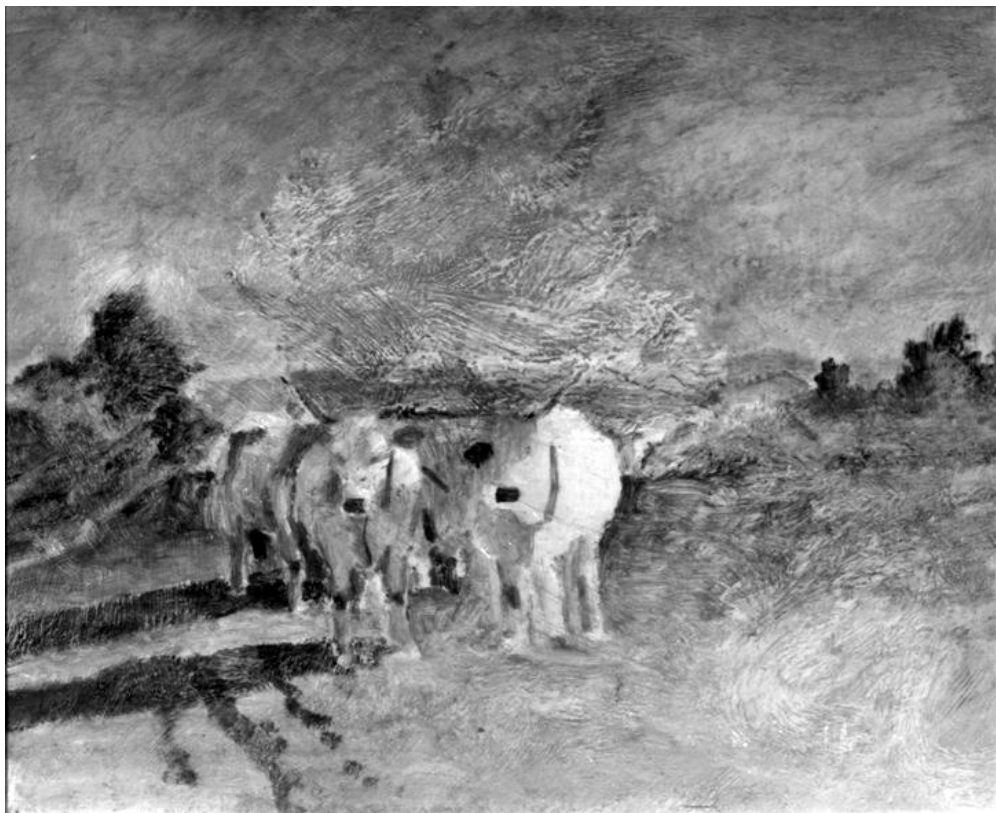


Fig. 5.34. Reflectographic image acquired by InGaAs detector

**References**

1. F. Albertin, M. Gambaccini, E. Peccenini, V. Pellicori, F. Petrucci. *Tecniche multispettrali integrate per lo studio di opere d'arte contemporanea* XCVI National Meeting SIF, Bologna, 2010.
2. F. Albertin, L. Boselli, V. Pellicori, E. Peccenini, F. Petrucci, F. Tisato. *Tecniche artistiche del novecento: nuove finalità per la diagnostica per immagini*. Meeting Science for Contemporary Art, AIAR, Ferrara, 2011.
3. F. Albertin, L. Boselli, M. Gambaccini, V. Pellicori, E. Peccenini, F. Petrucci, F. Tisato. *Wide Band IR Reflectography*, 11th International Workshop on Advanced Infrared Technology and Applications AITA, L'Aquila, 2011.
4. <http://xp9.ifac.cnr.it>

---

---

**CHAPTER 6**

**CONCLUSIONS**

---

---





**I**n this work a scanning device for wide band IR Reflectography has been described and inserted in a image diagnostics protocol to investigate paintings.

The system allows to acquire image at 12bit/pixel at suitable distance from the painting and covering an area of 90 x 90 cm<sup>2</sup>.

The problem of overheating founded on a painting with dark background has been solved using a suitable filtration of the lamps.

The main applications has been performed using an InGaAs detector with a spectral response extended up to 2,5 μm and spatial resolution of 2 lp/mm.

The optical system and acquisition have been developed to be able to support different types of single IR detector.

However, the device is still at a prototype level. Despite the lightweight, the electronics and the power sources should be compacted to make really transportable the system.

The wide band range has given good results on the detection of underdrawing, proving the better capability to detect the underdrawing than the most diffused Reflectography by Silicon CCD.

Moreover, some applications have shown unforeseen results exploiting the different reflectance of pigment: recognizing hidden painting, obtaining information on the pigment used and distinguishing retouches or repaintings made by different materials.

Thus, the reflectographic technique acquires new purposes. Besides the study of execution techniques and the investigation of underdrawing, it may become a really support to the restoration.



# Acknowledgements

I would like to express my gratitude to my tutors Ferruccio Petrucci, whose expertise, understanding, and patience, added considerably to my Ph.D experience; and Mauro Gambaccini for having offered me the opportunity of working at the Physics Department of Ferrara University.

I would also like to thank the services of Mechanics, Electronics and Computing of INFN Section of Ferrara, in particular Stefano Chiozzi for the help and valuable contribution to this work.

Thanks to Giovanni Villa and Gianluca Poldi of Bergamo University and the restorer Giovanna Scicolone for the realization of the test painting.

Thanks also to the support of TekneHub of Ferrara Tecnopole and the High Technology Network of the Emilia Romagna region.

A very special thanks goes out to the other members of my research group: Fauzia Albertin, Lara Boselli, Virginia Pallicori and Flavia Tisato. It was a pleasure to work with you.

